



Fakultät für Medizin

Institut für Molekulare Immunologie

Glutathione peroxidase 4 regulates autophagy and cell death during erythropoiesis

Özge Canlı

Vollständiger Abdruck der von der Fakultät für Medizin der Technischen Universität München zur Erlangung des akademischen Grades eines

Doctor of Philosophy (Ph.D.)

genehmigten Dissertation.

Vorsitzender: apl. Prof. Dr. Helmuth K. H. Adelsberger

Prüfer der Dissertation:

1. Priv.-Doz. Melek Canan Arkan-Greten, Ph.D.
2. Univ.-Prof. Dr. Georg W. Bornkamm
3. Priv.-Doz. Dr. Daniel Krappmann, Ludwig-Maximilian-Universität München

Die Dissertation wurde am 18.02.2013 bei der Fakultät für Medizin der Technischen Universität München eingereicht und durch die Fakultät für Medizin am 15.03.2013 angenommen.

Glutathione peroxidase 4 regulates autophagy and cell death during erythropoiesis

Özge Canli

PhD Thesis, 2013

Thesis Supervisor: Prof. Dr. med. Florian R. Greten

Keywords: GPx4, Anemia, Autophagy, Necroptosis, ROS, lipid peroxidation, caspase 8

Abstract

Maintaining cellular redox balance is vital for cell survival and tissue homeostasis since imbalanced production of reactive oxygen species (ROS) may lead to oxidative stress and cell death. Oxidative stress has been linked to several disorders; however, underlying molecular mechanisms are still not fully understood. Erythrocytes are especially highly sensitive to ROS accumulation due to their physiological function in oxygen transport. Previous studies have shown that oxidative stress in erythroid cells often results in shortened life span of red blood cells and in hemolysis. Glutathione peroxidase 4 (GPx4), one of the most important ROS scavenging selenoproteins, is a unique antioxidant enzyme that can directly reduce phospholipid hydroperoxide in mammalian cells. Using mice with a hematopoietic specific deletion of GPx4, it is demonstrated that GPx4 is essential for reticulocyte maturation. Loss of GPx4 in erythroid cells results in ROS accumulation and lipid peroxidation leading to impaired reticulocyte maturation and subsequently to anemia. Additional deficiency of vitamin E leads to further elevation of anemia proposing that vitamin E plays a critical role to compensate impaired erythropoiesis in the absence of GPx4. Moreover, autophagy, which is potentially a counteracting mechanism to oxidative stress, is impaired due to GPx4 depletion. Also, caspase 8, one of the main regulatory elements of cell death execution, is inhibited due to glutathionylation. In combination with impaired autophagy and functional inhibition of caspase 8, GPx4 ablation triggers RIP1/RIP3 dependent necroptosis. Inhibition of necroptosis normalizes reticulocyte maturation and reverts anemia. Interestingly, necroptosis occurs independent of upstream activators such as TNF α and FasL. The model proposes a novel receptor-independent pathway for the initiation of necroptosis that is initiated through the enhanced accumulation of ROS and formation of lipid peroxides as activators of RIP1/RIP3. Collectively, these results suggest that ROS and lipid peroxidation impair autophagy, functionally inhibit caspase 8 and induce necroptosis. Moreover, the data reveal the critical role of GPx4 and vitamin E in erythropoiesis.

Glutathion Peroxidase 4 reguliert Autophagie und Zelltod während der Erythropoese

Özge CANLI

PhD Thesis, 2013

Thesis Supervisor: Prof. Dr. med. Florian R. Greten

Keywords: GPx4, Anämie, Autophagie, Nekroptose, ROS, Lipid Peroxidation, Caspase 8

Zusammenfassung

Das Überleben von Zellen und Homöostase in Geweben setzt ein austariertes zelluläres Redox-Gleichgewicht voraus, weil unbalanzierte Produktion von reaktiven Sauerstoff-Verbindungen (reactive oxygen species, ROS) zu oxidativem Stress und Zelltod führt. Viele Studien haben die Verbindung von ROS zu einer Vielzahl von Störungen etabliert, doch grundlegende molekulare Mechanismen sind nur unzureichend charakterisiert. Aufgrund ihrer physiologischen Funktion als Sauerstofftransporter sind insbesondere Erythrozyten besonders anfällig gegenüber einer Akkumulation von ROS. Bisherige Arbeiten haben gezeigt, dass oxidativer Stress in Erythrozyten deren Lebensdauer verkürzt und zur Hämolyse führt. GPx4, eines der wichtigsten ROS-abbauenden Selenoproteasen, ist ein einzigartiges Enzym, das direkt Phospholipid-Hyperperoxide in Säugetier-Zellen abbauen kann. Hier zeigen wir in einer transgenen Mauslinie mit GPx4-Deletion in hämatopoetischen Zellen, dass GPx4 essentiell für die Ausreifung von Retikulozyten ist. In GPx4-defizienten erythroiden Zellen akkumulieren ROS und Lipidperoxide, die die Ausreifung von Retikulozyten stören und folglich zu Anämie führen. Die Anämie ist in Abwesenheit von Vitamin E stärker ausgeprägt, was die Rolle von Vitamin E in der Kompensation der gestörten Hämatopoese unter GPx4-Defizienz unterstreicht. Darüberhinaus ist Autophagie, ein Prozess um oxidativem Stress entgegenzuwirken, durch GPx4-Verlust gestört. Des Weiteren ist Caspase 8, einer der Hauptregulatoren im Ablauf von Zelltod, durch Glutathionierung inhibiert. In Kombination mit gestörter Autophagie und funktioneller Inhibition von Caspase 8 löst die Deletion von GPx4 eine RIP1/RIP3-abhängige Nekroptose aus. Nekroptose-Inhibition normalisiert die Reifung von Retikulozyten und verhindert Anämie. Interessanterweise läuft Nekroptose unabhängig von vorgeschalteten Aktivierungen wie $\text{TNF}\alpha$ und FasL ab. Dieses Modell stellt einen neuen Rezeptor-unabhängigen Signalweg zur Initiation von Nekroptose vor, in dem verstärkte Akkumulation von ROS und Lipidperoxiden zur Aktivierung von RIP1/RIP3 führen. Zusammenfassend zeigen diese Ergebnisse, dass ROS und Lipidperoxide Autophagie und die Funktion von Caspase 8 stören und Nekroptose induzieren. Darüberhinaus zeigen die Daten die Bedeutung von GPx4 und Vitamin E in der Erythropoese auf.

Acknowledgments

With immense gratitude, I would like to express my deepest appreciation to all those who contributed their time and effort to make this work possible.

I am sincerely grateful to;

My supervisor *Prof. Dr. Florian R. Greten*, for the momentous ideas, for the invaluable guidance, for endless support and encouragement, for his trust, for giving me the chance to take part in this exhilarating journey.

My advisor *Prof. Dr. Georg W. Bornkamm*, for his inspirational supervision, constructive participation and for the extensive discussions.

My advisor *Dr. M. Canan Arkan*, for her enlightening critiques and insights.

Dr. Marcus Conrad, Dr. Lothar Hültner, Dr. Michaela Aichler, Dr. Naidu Vegi, Dr. Timm Schroeder, Dr. Dirk Janik, Dr. Frauke Neff, Prof. Dr. Axel Walch, Philipp S. Hoppe, Cornelia Kuklik-Roos, Camilla Ladinig, Manuela Schneider, Josef Mysliwietz, Heidi Förster, from Helmholtz Zentrum München, for their valuable contributions.

Prof. Dr. Peter Vandenabeele and Saker Grootjans, for their generous collaboration.

PhD Program coordinator *Dr. Katrin Offe*, for her considerate guidance.

Technical assistants *Kerstin Burmeister*, for the expert help and for her easeful optimism; *Saskia Ettl*, for all the professional aid and for the genuine support.

My colleagues and dear friends; *Michaela A. Diamanti, Dr. Tiago De Oliveira, Begüm Alankuş, Paul Ziegler, Julia Varga, Charles Pallangyo, Dr. Hsin-Yu Fang, Olga Goncharova, Dr. Abdelhamid Beji* for the companionship, for the discussions, for the help, for the comfort, for sharing, for commiseration and for the joy.

Former members of the lab; *Dr. Moritz Bennecke, Dr. Julia Bollrath, Dr. Serkan Göktuna, Kristin Retzlaff, Dr. Tim Nebelsiek* for preceding; *Dr. Sarah Schwitalla,* for the companionship through the path, *Dr. Arun Mankan, Gülfem Öner, Julia Kaerlein, Birgit Wittig* for their support.

Members of Arkan lab; *Çiğdem Atay, Manon Schultz, Jessica Heringer, Franziska Romrig, Dr. Jamil Khasawneh* for the ease and for their friendship.

Dr. Anne Krug, Prof. Dr. Andreas Jung and *Prof. Dr. Jürgen Ruland* for the conducive tutoring during my rotation projects.

Members of Krug lab; *Dr. Katharina Eisenächer, Dr. Alexander Heiseke, Dr. Jacob Loschko, Dr. Andreas Schlitzer* for their genuine help.

My friends; *Dr. Yolanda Markaki, Roland Schüller, Deniz Saltukoğlu, Pınar Önal* for sharing the zest and the burden.

My dear friend; *Onur Gökçe* for the inspiration, for his challenging curiosity, for the care and for simply being there with me.

My beloved family; *Gözde Canlı, Türkan Canlı* and *Zeki Canlı,* for their gratuitous love and unbounded faith. I am truly indebted to their incessant devotion.

“Anneanne, seni çok seviyorum. Huzur içinde uyu.”

Contents

Abstract	i
Zusammenfassung	ii
Acknowledgments	iii
Table of Contents	vi
List of Figures	viii
List of Tables	viii
Abbreviations	x
1 Introduction	1
1.1 ROS, oxidative stress, antioxidant defense	1
1.1.1 Oxidative stress	1
1.1.2 Cellular redox regulation	5
1.1.3 GPx4	10
1.2 Erythropoiesis	17
1.2.1 Anemia	18
1.2.2 Role of ROS in RBC development and anemia	21
1.3 Mechanisms of cell death	22
1.3.1 Apoptosis	22
1.3.2 Autophagy	24
1.3.3 Necroptosis	28
2 Materials and Methods	31
2.1 Materials	31
2.1.1 Mouse models	31
2.1.2 Chemicals, solutions and equipment	32
2.2 Methods	32
2.2.1 Animal experiments	32
2.2.2 Cell isolation and primary cell culture	34
2.2.3 Colony formation assay	34
2.2.4 Culture experiments of fibroblasts	35
2.2.5 Flow cytometry	36
2.2.6 Histology	38
2.2.7 RNA analysis	41
2.2.8 Western blot	43
2.2.9 Immunoprecipitation	45
2.2.10 Glutathionylation assay	45

2.2.11	GSH measurement	46
2.2.12	ELISA	46
3	Results	47
3.1	Anemia in the absence of GPx4	47
3.2	ROS accumulation and lipid peroxidation in red blood cells	48
3.3	Vitamin E is essential for the increased erythropoiesis in GPx4 ^Δ mice	51
3.4	Autophagic flux is inhibited in the absence of GPx4	53
3.4.1	Genetic inhibition of autophagy does not revert anemia <i>in vivo</i>	55
3.5	Anemia occurring in the absence of GPx4 is not dependent on 12/15-Lox	57
3.6	GPx4-deficiency does not induce apoptosis in erythroid progenitors .	59
3.7	Caspase 8 is functionally inhibited due to glutathionylation	60
3.8	RIP1/RIP3-dependent necroptosis is responsible for cell death in GPx4-deficient fibroblasts and erythroid progenitor cells	61
3.8.1	Inhibition of necroptosis rescues anemia	65
3.8.2	ROS levels and lipid peroxidation are not affected by nec-1 . .	65
3.8.3	Necrosome formed in the absence of GPx4 is independent of FADD recruitment	68
3.8.4	Necroptosis in the absence of GPx4 is not dependent on TNF α or CD95L	68
3.9	Despite the DNA damage, inhibition of PARP does not rescue cell death of GPx4-deficient fibroblasts and the anemia in GPx4 ^Δ mice . .	69
4	Discussion	74
4.1	GPx4 deletion impairs cellular redox balance leading to accumulation of ROS and lipid peroxidation	74
4.1.1	Oxidative stress in RBCs causes anemia	75
4.1.2	Vitamin E acts as a ROS scavenger in the absence of GPx4 . .	75
4.2	Impaired autophagy in the absence of GPx4	76
4.3	Loss of GPx4 leads to necroptosis	77
4.3.1	Inhibition of caspase dependent cell death in GPx4 deficient cells	77
4.3.2	Necroptosis as a cell death mechanism in the absence of GPx4	79
5	Conclusion	81
	Bibliography	96
A	Appendix	97
A.1	Chemicals, Reagents and Kits	97
A.2	Antibodies	98
A.2.1	Flow cytometry antibodies	98
A.2.2	Western blot antibodies	98
A.2.3	Antibodies used for histology	98
A.3	siRNA	98
A.4	Genotyping	98

List of Figures

1.1	ROS and antioxidant defense systems	2
1.2	ROS and antioxidant defense systems	5
1.3	Catalytic cycle of GPx4	12
1.4	Structure of the GPx4 gene, encoding isoenzymes of GPx4	17
1.5	Erythropoiesis regulation.	19
1.6	Molecular mechanisms of autophagy.	26
1.7	TNFR1 elicited signaling pathways.	30
3.1	GPx4 deletion in erythroid cells	48
3.2	Loss of GPx4 in hematopoietic cells induces anemia that is compensated by increased erythropoiesis.	49
3.3	Lipid peroxidation and accumulation of ROS in red blood cells	50
3.4	Survival of peripheral erythrocytes and reticulocytes	51
3.5	Impaired reticulocyte maturation in the absence of GPx4	52
3.6	<i>In vitro</i> erythroid colony formation is abolished in GPx4 Δ BM	53
3.7	Vitamin E is essential for the increased erythropoiesis in GPx4 Δ mice	54
3.8	Autophagy is impaired in GPx4 Δ mice	56
3.9	Inhibition of autophagy does not revert anemia <i>in vivo</i>	57
3.10	Anemia occurring in the absence of GPx4 is not dependent on 12/15-Lox	58
3.11	GPx4-deficiency does not induce apoptosis in erythroid progenitors	59
3.12	Necroptosis in the absence of GPx4 is not dependent on caspase 8	60
3.13	Caspase 8 is functionally inhibited due to glutathionylation <i>in vitro</i>	62
3.14	Caspase 8 is functionally inhibited due glutathionylation <i>in vivo</i>	63
3.15	RIP1/RIP3-dependent necroptosis is responsible for cell death in GPx4-deficient fibroblasts and erythroid progenitor cells	64
3.16	Nec-1 treatment reverts anemia in GPx4 Δ mice	66
3.17	Necroptosis is responsible for the anemia in GPx4 Δ mice	67
3.18	Nec-1 does not reverse ROS levels or lipid peroxidation	67
3.19	Necrosome formed in the absence of GPx4 is independent of FADD recruitment	68
3.20	Necroptosis in the absence of GPx4 is not dependent on TNF α	69
3.21	TNF α or CD95 neutralization do not rescue anemia <i>in vivo</i>	70
3.22	Inhibition of PARP does not rescue cell death in GPx4 Δ fibroblasts	72
3.23	Inhibition of PARP does not rescue the anemia in GPx4 Δ mice	73
5.1	Summary of the proposed model explaining the cellular role of GPx4	83

List of Tables

1.1	Blood count values for C57BL/6J mice	21
1.2	Features of different forms of programmed cell death	23
2.1	Tissue dehydration program	38
2.2	Deparaffinization and rehydration protocol	39
2.3	Section dehydration protocol	39
2.4	Quantitative PCR Program	42
2.5	Quantitative PCR primers	43
2.6	Protein lysis buffer	43
2.7	5x Laemmli buffer	44
2.8	Transfer Buffer	45
A.6	12/15-Lox Genotyping PCR	99
A.7	ATG7 Genotyping PCR	99
A.8	Cre Genotyping PCR	99
A.9	GPx4 Genotyping PCR	99
A.10	RIP3 Genotyping PCR	99

Abbreviations

12/15-Lox 12/15-Lipoxygenase.

4-OHT 4-Hydroxytamoxifen.

8oxodG 8-Hydroxyguanine.

AIF apoptosis inducing factor.

Atg autophagy protein.

Bcl2 pro-apoptotic B cell lymphoma 2.

BM bone marrow.

BODIPY BODIPY 581/591 C11.

CAT catalase.

CMA chaperone-mediated autophagy.

Cox cyclooxygenase.

Cox2 cyclooxygenase-2.

Cys cysteine.

cyt c cytochrome c.

DCF 5-6- chloromethyl-2',7'- dichlorodihydrofluorescein diacetate, acetyl ester, CM-H₂DCFDA.

DTT dithiothreitol.

ELISA enzyme-linked immunosorbent assay.

EM Electron microscopy.

EPO erythropoietin.

FAD flavin adenine dinucleotide.

FADD FAS-associated death domain.

GPx glutathione peroxidase.

GPx4 glutathione peroxidase 4.

GSH glutathione.

GSSG glutathione disulfide.

Hb hemoglobin.

HCT hematocrit.
HIF1 hypoxia-inducible factor 1.
HRP horseradish peroxidase.
i.p. intraperitoneal.
IL6 interleukin 6.
Lox lipooxygenase.
MCH mean corpuscular hemoglobin.
MCHC mean corpuscular hemoglobin concentration.
MCV mean corpuscular volume.
NADPH nicotinamide adenine dinucleotide phosphate.
nec-1 necrostatin 1.
NF κ B nuclear factor kappa B.
PARP poly ADP-ribose polymerase.
PBS-T PBS-0.1%Tween20.
PFA paraformaldehyde.
PI promidium iodide.
PI3K class III phosphatidylinositol 3 kinase.
poly I:C polyinosinic: polycytidylic acid.
RBC red blood cell.
RDW red cell distribution width.
RIP1 receptor-interacting protein 1.
RIP3 receptor-interacting protein 3.
ROS reactive oxygen species.
RT room temperature.
Sec selenocysteine.
SOD superoxide dismutase.
TAK1 transforming growth factor β activated kinase 1.
TNF α tumor necrosis factor α .
TRAF2 tumor necrosis factor receptor-associated factor 2.
TRAIL TNF-related apoptosis-inducing ligand.
Trx thioredoxin.
TrxR thioredoxin reductase.
TUNEL TdT-mediated dUTP-biotin nick end labeling.

Chapter 1

Introduction

1.1 ROS, oxidative stress, antioxidant defense

ROS are formed as normal products of aerobic metabolism but can as well be produced at elevated rates under pathological conditions. ROS refers to chemically reactive molecules derived from oxygen, including highly reactive species, such as the hydroxyl radical, and some less reactive molecules, as superoxide and hydrogen peroxide.

ROS can be produced within cells by multiple enzymes that use molecular oxygen as substrate. They were first studied for their essential role in the host defense. When phagocytes are activated, they produce high amounts of ROS to kill intruding bacteria [1, 2, 3].

To maintain the redox state of tissues, biological systems keep a balance between the production and manifestation of oxygen radicals, to detoxify reactive intermediates and to repair the resulting damage (Figure 1.1).

1.1.1 Oxidative stress

Oxidative stress is defined as the imbalance in cellular redox in favor of the oxidants. Increased oxidative stress plays a crucial role in a variety of pathological conditions including cancer, degenerative diseases, and aging [4]. Due to their high reactivity, ROS are prone to cause damage to most biomolecules and are therefore potentially toxic, mutagenic or carcinogenic. They can readily react with most biomolecules, starting a chain reaction of free radical formation. In order to eliminate the unpaired

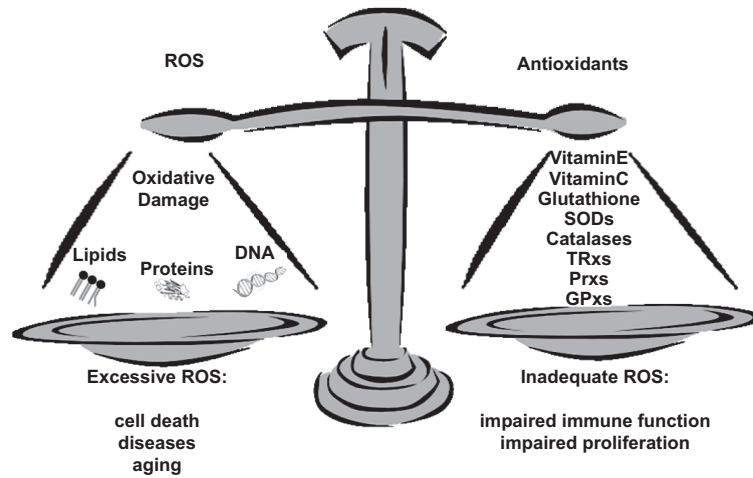


Figure 1.1: ROS and antioxidant defense systems. Cellular ROS levels are maintained via several enzymatic and non-enzymatic antioxidants. Excessive ROS lead to oxidative stress causing damage to lipids, proteins and nucleic acids, finally causing cell death. On the other hand, inadequate ROS interfere with regulation of cellular mechanisms, such as immune defense and proliferation.

electrons to stop this chain reaction, the newly formed radical reacts either with another free radical or with a free radical scavenger. In the absence of reducing agents, an imbalanced production of ROS can potentially harm biomolecules, such as nucleic acids, lipids and proteins.

DNA ROS have been shown to be mutagenic by causing chemical modifications to DNA [5]. A number of DNA alterations have been associated with redox imbalance such as cleavage of DNA, DNA-protein cross-links or oxidation of purines. There is compelling evidence that oxidative stress causes premutagenic lesions generating a diverse range of adducts in DNA. Several repair mechanisms take part in the elimination of such lesions. One of the major mutagenic base lesions generated by oxygen radicals is 8-Hydroxyguanine (8oxodG), which preferentially pairs with adenine instead of cytosine and thus generates transversion mutations after replication [6].

Lipids Free radical-mediated lipid oxidation, termed lipid peroxidation has been implicated in various diseases such as cardiovascular diseases, causing formation of atherosclerotic plaques by the oxidation of low density lipoproteins [7, 8]. Fatty acids are sensitive to oxidation especially due to the presence of polyunsaturated residues [9]. Excessive ROS cause lipid peroxidation by targeting fatty acids [5, 10]. Imbalanced lipid peroxidation is a deleterious process leading to disruption of biomembranes, thus to cellular dysfunction. Accumulation of reactive lipid molecules specifically modifies cysteinyl thiols and modulate protective cell signaling pathways. On the other hand, regulated lipid peroxidation has multiple functions in cell signaling dependent on the site and mechanism of oxidation [11]. Various antioxidants, such as vitamin E, vitamin C, and enzymes as superoxide dismutase (SOD), catalase (CAT), glutathione peroxidase (GPx) take part in the regulation of lipid peroxidation to prevent membrane oxidation or to minimize the damage by eliminating cytotoxic molecules [5].

Proteins ROS have been shown to react with several amino acid residues, generating modified proteins, leading to loss or gain of function for enzymes or proteins, thus to alterations in cell signaling pathways [12, 10]. Oxidation of proteins can lead to several modifications, including; hydroxylation of aromatic groups and of aliphatic amino acid side chains, nitration of aromatic amino acid residues, nitrosylation of sulfhydryl groups, sulfoxidation of methionine residues, chlorination of aromatic groups, conversion of some amino acid residues to carbonyl derivatives, cleavage of the polypeptide chain and formation of cross-linked protein aggregates [13]. Among the most susceptible amino acids are sulfur or selenium containing residues [14] and cysteine (Cys) residues with their sensitivity to glutathionylation [15]. Oxidation of Cys thiol groups leads to sulfenic acid formation and extensive exposure to oxidants cause sulfinic or sulfonic acid formation [16]. The level of oxidized proteins increases with aging and also in a number of age related diseases, including amyotrophic lateral sclerosis, Alzheimer's disease, respiratory distress syndrome, muscular dystrophy, cataractogenesis, rheumatoid arthritis, progeria, Werner's syn-

drome, atherosclerosis, diabetes, Parkinson's disease, essential hypertension, cystic fibrosis, and ulcerative colitis [17, 18, 19]. The steady-state level of oxidatively modified proteins is dependent on a multitude of factors that influence the rates of ROS generation, the ability of cells to scavenge ROS, and also the levels and activities of the proteasome and other proteases that catalyze the degradation of oxidized proteins [13].

S-Glutathionylation is a reversible posttranslational modification of Cys residues by the addition of glutathione (GSH) via formation of disulfides [15]. It is a regulatory mechanism under normal conditions; however, its increase in response to oxidative/nitrosative stress interferes with cellular signaling pathways. It is associated with post-translational regulation of a variety of regulatory, structural and metabolic proteins taking part in signaling or metabolic pathways. Oxidative stress through the imbalance in glutathione disulfide (GSSG)/GSH ratio leads to irreversible glutathionylation of proteins causing functional inhibition. S-glutathionylation is suggested to be a protective measure to protect active site cysteines against irreversible oxidation, such as, formation of sulfinic/sulfonic acid and inactivation [20, 21]. However, recent studies demonstrated inactivation of apoptotic pathways due to glutathionylation of caspases including caspase-1 [22] and caspase-3 [23].

Oxidative stress and cell death

An increase in ROS production or a defect in ROS scavenging can disrupt redox homeostasis, leading to an overall increase of intracellular ROS levels and finally to oxidative stress. Cellular ROS can determine the fate of cells, in general, ROS at low levels act as signaling molecules that promote cell proliferation and cell survival, however, uncontrolled increase in ROS can cause cell death. Alterations in redox homeostasis can promote cell death or cell survival, depending on the magnitude of the stimuli and genetic stability of the cells [24] (Figure 1.2). In addition, oxidative stress via inactivation of regulatory elements can determine the death execution mechanism. The role of ROS and oxidative stress in the context of different types of cell death is further discussed in Section 1.3.

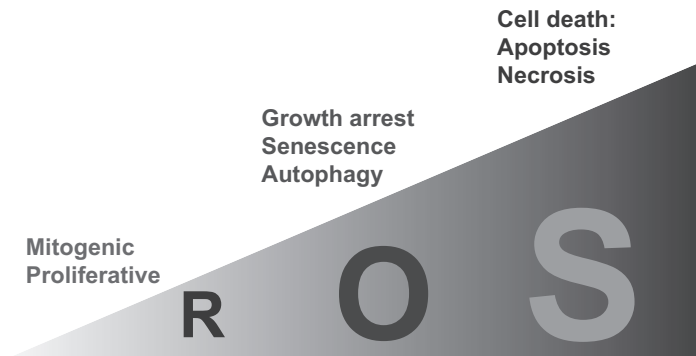


Figure 1.2: ROS and antioxidant defense systems. Cellular ROS levels are maintained via several enzymatic and non-enzymatic antioxidant defense systems. Excessive ROS lead to oxidative stress causing damage to lipids, proteins and nucleic acids, finally causing cell death. On the other hand, inadequate ROS interfere with cellular metabolisms and may lead to impaired immune defense and cell proliferation.

1.1.2 Cellular redox regulation

The delicate balance between ROS generation and elimination is maintained by several mechanisms, and a dysfunction of any of these mechanisms could lead to alterations in cellular redox state. Cells are equipped with enzymatic and non-enzymatic antioxidant systems to eliminate ROS and maintain redox homoeostasis (Figure 1.1).

Non-enzymatic antioxidants

Three non-enzymatic antioxidants of particular importance are: Vitamin E, vitamin C and glutathione.

Vitamin E Vitamin E encompasses a group of potent, lipid-soluble antioxidants. α -tocopherol, the most abundant form of vitamin E in nature, is the major lipid-soluble antioxidant, and plays a vital role in protecting membranes from oxidative damage [25]. It is a potent peroxy radical scavenger and a chain-breaking antioxidant that prevents the propagation of free radicals in membranes and in plasma lipoproteins [26]. The hydroxyl group of tocopherol reacts with the peroxy radical to form the corresponding lipid hydroperoxide and the tocopheryl radical. The to-

copheryl radical reacts with vitamin C or other hydrogen donors to convert vitamin E to its reduced state [27].

Vitamin C Vitamin C (or ascorbic acid) is an electron donor and therefore a reducing agent. It is a water-soluble antioxidant that can reduce radicals from a variety of sources [28]. Ascorbic acid acts by donating two electrons from a double bond between the second and third carbons of the 6-carbon molecule [29]. The species formed after the loss of one electron is a free radical, ascorbyl radical [30, 28]. Once formed, ascorbyl radical can be reduced back to ascorbic acid by enzymatic pathways or by reduction of glutathione [30]. Interestingly, vitamin C also functions as a pro-oxidant under certain circumstances [31, 32].

Glutathione GSH is an important water soluble antioxidant and an essential co-factor for antioxidant enzymes due to its high electron donating capacity linked with its sulfhydryl group [33]. The oxidized form of glutathione is a sulfur linked compound known as GSSG. Reacting with radicals oxidizes glutathione, which is reduced in a redox cycle involving glutathione reductase and the electron acceptor nicotinamide adenine dinucleotide phosphate (NADPH) [33, 34]. The GSSG/GSH ratio can be used as an indicator of oxidative stress and when not balanced causes toxicity for the cells [35]. GSH depletion has been shown to cause cell death [36, 37, 38]. Although initial studies suggested that GSH depletion was only a by-product of oxidative stress generated during cell death, recent discoveries suggest that GSH depletion and post-translational modifications of proteins through glutathionylation are critical regulators of apoptosis [39]. In addition, recent data suggested that glutathionylation of caspases inhibits apoptotic pathways and alters immune responses [22, 23].

Antioxidant enzymes

The main enzymatic antioxidants consists of 5 enzyme families; SODs, catalases, thioredoxins, peroxiredoxins and glutathione peroxidases.

Superoxide dismutases SODs are enzymes that play a pivotal role in metabolizing superoxide anion radicals derived from extracellular stimulants and by-products of oxygen metabolism through the electron transport chain in mitochondria [40]. SODs employ Fe, Mn, Ni, Cu or Zn ions for activity [41, 42]. The family is composed of several enzymes with the ability to convert superoxide to dioxygen and hydrogen peroxide, with consumption of hydrogen ion. In mammals there are three isoforms of SODs: the cytoplasmic Cu/ZnSOD (SOD1), the mitochondrial MnSOD (SOD2), and the extracellular Cu/ZnSOD (SOD3) [43]. SOD depletion has been linked to several diseases including amyotrophic lateral sclerosis (ALS) [44, 45] and hemolytic anemia as a result of oxidative stress [46, 47].

Catalases Catalases of many organisms are mainly heme-containing enzymes [48]. In mammalian cells they are mostly localized in peroxisomes, where they catalyze the conversion of hydrogen peroxide to water and molecular oxygen [49, 50]. In mammalian tissues, catalase activity is highest in liver and erythrocytes, relatively high in kidney and adipose tissue, intermediate in lung and pancreas, and very low in heart and brain [50]. Catalase protects hemoglobin by removing over half of the hydrogen peroxide generated in normal human erythrocytes, which are exposed to substantial oxygen concentrations [51]. It has been implicated as an important factor in inflammation [52], mutagenesis [53], tumorigenesis [54] and in prevention of apoptosis [55]. Catalase and glutathione peroxidase are believed to be the most active systems in detoxification of hydrogen peroxide in human erythrocytes [51].

Thioredoxins The thioredoxin (Trx) system consists of the two types of antioxidant oxidoreductase enzymes; Trx and thioredoxin reductase (TrxR), both being ubiquitous in mammalian and prokaryotic cells [56]. TrxR catalyzes the reduction of the active site disulfide in Trx using NADPH and flavin adenine dinucleotide (FAD). Mammalian TrxR with its highly reactive active site composed of a selenocysteine (Sec) residue has a high reductive capacity and can act on several substrates in addition to Trx [49]. Reduced Trx is a general protein disulfide reductant [49]. In

mammals, extracellular forms of Trx also have cytokine-like effects [56]. There are a number of clinical conditions involving Trx such as acute ischaemic heart disease and hepatocellular carcinoma [57, 58, 59, 60].

Peroxiredoxins Peroxiredoxins (Prx; thioredoxin peroxidases) are capable of directly reducing peroxides such as hydrogen peroxide and different alkyl hydroperoxides [61]. Prxs are also efficient peroxynitrite reductases [62, 63]. They share a common reactive Cys residue in the N-terminal region and use thioredoxin or glutathione as the electron donor [64]. There are 13 known members of peroxiredoxins and six subclasses are expressed in mammals [61, 65, 66]. The oxidized Prx formed in the catalytic cycle in mammalian cells can be reduced by Trx [61]. Peroxiredoxins have been shown to inhibit apoptosis induced by p53 [67] and by hydrogen peroxide (H_2O_2) [68]. Recent evidence suggests that they regulate peroxide-mediated signaling cascades [64].

Glutathione peroxidases GPxs catalyze the reduction of hydrogen peroxide and organic hydroperoxides to water or corresponding alcohols using water or reduced GSH as an electron donor. The activity of GPx was first described in 1957, and its function was hypothesized to be protection of red blood cells against hemolysis by oxidation (later called GPx1) [69]. GPxs are believed to be the major components of the human antioxidant defense.

In humans, there are seven known members of the family, five of which are selenoenzymes and the other two containing Cys instead of Sec. The GPx family includes the following members: the ubiquitously expressed cytosolic GPx (cGPx/GPx1) [70], a gastrointestinal specific enzyme which is exclusively expressed in gastrointestinal tract in rodents but also in liver in humans (GI-GPx/GPx2) [71, 72], a secreted protein found in plasma (pGPx/GPx3) [73], a ubiquitously expressed enzyme that acts on oxidized lipids, phospholipid hydroperoxide glutathione peroxidase (PHGPx/GPx4) [74, 75, 73], a sperm nuclei specific enzyme (snGPx4) [76], and a newly discovered glutathione peroxidase located in olfactory epithelium and embry-

onic tissues (GPx6) [76]. The nonseleno variants include the GPx5 with restricted expression to the epididymis [77] and the ubiquitously expressed nonselenocysteine (NPGPx/GPx7) [78]. These enzymes differ in their tissue distributions and their substrate specificity for peroxide degradation [79]. The common feature of seleno GPxs is the conserved catalytic triad containing Sec, Gln, and Trp, which act through oxidation and reduction of Sec during the catalytic cycle. GPx1,2 and 3 act as homotetrameric proteins, whereas GPx4 functions as a monomeric enzyme.

GPx1 is a ubiquitous cytosolic enzyme and can reduce hydrogen peroxide and some organic hydroperoxides including cholesterol and long-chain fatty acid peroxides, but not fatty acid hydroperoxide in phospholipids [80]. It uses restrictively glutathione as reducing substrate, thus GPx1 activity is often discussed in parallel with glutathione reductase activity, which maintains a constant supply of GSH from GSSG for enzyme activity [79]. Studies with genetically modified mice provided information on the physiologic functions of GPx1 [81, 82]. Mice deficient in the cellular GPx1 are healthy and fertile without increased oxidative stress or sensitivity to hyperoxia suggesting that GPx1 plays a limited role during normal development and under physiological conditions [83]. However, GPx1 was found to be the major mediator of the protective effects of selenium in mice subjected to paraquat and H₂O₂ induced oxidative stress [84, 85].

GPx2 is found in the cytosol and functions as a tetramer. It has a high sequence identity and similar substrate specificity with GPx1 [72]. GPx2 knockout mice also develop normally, however, the absence of both GPx1 and GPx2 resulted in growth retardation and colitis, which led to ileal tumor formation [72, 86]. Interestingly, Gpx2, but not Gpx1, was sufficient in rescuing these phenotypes, suggesting a specific role of GPx2 in protecting the gastrointestinal tract against inflammation and cancer development [86]. GPx2 is predicted to have a vital function based on the high stability of its mRNA under selenium-limiting conditions and the rapid production of the GPx2 protein during selenium repletion compared to other selenoproteins [87].

1.1.3 GPx4

An interesting characteristic of mammalian selenoproteins is the so-called selenium hierarchy, which determines whether or not a selenoprotein is expressed under selenium deficiency and GPx4 has a very high rank within this hierarchy based on its stable expression even when selenium is rare, indicating a strong dependence on this selenoprotein [88].

GPx4 was originally identified as an inhibitor of lipid peroxidation in pig livers with peroxidative activity on phosphatidylcholine in liposomes and biomembranes in the presence of GSH [89, 90] and later detected in human tumor cell lines [91]. Although the active site of GPx4 is highly similar to the other enzymes in the family, the overall sequence similarity is lower than 50% [92].

In addition to being a major antioxidant enzyme, GPx4 is especially important since it has been implicated in the regulation of various processes including sperm maturation [93], gene expression [94], development [95, 96], eicosanoid biosynthesis [97], chromatin condensation [98], DNA damage [99] and cell survival or cell death in several studies [100, 101, 102, 103, 104, 95]. Moreover, GPx4 deletion is lethal during embryogenesis [95, 96].

Biochemical and cellular functions of GPx4

GPx4 is a peculiar member of the GPx family due to a couple of reasons. For instance, whereas the other GPx enzymes function in tetrameric forms, GPx4 was found to be a monomeric enzyme [91] containing a single Sec [90]. GPx4 shares the structural preconditions for its enzymatic activity with the other GPx isoforms with a broad affinity toward its substrate hydroperoxides and its reducing equivalents. In contrast to other GPx isoforms, the active site of GPx4 does not contain an exposed surface loop providing the hydrophobic surface to be accessible allowing close associations with membranes and lipoproteins [105]. In addition to reducing small hydrophilic peroxides such as hydrogen peroxide, GPx4, with its unique structural advantage, can act on more complex substrates such as phospholipids or cholesterol hydroperoxides incorporated into membranes or lipoproteins [90, 106, 107]. As an

enzymatic antioxidant, it is capable of reducing a large array of hydroperoxy lipids including peroxidized phospholipids and cholesterol esters [107]. More importantly, GPx4 is the only enzyme in the family whose deletion is lethal during embryogenesis [95, 96].

GPx4 uses GSH as reducing agent when it is sufficient. In the case of GSH limitation GPx4 has the capacity to accept thiol groups in proteins as reducing agents, for instance, in developing sperm cells [108]. GPx4 is crucial during development owing to the Cys residues on its protein surface, which are critical for its catalytic cycle and have been implicated in its ability to form extensive enzymatically inactive protein polymers in addition to the thioloxygenase activity that induces protein cross-links [108, 109, 110]. GPx4 is expressed at low levels in most mammalian cells, but at high levels in the testis [87]. Low testicular levels of GPx4 have been related to male infertility [111], but these alterations could not be linked to naturally occurring mutations in the GPx4 gene [112].

The human GPx4 gene is located on chromosome 19, and three different GPx4 variants (cytosolic isoform (c-GPx4), mitochondrial isoform (m-GPx4), and nuclear isoform (n-GPx4)) originate from this gene [87, 95] (Figure 1.4). The three different isoenzymes exhibit similar enzymatic properties but they can be distinguished by their specific N-terminal sequences that are determined by alternative usage of three translational initiation sites [100, 113, 114, 115]. These different N-terminal localization signals determine subcellular localization of the enzyme [87, 95].

The catalytic Sec residue at position 46 in GPx4 is believed to be important for its function based on the observation that Sec to Cys conversion leads to strongly impaired activity [116]. Kinetic analysis of the GPx4 reaction suggested a redox cycle consisting of three elementary reactions (Figure 1.3). In the first step, hydroperoxy substrate oxidizes selenol, which yields the selenic acid derivative. In the second step, the oxidized enzyme reacts with a thiol group, mostly with reduced glutathione, leading to seleno-disulfide bond. The last step is the reduction of the enzyme using a second glutathione molecule, yielding one oxidized glutathione disulfide molecule. A defect in this cycle causes an imbalance in the critical cellular GSSG/GSH ratio.

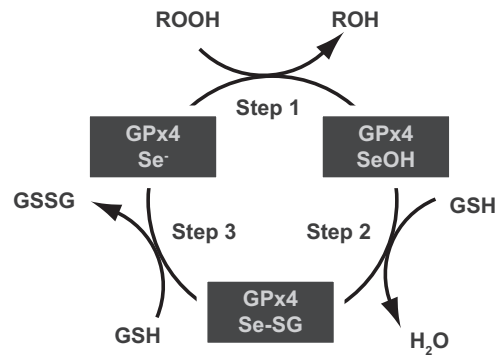


Figure 1.3: Catalytic cycle of GPx4. The catalytic cycle consists of three consecutive elementary reactions. The first step involves oxidation of the dissociated selenol by the hydroperoxy substrate, yielding a selenic acid derivative. In the second step, the oxidized enzyme reacts with a thiol group, mostly a reduced glutathione. The last step of the catalytic cycle involves regeneration of the reduced enzyme by a second glutathione molecule yielding one oxidized glutathione disulfide molecule.

GPx4 as a regulator of cell survival :

Beyond its antioxidant activity GPx4 is implicated as a regulator of cell survival protecting cells from various apoptotic triggers and cell death. For instance, over-expression of GPx4 is shown to be protective against hydroperoxide-mediated injury in different studies [102, 117, 100]. GPx4 expression also rescued cell death due to oxidative stress in Burkitt lymphoma cells at low cell density [118]. over-expression of mitochondrial, but not cytosolic form suppressed hypoglycemia-induced apoptosis in RBL-2H3 cells by preventing the cytochrome c (cyt c) release from mitochondria [119, 101]. On the other hand, Schneider *et al.* showed that deletion of mitochondrial GPx4 causes male infertility but does not interfere with embryogenesis and postnatal development in a study with mice lacking specifically the mitochondrial isoform [120]. Furthermore, the study comparing the roles of the GPx4 isoforms demonstrated that the short form of GPx4 lacking the N-terminal mitochondrial signal is present in somatic tissue mitochondria and is essential for survival in mice, whereas the long form is important for male fertility [121].

GPx4 over-expression has been reported to suppress cell death in several different studies. over-expression of GPx4 prevented oxidant-induced toxicity leading to apoptosis in rabbit aortic smooth muscle cells [122]. In a study with human breast cancer cells (MCF-7), GPx4 provides significant protection against singlet oxygen-generated lipid peroxidation and remarkably increases cell survival [123]. Hurst *et. al* showed that GPx4 over-expressing breast tumor epithelial cell line is highly protected against cholesterol hydroperoxide-induced lethality [124]. Nomura *et. al* demonstrated that over-expression of mitochondrial GPx4 but not non-mitochondrial forms prevented apoptosis via reversing the release of cyt c from mitochondria and the activation of caspase-3 upon exposure to 2-deoxyglucose and also etoposide, staurosporine, UV irradiation, cycloheximide, and actinomycin D [101]. Another study, using transgenic mice either overexpressing GPx4 or deficient in GPx4, demonstrated the protective effects of the enzyme against cyt c from mitochondria [125].

The major phenotypes of GPx4 deficiency are extensive membrane oxidation and cell death [103, 126]. Interestingly, neuronal degeneration in GPx4 deficient cells does not involve caspase activation, but instead leads to the activation of apoptosis inducing factor (AIF)-dependent pathway [103].

GPx4 in development :

In addition to its antioxidant and antiapoptotic features, GPx4 is shown to be vital during development and its deletion is lethal during embryogenesis [95, 96].

During different stages of development in tissues, the transcriptional regulation of different GPx4 isoforms seems to have importance indicated by their tight and distinct regulation of expression. Interestingly, GPx4 has a unique cellular distribution in brain and during development is expressed in principal neurons of the brain [83, 127]. During early stages of embryonic development (E6.5-E15.5), m-GPx4 and c-GPx4 are expressed in similar profiles, however, in later developmental stages (E16.5) and after birth, the concentration of the m-GPx4 decreases, whereas c-GPx4 mRNA remains unchanged [104]. It has been implicated as a structural protein in

sperm maturation based on its ability to use protein thiol groups of neighbouring proteins as substrate when under glutathione limitation [93, 120]. During late spermatogenesis the predominantly expressed form is the nuclear isoform, which is not detected in most other cells and tissues [115]. However, surprisingly mice carrying a targeted deletion of only the nuclear variant of GPx4 using advantage of its unique promoter, do not show any lethality unlike the full knockout animals, ruling out any significant contribution of the nuclear form of GPx4 to mouse development. Besides their full viability, males were fully fertile without any morphological alterations in the sperms despite the high expression of nuclear form in the sperms. On the other hand, the cells isolated from these mice show delayed chromatin condensation and this observation has been related to the sulfhydryl oxidase activity of n-GPx4 [98]. Whereas deletion of the nuclear form is compatible with spermatogenesis, deletion of the mitochondrial form causes abolished spermatogenesis [120].

GPx4 in cell signaling :

The major phenotypes of GPx4 deficiency are extensive membrane oxidation and cell death [103, 126]. GPx4 has been shown to inhibit arachidonic acid-metabolising enzymes such as lipoxygenase (Lox) and cyclooxygenase (Cox). These enzymes require a certain hydroperoxide state for their enzymatic activity, which depends on cytoplasmic GPx4 activity on the regulation of the cellular redox balance by reducing lipid hydroperoxides [128, 129, 130, 97, 131, 132]. It was shown that down-regulation of GPx4 due to selenium depletion leads to an increase in Lox activity [97]. In another study with a human carcinoma cell line, knock-down of GPx4 is shown to be leading to upregulation of Lox and Cox1 [132]. On the other hand, over-expression of GPx4 is shown to impair arachidonic acid metabolism [131]. Recently, GPx4 has been shown to have role in tumor angiogenesis via suppressing lipid peroxidation derived from 12/15-Lipoxygenase (12/15-Lox) activity or cyclooxygenase-2 (Cox2) possibly via modulation of ROS sensitive tyrosine kinase signaling pathways [133, 134, 135].

GPx4 has previously been shown to modulate the activity of transcription factors including nuclear factor kappa B (NF κ B) and Nrf2 [136, 137, 138, 139]. Wenk *et al.* showed that cells overexpressing GPx4 exhibited impaired NF κ B activation, elevated phosphorylation and nuclear translocation of p65 and as a consequence reduced interleukin 6 (IL6) release concluding that lipid peroxides initiate the NF κ B-mediated induction of IL6, which results in the induction of MMP-1, a matrix metalloproteinase frequently upregulated during invasion and metastasis of various tumors [139]. The impact of GPx4 expression on NF κ B activity in embryonic development has not yet been investigated, however impaired NF κ B activation has been shown to cause embryonic lethality due to increased apoptosis of the liver parenchyma and impaired embryonic hematopoiesis [140].

In addition to being the major antioxidant to eliminate destructive lipid peroxides, GPx4 also reduces thymidine peroxides, suggesting a possible role for GPx4 in the repair of DNA damage [99].

Regulation of expression

Three different mRNA species have been shown to be transcribed from the GPx4 gene [75, 141, 74, 142]. In mice exon 3 contains the Sec codon and exon 7 encodes the cis-acting Sec insertion sequence [143]. Figure 1.4 illustrates the structural orientation of GPx4 gene. Transcripts, which start from the most upstream transcription initiation site of the gene in exon 1, contain translational start sites for the mitochondrial and the cytosolic GPx4 [141]. This start site is dominantly used in spermatogenic cells, but the mechanisms that induce transcription from this site remain largely unknown. A second transcription initiation site is located in exon 1a corresponding to ubiquitously expressed mRNA in most mammalian cell types that contains the translational start site only for the cytosolic isoform. The corresponding regulatory region represents the promoter of a housekeeping gene, that is a classical TATA-box under the control of general transcription factors [144]. The third transcription initiation site is located upstream of exon 1b and generates mRNA species coding for the nuclear GPx4 [142]. Transcription from this site is regulated by the

cAMP-response element modulators [76].

All three isoforms of GPx4 are found in early mouse embryos and at later stages GPx4 expression is detected in most developing organs in particular the limbs [104, 145]. Whereas the mRNA levels for the cytosolic GPx4 remain mostly constant throughout embryonic development, expression profiles of mitochondrial and nuclear isoforms appear to be under stage-dependent control with similar expression kinetics, namely, reduction in expression at later stages of embryonic development compared to the early stages [104].

To explore the role of GPx4 during embryonic development, targeted constitutive GPx4 knockout mice were generated [95, 96]. In contrast to the other enzymes in the GPx family, GPx4 knockout was lethal during midgestation suggesting that GPx4 enzymatic activity is vital at this embryonic stage [95, 96, 105]. The developing brain appears to be the dominant site for GPx4 expression in embryonic mice and rats and the suppression of expression leads to abnormal development of mid and hindbrain structures [104, 127].

During the development, one of the key functions of GPx4, namely its anti-apoptotic activity, seems to be the determining factor for GPx4 expression regulation. In developing embryos, GPx4 expression correlates with areas of reduced apoptosis in developing limbs [146]. Also, impaired GPx4 expression in developing embryos resulted in increased DNA fragmentation as an indicator of increased apoptotic cell death [104, 95]. These data suggest that the local and stage dependent expression of GPx4 during development is mainly determined by its anti-apoptotic function.

Mice carrying a targeted deletion of only the nuclear variant of GPx4 taking advantage of its unique promoter, do not show any lethality unlike the full knockout animals, ruling out any significant contribution of the nuclear form of GPx4 to mouse development. Besides their full viability, males were fully fertile without any morphological alterations in the sperms despite the high expression of nuclear form in the sperms [98].

The molecular mechanisms controlling the complex isoform-specific expression patterns of GPx4 in different tissues are not fully understood. Several promoter

sites and transcription factors revealing a complex network of functional interactions have been identified so far using mostly reporter gene assays and most of them are confirmed to be conserved between human and mice [144, 147, 148]. Main regulatory sites identified are illustrated in Figure 1.4.

In addition to transcriptional regulation, post-transcriptional modifications such as alternative splicing also play role in the regulation of GPx4 on the basis of different signaling stimuli or developmental stages [129, 149, 76, 150, 151].

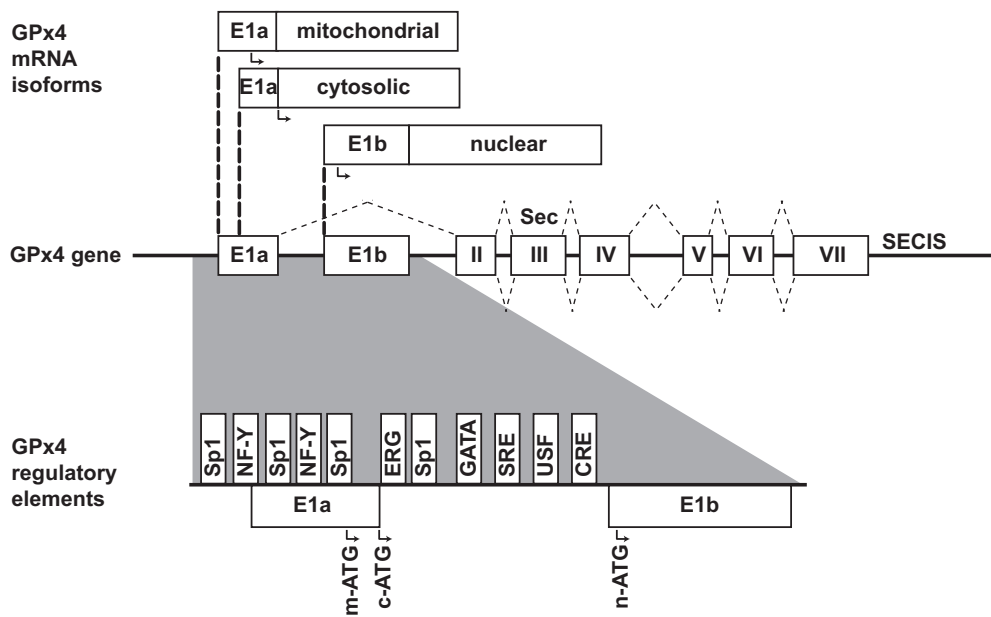


Figure 1.4: Structure of the GPx4 gene, encoding isoenzymes of GPx4. GPx4 gene is illustrated with the mRNA variants and the corresponding promoter regions. Important regulatory elements are shown with regard to the promoter regions.

1.2 Erythropoiesis

More than 5 liters of blood circulate in an average human adult body. Blood delivers immune cells to the potential sites of infection and contains platelets that can form a plug in a damaged blood vessel to prevent blood loss. Most importantly it carries oxygen and nutrients to living cells and takes away the waste products via erythrocytes [152].

Every second, 2-3 million red blood cell (RBC) are produced in the bone marrow (BM) and released into the circulation. They are the most common cell type in the blood (4-6 million cells in cubic millimeter blood). With a diameter of 6-8 μm , RBCs have the ability to squeeze in through the smallest blood vessels. They circulate around the body for up to 120 days in humans and 60 days in mice [153]. The old or damaged RBCs are removed from the circulation by macrophages in the spleen and liver [152]. The mature RBC lacks a nucleus, allowing the cell to store more hemoglobin, consequently enabling more oxygen transport [152].

The term erythropoiesis is used to describe the process of RBC formation or production, by which the hematopoietic stem cells differentiate into mature, non-nucleated erythrocytes (Figure 1.5). The process works via a physiological feedback loop through the hormone erythropoietin (EPO). EPO is produced mainly in the kidney in response to hypoxic stress. After its release into the circulation EPO binds to EPO receptors on the erythrocyte progenitor cells and stimulates the RBC production in BM. An increase in RBC mass, in turn, relieves the hypoxia and decreases EPO production [154, 155].

The EPO gene is known to consist of five exons, with important regulatory elements downstream of the gene. The critical element for the regulation of the EPO gene during hypoxia is the 3' enhancer that is the binding site for hypoxia-inducible factor 1 (HIF1) [156, 154]. Adaptation to hypoxia has a considerable clinical importance, as it influences the pathophysiology of common diseases such as anemia, polycythemia, tissue ischemia and cancer [157, 158, 154].

The rate of RBC production increases dramatically in response to clinical or physiologic stimuli that threaten tissue oxygenation, via enhanced proliferation of erythroid progenitors [159].

1.2.1 Anemia

Anemia is defined as a state in which the quality or quantity of circulating RBCs are below normal. Blood hemoglobin (Hb) concentration is used as a key indicator of anemia since it can be measured directly [160]. The degree of anemia may be scaled

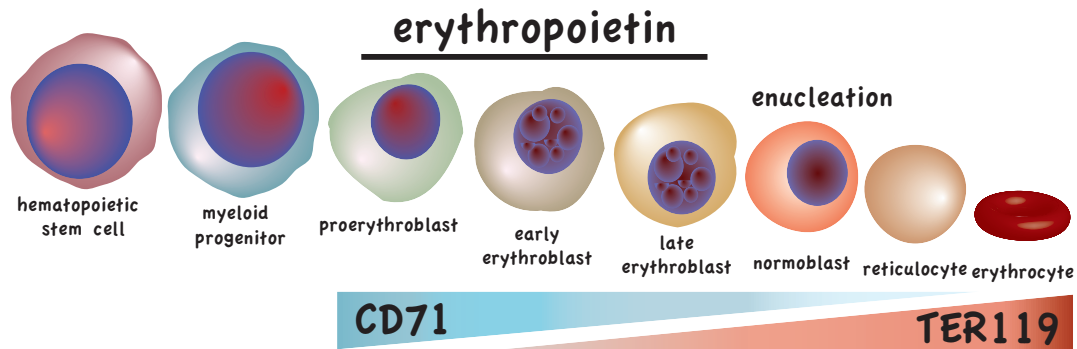


Figure 1.5: Erythropoiesis regulation. The development of erythrocytes in the bone marrow is regulated by the hormone erythropoietin that stimulates the differentiation of myeloid progenitor cells into erythroid precursors. Beginning with the proerythroblasts there are intermediate stages before the formation of enucleated reticulocytes. These cells are released into the circulation where they mature into functional erythrocytes. Before the maturation the cells express transferrin receptor CD71, which is important for the iron regulation. The maturation to erythrocytes results in loss of CD71 expression. TER119, which is associated with Glycophorin A, is a common marker for erythroid cells from the early erythroblasts to mature erythrocyte stages of development.

as mild, moderate, and severe anemia based on Hb levels. The National Cancer Institute and others have agreed on the following classification for anemia: mild, Hb 10 g/dL to normal limits; moderate, Hb 8.0 to 10.0 g/dL; severe, Hb 6.5 to 7.9 g/dL; and life-threatening, Hb less than 6.5 g/dL [160].

The body tries to counterbalance the effects of anemia by several mechanisms: first, the red cells of anemic patients generate increased amounts of phosphoglycerate, which leads to a decrease in oxygen affinity to Hb and increase in oxygen dissociation [160]. Second, increased cardiac output can compensate for the peripheral oxygen deficiency [160]. Also, the increase in the respiratory rate improves blood oxygenation [160]. In addition, blood is shifted from nonvital donor organs to oxygen-sensitive recipient organs such as muscle, heart, kidneys, and central nervous system [160]. Increased oxygen supply of vital organs also can be achieved by reduction of pH in tissues and capillary blood leading to more efficient unloading of

oxygen from Hb [160]. Furthermore; the rate of red cell production may increase as a response to compensatory EPO release [160].

Interestingly, GSH deficiency has been shown to cause a compensated hemolytic anaemia [161]. This phenotype is claimed to be related to the essential function of GSH in maintaining the cell membrane integrity.

Indicators of anemia in complete blood count

RBC RBC count shows the total number of RBCs in dL of blood. Low RBC count is the main indicator of anemia.

Hb The test measures the amount of Hb in blood and is a good indicator for the ability of blood to carry oxygen throughout the body. Low hemoglobin levels might indicate anemia. The average level for mice is 15.6-16.2 g/dL [162].

HCT Hematocrit (HCT) test, also called packed cell volume test, measures the amount of volume red blood cells take up in the blood. The value is given as a percentage of red blood cells in a volume of blood. The average normal levels for mice are between 48.1-51.1 % [162].

The normal values for wild type B6 mice of RBC, Hb, HCT and reticulocytes are listed in Table 1.1.

RBC indices (MCV, MCH and MCHC) There are three main red blood cell indices: mean corpuscular volume (MCV), mean corpuscular hemoglobin (MCH), and mean corpuscular hemoglobin concentration (MCHC). MCV shows the size of the red blood cells. MCH value is the amount of hemoglobin in an average red blood cell. MCHC measures the concentration of hemoglobin in an average red blood cell. These numbers help in the diagnosis of different types of anemia. Red cell distribution width (RDW) is another parameter that can be used for diagnosis. This shows whether the cells differ in size or shape. The average normal levels for mice are: MCV, 47.6-48.4 fL, MCH, 15.6-16.0 pg and MCHC, 32.6-33.1 g/dL [162].

Table 1.1: Blood count values for C57BL/6J mice

	Female		Male	
	Mean	SD	Mean	SD
RBC ($10^6/\mu\text{L}$)	10.2	± 0.584	10.3	± 0.548
Hb (g/dL)	16	± 1.22	16	± 1.21
HCT (%)	49.8	± 3.99	50.3	± 3.68
Ret ($10^9/\text{L}$)	449	± 272	427	± 120

Data from <http://phenome.jax.org>.

1.2.2 Role of ROS in RBC development and anemia

Recent evidence suggests that oxidative stress contributes significantly to the regulation of hematopoietic cell homeostasis. Especially the RBC and hematopoietic stem cells are highly sensitive to ROS accumulation. Potential DNA damage due to ROS accumulation causes alterations in hematopoietic stem cell cycle. These abnormalities may lead to accelerated aging of hematopoietic stem cells or to hematopoietic malignancies [163]. In erythrocytes, imbalanced ROS accumulation often leads to hemolysis and shortened life span [163].

Regulation of oxidative stress is particularly important to erythropoiesis [163]. Erythroid precursors synthesize and accumulate hemoglobin as they mature. In addition, insertion of iron to heme in mitochondria of erythroid precursors requires oxidation reactions [163, 164]. In most cells, the major source of ROS is the mitochondrion [165]. However in mature red cells, lacking mitochondria, the major source of ROS is the oxygen carrier protein Hb, which undergoes autoxidation to produce superoxide [164]. Circulating erythrocytes are highly prone to oxidative damage since they carry oxygen bound to hemoglobin and for this reason ROS regulation in RBCs has particular importance.

It has been shown in several studies that compromised protection from ROS, for instance due to enzymatic deficiencies in intracellular reductive molecules or in molecules that protect globin, results in diseases of RBCs, associated mainly with shortened life span and with hemolysis, leading to anemia [166, 167, 168, 169]. In

some cases increased proliferation and differentiation of erythroid progenitors can compensate for the loss of erythroid cells and might lead to splenomegaly. In order to avoid such anomalies, erythroid cells rely on several antioxidant enzymes that protect the cells against oxygen radicals such as GPx1, as proved to be important using a deficient mouse model by Johnson *et al.* [163, 170]. Additional studies showed that several antioxidant mechanisms are involved in the homeostasis of erythrocytes such as; superoxide dismutases, catalase and glutathione peroxidases, and nonenzymatic scavengers such as glutathione, Prx, ascorbic acid, and carotenoids [171, 172, 173, 174, 175, 166].

1.3 Mechanisms of cell death

Cell death is a fundamental cellular response that has a crucial role in tissue homeostasis by eliminating unwanted cells. Programmed cell death is the general name of genetically regulated cell death. In addition to apoptosis, autophagic cell death and necroptosis are also categorized as the alternative mechanisms of cell death. Moreover, there are some other mechanisms that are distinct from the typical forms, such as; epidermis specific cornification, mitotic catastrophe occurring after a failed mitosis, anoikis-associated cell death due to loss of the attachment, poly ADP-ribose polymerase (PARP)1 and AIF dependent parthanatos, caspase-1 dependent pyroptosis and caspase 1 independent pyronecrosis [176, 177]. Recently, ferroptotic death is defined as a morphologically, biochemically, and genetically distinct mechanism of cell death, which is based on the iron-dependent, oxidative death [178]. Different forms of cell death are summarized in Table 1.2.

1.3.1 Apoptosis

Apoptosis is the first described form of regulated cell death based on some principle morphological features [179]. Key features of apoptosis include cleavage of cytoskeletal proteins by proteases, reduction of cellular volume, chromatin condensation, nuclear fragmentation, and the formation of plasma-membrane blebs. Unlike necrosis, plasma membrane integrity is preserved until late in the process of apoptosis

Table 1.2: Features of different forms of programmed cell death

	Apoptosis	Non-Apoptotic		
Morphology	Cell blebbing Chromatin condensation Cell shrinkage	Autophagosomes Autolysosomes	Organelle swollen Early cytoplasmic membrane rupture	
Biochemical features	Caspase activation	mTOR suppression Atg activation	TNFR1 activation	PARP activation ATP depletion HMGB1 release
Key organelles	Mitochondria	Lysosomes Autophagosomes	Cell membrane	Nuclei
Key Regulators	Caspases Bcl-2 family	Atgs mTOR III PtdIns3K	RIP1 RIP3 JNK	PARP AMPK
Main inducers	Cell death ligands DNA damage agents	Starvation mTOR inhibitors	Cell death ligands	DNA damage agents
Chemical inhibitors	Caspase inhibitors	Wortmannin 3-MA Chloroquine	necrostatin	PARP inhibitors

[180, 176].

Several pathways have been identified in the regulation of apoptotic cell death. The two major pathways are death receptor mediated signaling and mitochondria mediated signaling (also called intrinsic pathway). Binding of death ligands such as TNF, FASL (also known as CD95L) or TNF-related apoptosis-inducing ligand (TRAIL) to the death receptors (TNF receptor family) recruits the adaptor protein FAS-associated death domain (FADD). FADD in turn recruits caspase 8, which ultimately activates caspase-3 as the executioner of apoptosis [181, 182, 183, 180].

Interplay between proapoptotic and antiapoptotic members of the pro-apoptotic B cell lymphoma 2 (Bcl2) family controls the mitochondrial apoptotic pathway [184]. Initiators of the pathway include intracellular reactive oxygen species, DNA damage and the unfolded protein response. The basic mitochondrial pathway of apoptosis in vertebrates begins with the permeabilization of the mitochondrial outer membrane by proapoptotic members of the Bcl2 family, resulting in a release of proteins such as cytochrome c from the mitochondria to cytosol [185, 186]. Cytochrome c release triggers recruitment of caspase-9 to form the apoptosome. Activated caspase-9 then cleaves and activates the executioner caspases [187, 188, 189].

The inability of caspase inhibitors to completely protect cells from death lead researchers to identify caspase-independent programmed cell death mechanisms.

1.3.2 Autophagy

Autophagy (from Greek, self-eating) is a highly regulated cellular process that mediates the degradation of intracellular components, single macromolecules and organelles inside lysosomes [190, 191]. Autophagy was first described by Christian de Duve in 1963 as a lysosome-mediated degradation process for non-essential or damaged cellular elements [192, 193, 194]. Physiologically, it preserves the balance between organelle biogenesis, protein synthesis and their clearance [195].

There are three classes of autophagy described based on how protein substrates are localized to the lysosome for degradation:

Macroautophagy Macroautophagy (generally referred to as autophagy) is a multi-step process, involving the formation of double-membrane vesicles known as autophagosomes. Autophagosomes mature and fuse with lysosomes to degrade their contents in the acidic environment mediated by acidic hydrolases. More than 30 autophagy proteins (Atgs), which are conserved from yeast to mammals, participate in autophagy at different steps throughout the process [196, 197].

Microautophagy Microautophagy is a process in which lysosomes directly wrap around cytosolic constituents and ingest cargo by membrane involution [198, 199, 200].

Chaperone-mediated autophagy Chaperone-mediated autophagy (CMA) targets chaperones to proteins that contain a motif biochemically related to the pentapeptide KFERQ. The chaperone/protein complex then binds to lysosome-associated membrane protein-2A (LAMP-2A) receptors on the lysosomal membrane, and translocates the target proteins into the lysosomes for degradation [201, 202].

The data from the mouse studies revealed Atg5, Atg7 and beclin-1 as essential elements for autophagy. Autophagy starts with the stepwise engulfment of cytoplas-

mic material by the phagophore, which sequesters material in double-membraned vesicles named autophagosomes or autophagic vacuoles. In most cases, the first regulatory process involves the mTOR kinase, which inhibits autophagy by phosphorylating Atg13. This phosphorylation attenuates the Atg1 kinase activity upon dissociation of Atg13 from Atg1 and Atg17. When mTOR is inhibited, reassociation of dephosphorylated Atg13 with Atg1 stimulates its catalytic activity and induces autophagy.

Vesicle nucleation involves the activation of mammalian Vps34, class III phosphatidylinositol 3 kinase (PI3K). Vps34 activation depends on the formation of a multiprotein complex, which includes beclin-1.

Vesicle elongation process is regulated by two ubiquitin-like conjugation systems. One pathway involves the covalent conjugation of Atg12 to Atg5 with the help of the E1-like enzyme Atg7 and the E2-like enzyme Atg10. The second pathway involves the conjugation of phosphatidylethanolamine to LC3 (Atg8 homolog) by the sequential action of the protease Atg4, the E1-like enzyme Atg7 and the E2-like enzyme Atg3. Lipid conjugation leads to the conversion of the soluble form of LC3 (LC3-I) to the autophagic-vesicle-associated form (LC3-II). Autophagosomes undergo maturation by fusion with lysosomes to create autolysosomes. In the autolysosomes, the inner membrane as well as the luminal content of the autophagic vacuoles are degraded by lysosomal enzymes acting exclusively in this acidic compartment [196, 190, 191]. Schematic illustration of regulation of autophagy is shown in Figure 1.6.

Defining the stages of autophagy and its progress in a tissue or cell is important for understanding its function and regulation. There are several methods for the detection and analysis of autophagy. Ultrastructural analysis by Electron microscopy (EM) of autophagosomes is one of the most classical approaches for the detection of autophagy based on its unique morphological characteristics [196, 193]. Another widely used tool for detection of autophagy is monitoring the post-translational modifications of LC3. LC3-I and LC3-II can be distinguished by their difference in mobility on gel electrophoresis. LC3-II insertion into the autophagosomal membrane is a consistent key step in autophagosomal formation, and its level reflects the

relative amount of autophagosomes in the cell [203, 196, 204].

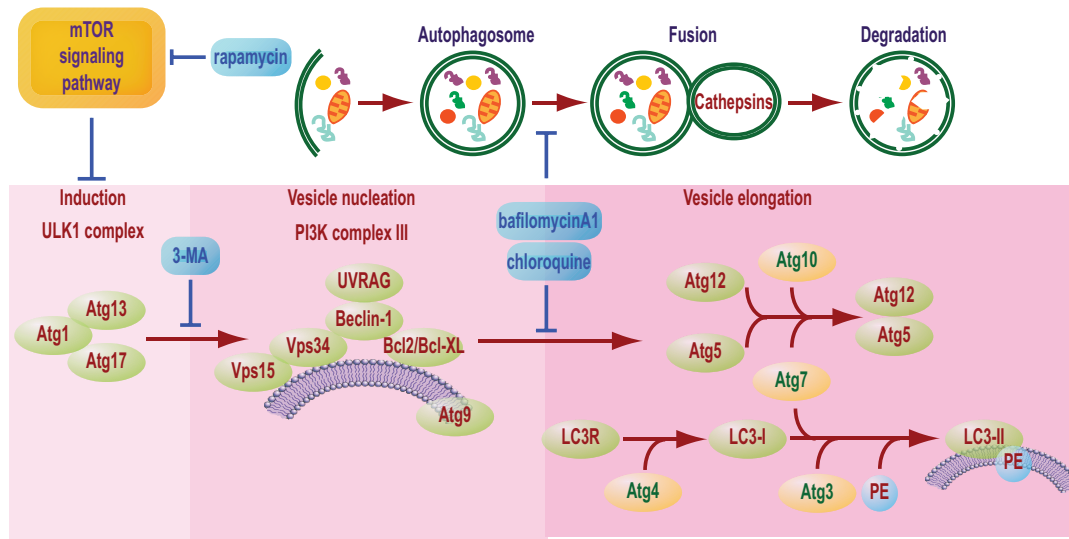


Figure 1.6: Molecular mechanisms of autophagy. Autophagy starts with the engulfment of cytoplasmic material by the phagophore, which sequesters material in double-membraned vesicles named autophagosomes. The first regulatory process involves the mTOR signaling, which inhibits autophagy by phosphorylating Atg13. This phosphorylation leads to the dissociation of Atg13 from a protein complex that contains Atg1 kinase and Atg17, and thus attenuates the Atg1 kinase activity. When mTOR is inhibited, reassociation of dephosphorylated Atg13 with Atg1 stimulates autophagy. Among the initial steps of vesicle nucleation is the activation of mammalian Vps34, a class III PI3K. Vps34 activation depends on the formation of a multiprotein complex in which beclin-1, UVRAG, Vps15. Bcl2 and Bcl-XL act as main regulators. Two ubiquitin-like conjugation systems are part of the vesicle elongation process. One pathway involves the covalent conjugation of Atg12 to Atg5, with the help of the E1-like enzyme Atg7 and the E2-like enzyme Atg10. The second pathway involves the conjugation of PE to LC3 by the sequential action of the protease Atg4, the E1-like enzyme Atg7 and the E2-like enzyme Atg3, leading to the conversion of the soluble form of LC3 (LC3-I) to the autophagic vesicle associated form (LC3-II). Autophagosomes undergo maturation by fusion with lysosomes to create autolysosomes. In the autolysosomes, the inner membrane as well as the luminal content of the autophagic vacuoles are degraded by lysosomal enzymes that act optimally within this acidic compartment.

Under basal cellular conditions, the balance between protein synthesis and degradation contributes to the maintenance of cellular homeostasis and guarantees continuous renewal of proteome and organelles [205]. Failure of the autophagic system results in marked accumulation of abnormal proteins and defective organelles, which

leads to functional failure, and often to cell death [190]. Autophagy is also essential for cellular adaptation to environmental changes and in the cellular response to extracellular and intracellular stressors, which explains its involvement in processes such as cellular growth, differentiation, development, and host defense.

Among various biological functions of autophagy, its dual role in cell death and cell survival is subjected to further investigation. On one hand, autophagy has been described as an important cell survival mechanism, especially in cells under stress conditions [206, 207]. On the other hand, it can lead to the cell death in which autophagy itself serves as the executor of the cell death machinery [208]. So far, although autophagic cell death and its physiological relevance in development have mainly been established in lower eukaryotes and invertebrates such as *Dictyostelium discoideum* and *Drosophila melanogaster*, it has never been shown to be the cause of death in mammalian cells under physiologically relevant conditions [208, 191].

ROS and autophagy

Current findings implicate ROS in the regulation of autophagy through a variety of stimulating factors depending on cell types [209, 210, 211, 212]. Conversely, autophagy can also suppress ROS accumulation. The crosstalk between autophagy, redox signaling and ROS is not well understood. It is suggested that accumulation of toxic proteins and the decrease in mitochondrial function lead to further oxidative stress when the autophagic process is disrupted [213, 195]. Dysregulated redox signaling or mitochondrial dysfunction can also influence autophagic activities mainly through ROS accumulation and the substantial by-products [195].

Under oxidative stress, large amounts of ROS oxidize proteins and alter their functions. These oxidized proteins may form aggregates and become toxic to cells. Autophagy is an effective mechanism for degradation of these oxidized proteins [214, 215, 216]. CMA has been shown to degrade oxidized protein substrates [214]. Oxidative stress is also shown to induce autophagy-mediated degradation of oxidized proteins in *Arabidopsis* [216].

1.3.3 Necroptosis

Necroptosis refers to a specific form of caspase-independent, non-apoptotic or necrotic cell death that is mediated by cell death ligands tumor necrosis factor α (TNF α), FasL (CD95) and TRAIL via cell death receptors and a unique downstream signaling pathway through the activity of the kinases receptor-interacting protein 1 (RIP1) and receptor-interacting protein 3 (RIP3) [217, 218, 219]. It was first described in murine fibrosarcoma L929 cells treated with TNF α [220] and subsequently found in many other cell types [221, 219]. The schematic illustration of the execution of the pathway is shown in Figure 1.7.

Upon ligand binding, TNFR1 undergoes a conformational change that allows the cytosolic portion of the receptor to recruit TNFR complex I, which includes TRADD, RIP1, cIAPs, TRAF2 and TRAF5. cIAP-mediated ubiquitylation of RIP1 leads to recruitment of transforming growth factor β activated kinase 1 (TAK1), TAK1-binding proteins TAB2 and TAB3, which activate the canonical NF κ B pathway. Conversely, deubiquitylation of RIP1 triggers caspase dependent or caspase independent cell death. Normally, caspase 8 triggers apoptosis by activating the classical caspase cascade. It also cleaves, and hence inactivates, RIP1 and RIP3. If caspase 8 is inhibited, phosphorylation of RIP1 and RIP3 results in necroptosis (Figure 1.7).

After the first description and designation of the name necroptosis by Degretev *et al.* to the particular type of programmed necrosis [222], it was characterized as a unique pathway of cell death that depends on the activity of the kinases RIP1 [223] and RIP3 [224, 225, 226]. So far, the described mechanisms of necroptosis requires TNFR1 signaling upon binding of cell death ligands TNF α , FasL and TRAIL and a unique downstream pathway that involves the activation of RIP1/RIP3 in the case where caspases are inhibited or cannot be activated effectively [224, 219]. caspase 8 plays a critical role in modulating the molecular switch between apoptosis or necroptosis in response to TNFR1 activation [227, 228].

To date, several molecules and pathways have been implicated as effectors of

necroptosis including; PARP1 [229], AIF [230], ROS [231, 232], NADPH oxidase 1 (NOX1) [233], pro-apoptotic Bcl2 family members [234] and many others.

Identification of a potent small-molecule inhibitor of necroptosis, necrostatin 1 (nec-1), which targets RIP1, provided an important tool for the study of necroptosis [222, 235]. Nec-1 is a small molecule that allosterically blocks the kinase activity of RIP1. It inhibits necroptosis without affecting RIP1-mediated activation of NF κ B, mitogen-activated protein kinase p38 and JNK1.

The study by Xu *et al.* in HT-22 cells suggest that glutamate-induced glutathione depletion leads to necroptotic cell death based on its inhibition with nec-1 [236].

ROS and necroptosis

Mitochondrial energy metabolism was linked to execution of necrosis first in the early 1990s in L929 cells [231]. Mitochondrial ROS production as well as generation of lipid peroxides were shown to be essential prerequisites for execution of most cases of TNF-dependent necrosis [221, 219]. Although ROS production is not essential for all instances of TNF-induced necrosis, the kinase activity of RIP may link TNFR1 signaling, mitochondrial bioenergetics and ROS production [224, 219]. Non-mitochondrial ROS production by the plasma membrane NADPH oxidase NOX1 also contributes to TNF-induced necrotic cell death [233]. TNF can stimulate ROS formation by favoring JNK1-dependent degradation of the ubiquitous iron-binding protein ferritin leading to an increase in redox-active iron [237]. To date, ROS are identified as downstream mediators of TNF-induced necroptosis.

Recently, GPx family was identified as an effector in genome-wide siRNA screen for regulators of necroptosis together with several other gene sets however the exact mechanism of their involvement is not known [234]. Recently identified cell death mechanism, ferroptosis is characterized by oncogenic RAS-selective lethal small molecule erastin triggered iron-dependent cell death [178]. Despite its similarities with necroptosis, the failure of its inhibition with nec-1 led to the distinction of this pathway.

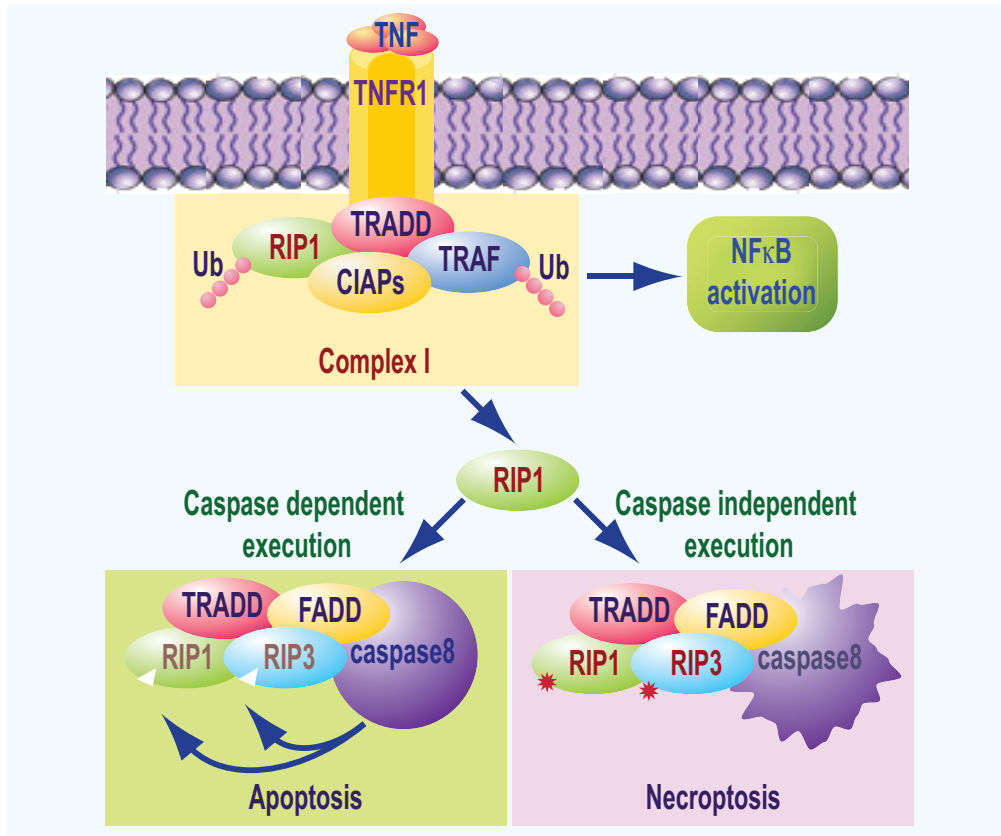


Figure 1.7: TNFR1 elicited signaling pathways. Upon TNF binding, TNFR1 undergoes a conformational change, allowing for the intracellular assembly of the TNFR complex I, which includes TRADD, RIP1, cIAPs, TRAF2 and TRAF5. cIAP-mediated ubiquitylation of RIP1 leads to activation of canonical NF κ B pathway. Conversely, deubiquitylation of RIP1 exerts lethal functions, which can be executed by two distinct types of cell death; caspase dependent or caspase independent. The internalization of TNFR1 is accompanied by a change in its binding partners that leads to the cytosolic assembly the complex, consisting of TRADD, FADD, caspase 8, RIP1 and RIP3. Normally, caspase 8 triggers apoptosis by activating the classical caspase cascade. It also cleaves, and hence inactivates, RIP1 and RIP3. If caspase 8 is inhibited, phosphorylated RIP1 and RIP3 engage the effector mechanisms of necroptosis.

Chapter 2

Materials and Methods

2.1 Materials

2.1.1 Mouse models

Mx1 Cre

The Cre recombinase is expressed under the control of the Mx1 promoter, an interferon-responsive promoter silent in healthy mice, but can be induced to high levels of transcription by administration of interferon alpha, interferon beta, or synthetic double-stranded RNA [238].

Rosa26-CreER^{T2}

A knock-in mouse line harboring the CreER^{T2} coding region under the control of the ROSA26 locus was created [239]. Cre recombinase expression is induced by tamoxifen administration. Analysis revealed ubiquitous recombination in the embryo and efficient recombination in peripheral and hematopoietic tissues.

GPx4^{fl/fl}

Mice harboring a loxP flanked (floxed, fl) GPx4 allele were achieved by loxP sites inserted to exons 5 to 7 of the gene [103]. Flp-mediated removal of the neo gene was achieved by breeding floxed GPx4 mice with mice expressing Flp recombinase. Germline transmissions of the loxP flanked GPx4 allele in mice allow conditional knock-out in the presence of Cre recombinase.

12/15-lipoxygenase knockout mice

Insertion of neomycin resistance cassettes with the help of a targeting vector constructed from genomic fragment containing exons 1-8 with the disruption of exon 3 led to 12/15-Lox deficient mice (strain name: B6.129S2-Alox15tm1Fun/J) [240].

Atg7^{fl/fl}

Atg7 conditional knockout mice were obtained via the targeting vector designed to conditionally disrupt exon 14, which is encoding the essential residue for activation of the substrates, by Cre-loxP technology [241].

RIP3-deficient mice

Exons 1 to 3, encoding amino acids 1 to 158 of mouse RIP3, were replaced with a PGK-neo selection cassette flanked by loxP sites and obtained ES cell clones with a disrupted allele were injected into blastocysts to generate chimeric mice [242].

2.1.2 Chemicals, solutions and equipment

For the detailed list of chemicals and reagents that have been used, refer to Appendix A.1, A.2.

2.2 Methods

2.2.1 Animal experiments

Animal facility

All mice were grown and treated in a pathogen free animal facility according to German national and EU regulations.

Genotyping

For the genotyping primers and protocols refer to Appendix A.4.

Induction of Mx1 promoter

Mx1 promoter was induced by a single i.p. injection of 250 μ l 1 mg/ml polyinosinic: polycytidylic acid (poly I:C) dissolved in PBS.

Blood withdrawal and blood count

For blood count or flow cytometry analysis, blood was collected from the facial vein. The mouse was anesthetized with isoflurane, the facial vein above the freckle was pricked with a lancet and the blood was collected in a 1.2 ml K₂EDTA blood collection tube (Sarstedt).

For the complete blood count, the blood collected in EDTA was diluted 1:3-1:4 and analyzed with Sysmex XT-2000i using the complete blood count differential with reticulocytes (CBC-Ret) protocol.

Serum separation

For serum analysis blood was collected directly in microcentrifuge tubes without EDTA, incubated 20 minutes at room temperature (RT) for complete clotting and centrifuged 10 minutes at 2000 g. The serum was transferred to a clean tube and stored at -20°C.

Biotin labeling to determine the survival of peripheral erythrocytes and reticulocytes

To determine the survival of erythrocytes and reticulocytes, the cells were labeled with biotin [243]. For biotin labeling experiments mice were injected daily for 3 days with biotin-nhs (1mg/day i.v.; Calbiochem, 203118) starting on the day of poly I:C administration (day 0). 100 μ l blood was collected weekly starting from day 0 and subjected for flow cytometry analysis.

Bone marrow transplantation

Preparation of the bone marrow: After sacrificing the mice, the bone marrow from femur and tibia was flushed with sterile PBS (Invitrogen) using a 25 G needle, under sterile conditions. The cells were homogenized by pipetting and passed

through a 100 μm cell strainer. The whole marrow was subjected to MACS (Miltenyi) purification according to the manufacturers' instructions for the separation of the T cells, using FITC-anti-CD3 antibody (eBiosciences) and anti-FITC magnetic beads (Miltenyi). The CD3 negative cells were dissolved in PBS at a density of 10^7 cells/ml.

Irradiation and transplantation: The recipient mice were subjected to whole body γ -irradiation of 9 Gy and injected i.v. with $1-2 \times 10^6$ cells. The transplanted animals were kept on broad spectrum antibiotic water (1.4 mg/ml Ciprobay (Bayer)) for two weeks.

2.2.2 Cell isolation and primary cell culture

Isolation of splenocytes

After sacrificing the animals, the spleen was removed using sterile forceps and scissors and placed into a petri dish in sterile PBS. The spleen was homogenized in between two glass slides. The cell suspension was homogenized better by pipetting for complete dissociation and was passed through a 100 μm cell strainer. The cells were centrifuged at 800 g for 5 minutes and resuspended in appropriate buffer.

Isolation of bone marrow cells

After sacrificing the mice, the bone marrow from femur and tibia was flushed with sterile PBS (Invitrogen) using 25 G needle, under sterile conditions. The cells were homogenized by pipetting, passed through a 100 μm cell strainer, centrifuged at 800 g for 5 minutes and resuspended in appropriate buffer.

2.2.3 Colony formation assay

Bone marrow cells were cultured in methylcellulose semisolid media with or without α -tocopherol, nec-1 and nec-1i. O-dianisidine-positive erythroid colonies were counted after 6-8 days.

2.2.4 Culture experiments of fibroblasts

Primary mouse embryonic fibroblasts with floxed GPx4 alleles were isolated from conditional GPx4 knockout embryos at E12.5 [103]. Cells were stably transfected with MERCreMER (MER, mutated-estrogen receptor). MERCreMER is retained in the cytosol by forming a complex with heat-shock protein 90 [244]. Only upon addition of 4-Hydroxytamoxifen (4-OHT) to the culture medium MERCreMER is released from the inhibitory complex and translocates to the nucleus where Cre-mediated recombination takes place.

The fibroblasts were cultured under standard conditions in Dulbecco's modified Eagle's medium (DMEM, GIBCO) supplemented with 10% FCS (Biochrom) and 1% penicillin/streptomycin (GIBCO). Deletion of GPx4 was induced with 1 μ M 4-OHT (Sigma) in 70% ethanol at a cell density of 2500 cells/cm². Refer to Appendix A.1 for the detailed list of reagents used.

Cell counts

The cells were harvested with Trypsin/EDTA and counted with a hemacytometer in the presence of 1% trypan blue. Trypan blue negative cells were considered as viable cells.

siRNA mediated transfection

siRNA smart pools were purchased from Thermo Scientific Dharmacon (for detailed information refer to Appendix A.3). Fibroblasts were seeded at 40% density 16 hours before transfection and starved for 2 hours before the transfection in OPTI-MEM (GIBCO). The transfection was performed using lipofectamine (Invitrogen) in the presence of 200 μ M siRNA and the cells were kept in transfection medium (OPTI-MEM+Lipofectamine+siRNA) for 4 hours. The medium was changed to DMEM/10%FCS/ 1% penicillin/streptomycin and the GPx4 deletion was induced 24 hours after the transfection.

Inhibitor treatments

All inhibitors were applied at the time of 4-OHT application. Nec-1 and inactive compound (Calbiochem) were dissolved in DMSO and used at 2.5-25 μ M. Human recombinant TNF α (R&D systems) was used at 100 ng/ml, TAK1 inhibitor 5Z-7-Oxozeaenol (Sigma) was used at 1 μ M, caspase inhibitor 1 (zVAD) (Calbiochem) was used at 10 μ M, TNF antagonist enbrel was used at 10 nM-1 μ M, PARP inhibitor Olaparib (Selleckchem) was used at 50 nM concentration.

2.2.5 Flow cytometry

Surface marker staining

For flow cytometry analysis the cells were washed with FACS buffer (2% FCS/2 mM EDTA/PBS). Before the surface marker stainings, the cells were blocked for unspecific binding for 10 minutes with CD16/CD32 blocking antibody (BDbiosciences) diluted in FACS buffer 1:100. The cells were washed twice with FACS buffer with centrifugation at 1500 rpm for 5 minutes. The cells were stained with the fluorophore conjugated antibodies (0.1-0.2 μ g/ 10^6 cells). The cells were washed twice with PBS and used directly for flow cytometry analysis. In the case where promidium iodide (PI) staining was done, PI was added directly on the cells just before counting. For the detailed list of antibodies used for flow cytometry analysis please refer to Appendix A.2.1.

Measurement of ROS accumulation

Redox sensitive fluorescent probe 5-6- chloromethyl-2',7'- dichlorodihydrofluorescein diacetate, acetyl ester, CM-H₂DCFDA (DCF) (Invitrogen) was used to measure the cellular ROS. 10^6 cells were labeled for 30 minutes at 37°C with 1 μ M DCF in 50 μ l RPMI. For the H₂O₂ treated cells the medium contained 100 nM H₂O₂. After the incubation, the cells were washed with FACS buffer and stained for appropriate surface markers and PI as described in Section 2.2.5.

Measurement of lipid peroxidation

Cellular lipid peroxidation was detected via BODIPY 581/591 C11 (BODIPY). 10^6 cells were incubated with $2 \mu\text{M}$ BODIPY for 60 minutes at 37°C in $100 \mu\text{l}$ RPMI. After the incubation, the cells were washed with FACS buffer and stained for appropriate surface markers and PI as described in Section 2.2.5.

Annexin V staining

After surface marker staining (Section 2.2.5), the cells were resuspended in Annexin V buffer containing Annexin V antibody. The cells were subjected to flow cytometry after 15 minutes of incubation at room temperature.

BrdU incorporation analysis

Mice were injected i.p. with BrdU solution (100 mg/kg) in sterile PBS (APC BrdU Flow Kit, BDPharmingen) 2 hours prior to sacrifice. Splenocytes were isolated as described in Section 2.2.2. The cells were stained for surface markers as described in Section 2.2.5. BrdU staining was performed according to the manufacturer's instructions. In summary; the cells were fixed and permeabilized with BD Cytotfix/Cytoperm Buffer, treated with $300 \mu\text{g/ml}$ DNase for 1 hour at 37°C to expose incorporated BrdU, stained with a fluorescent antibody against BrdU and subjected to flow cytometry analysis.

Reticulocyte maturation analysis

Reticulocyte maturation was monitored by staining total peripheral blood cells with $\alpha\text{-CD71}$, $\alpha\text{-TER119}$, the DNA-binding dye thiazol orange ($2 \mu\text{g/ml}$) (Biomol) and Mitotracker Deep Red (Invitrogen) that stains mitochondria.

Flow cytometry analysis

The cells were counted with FACScalibur (BDbiosciences) or with Galios flow cytometer (Beckman Coulter) and the data was analyzed using the analysis software FlowJo.

2.2.6 Histology

Tissue preparation

After sacrificing the animals, the tissues were collected and fixed overnight in 4% paraformaldehyde (PFA) at 4°C. The following day, fixed samples were dehydrated in Leica dehydrator using the program in Table 2.1. After dehydration the tissues were embedded in paraffin and stored at RT. For the histological stainings, 2-4 μm sections were cut with a microtome and fixed on glass slides. Just before the histological stainings, the sections were deparaffinized and rehydrated using the protocol described in Table 2.2.

Table 2.1: Tissue dehydration program

Reagent	Time (minutes)
70% ethanol	45
86% ethanol	45
96% ethanol	45
96% ethanol	60
100% ethanol	60
100% ethanol	60
100% ethanol	60
xylene	45
xylene	70
xylene	75
paraffin wax	60
paraffin wax	60
paraffin wax	60

Immunohistochemistry

For immunohistochemistry stainings, after the sections were deparaffinized and rehydrated (Table 2.2) two different permeabilization protocols were followed: for surface marker stainings the tissues were incubated in 0.3% Triton/PBS 10-20 minutes at RT and for all nuclear or cytoplasmic stainings the sections were microwaved in antigen unmasking solution (VectorLab) for 20 minutes, cooled down to RT and washed with

Table 2.2: Deparaffinization and rehydration protocol

Reagent	Time (minutes)
xylene	5
xylene	5
100% ethanol	2
100% ethanol	2
96% ethanol	2
96% ethanol	2
80% ethanol	2
80% ethanol	2
70% ethanol	2
70% ethanol	2
50% ethanol	2
50% ethanol	2
PBS	5

Table 2.3: Section dehydration protocol

Reagent	Time (minutes)
50% ethanol	2
70% ethanol	2
80% ethanol	2
96% ethanol	2
100% ethanol	2
xylene	5
xylene	5

PBS. In order to block endogeneous peroxidases the sections were incubated in 3% H₂O₂/PBS solution for 5 minutes. To avoid unspecific binding of the antibody the sections were blocked with 3% BSA/PBS+streaptavidin (VectorLab) for 30 minutes at RT. After blocking, the primary antibody was applied in 3% BSA/PBS+biotin (VectorLab) in variable conditions (Appendix A.2.3). The sections were intensively washed with PBS for 15-30 minutes and incubated with the appropriate biotin conjugated secondary antibody for 30 minutes at RT. After being washed twice with PBS for 5 minutes each, the slides were incubated for 30 minutes at RT with ABC complex containing avidin DH and biotinylated horseradish peroxidase H reagents (VectorLab). For the color reaction DAB kit (VectorLab) was used that consist of 3,3'-diaminobenzidine, the reaction buffer and peroxide, all mixed fresh just before starting the reaction. The reaction was stopped with distilled water after the visualization of the color reaction under microscope. The sections were stained with hematoxylin for 1 minute for counter staining. After washing 3 times with distilled water the sections were dehydrated according to the protocol in Table 2.3, air dried completely and covered with mounting medium (VectorLab) and a cover slide.

Immunohistofluorescence

For immunofluorescent stainings, after the sections were deparaffinized and rehydrated (Table 2.2) two different permeabilization protocols were followed: for surface marker stainings the tissues were incubated in 0.3% Triton/PBS 10-20 minutes at RT and for all nuclear or cytoplasmic stainings the sections were microwaved in antigen unmasking solution (VectorLab) for 20 minutes, cooled down to RT and washed with PBS. To avoid unspecific binding of the antibody the sections were blocked with 3% BSA/PBS for 30 minutes at RT. After blocking, the primary antibody was applied in 3% BSA/PBS in variable conditions (Appendix A.2.3). In some cases fluorophore-conjugated primary antibodies were used and in other cases, the sections were intensively washed with PBS for 15-30 minutes and incubated with the appropriate fluorophore-conjugated secondary antibodies for 30 minutes at RT. After being washed twice with PBS, the sections were shortly dried and covered with DAPI con-

taining conservation medium (ProLong Gold, Invitrogen) enabling counter staining of the cell nucleus via binding with the DNA. The sections were either directly used for imaging or stored at 4°C in dark.

TUNEL assay

TdT-mediated dUTP-biotin nick end labeling (TUNEL) assay was used to label apoptotic cells. The staining was carried out with the commercial kit ApoAlert DNA-Fragmentation Assay (Clontech) using the protocol for PFA-fixed, paraffin embedded samples. After the sections were deparaffinized and rehydrated (Table 2.2), they were incubated with 0.85% NaCl solution for 5 minutes at RT. The sections were washed with PBS twice and fixed with 4%PFA/PBS for 15 minutes at RT. The washing step was repeated and the sections were permeabilized in 20 $\mu\text{g}/\text{ml}$ proteinase K/PBS. After washing again the sections were equilibrated in equilibration buffer for 15 minutes at RT just before the reaction mixture was applied. The reaction was carried out in a reaction mixture containing; 30 μl equilibration buffer, 3 μl nucleotide mix, 0.33 μl TdT enzyme per section at 37°C in dark for 60 minutes. The reaction was terminated by 15 minutes incubation in 2X SSC buffer. The sections were rinsed with PBS and covered with DAPI containing conservation medium (ProLong Gold, Invitrogen) and coverslide. The sections were either directly used for imaging or stored at 4°C in dark.

2.2.7 RNA analysis

RNA isolation

RNA isolation was performed using RNeasy Mini Kit (Qiagen) in an RNase free environment. The cells were directly lysed in RTL buffer including 1% β - mercaptoethanol via pipetting vigorously and tissues using tissue homogenizer. For complete homogenization the lysate was applied to Qiasredder column (Qiagen). The rest of the protocol was carried out according to the manufacturers' instructions and the RNA was eluted with 20-50 μl RNase free water. The concentration and purity of RNA was determined and the RNA was either directly used for cDNA synthesis or

stored at -80°C.

cDNA synthesis

1-3 μg RNA was subjected to reverse transcription. The reaction was performed in a final volume of 15-20 μl . First, the 1 μg RNA, 2.5 μM OligodT (Invitrogen) and 0.5mM dNTP-mix (Invitrogen) were incubated at 65°C for 5 minutes for denaturation. The mixture was cooled down on ice for 2 minutes and mixed with 1X reaction buffer (Invitrogen), 5 mM dithiothreitol (DTT), 0.5 U RNaseOUT (Invitrogen) and 10 U Superscript II reverse transcriptase (Invitrogen) per 1 μg of RNA. The reaction was performed for 60 minutes at 50°C. The reaction was stopped by 1:4-1:10 dilution with distilled water and the cDNA was stored at -20°C.

Quantitative PCR

For quantitative PCR analysis gene specific primers were designed for the gene of interest (Table 2.5). For the reaction mix in a total volume of 20 μl , 0.5-1 μl of cDNA, 1X SYBR-Green MasterMix, 2 mM forward primer and 2 mM reverse primer were used. The reaction was carried out in StepOnePlus Real Time PCR system (Applied Biosystems) using the conditions in Table 2.4. The expression levels were normalized based on the levels of the housekeeping gene Cyclophilin (Relative expression = $2^{(CT_{\text{housekeeping}} - CT_{\text{targetgene}})}$). Primers used for quantitative PCR analysis were listed in (Table 2.5).

Table 2.4: Quantitative PCR Program

	Temperature (°C)	Time (seconds)
	50	60
	95	600
40 cycles	95	30
	60	60

Table 2.5: Quantitative PCR primers

Target Gene	Primer Forward (5'-3')	Primer Reverse (5'-3')
p62	CCTCAGCCCTCTAGGCATTG	CTGTGCCTGTGCTGGAAC
cyclophilin	ATGGTCAACCCACCGTGT	TTCTGCTGTCTTTGGAAC

2.2.8 Western blot

Protein preparation

Tissue and cell lysis The cells or tissues were lysed in ice cold lysis buffer (Table 2.6) via mechanical disruption using micro-pistill. For complete lysis the homogenized samples were incubated on ice for 20 minutes. The lysates were centrifuged at 13000 rpm for 10 minutes to precipitate the cell debris and the supernatant containing the total protein was either used directly or stored at -80°C .

Table 2.6: Protein lysis buffer

50 mM tris (pH 7,5) (Roth)
250 mM NaCl (Sigma)
30 mM EDTA(Fluka)
30 mM EGTA (Sigma)
25 mM sodiumpyrophosphate (Sigma)
1% triton-X 100 (Sigma)
0,5% NP40 (Sigma)
10% glycerol (Merck)
1 mM DTT (Sigma)
50 mM β -glycerophosphate (Sigma)
25 mM sodium fluoride (Sigma)
5 mM sodium orthovanadate (Sigma)
2 nM PMSF (Sigma)
1 tablet of complete-protease inhibitor cocktail (Roche)/50 ml

Protein content measurement Protein concentrations were determined spectrophotometrically at a wavelength of 595 nm by Bradford protein assay (Biorad) using BSA to obtain a standard curve.

Before applying the proteins to SDS-PAGE, the protein samples were normalized based on the concentration and diluted in Laemmli buffer (Table 2.7) and boiled 5 minutes at 95°C.

Table 2.7: 5x Laemmli buffer

200 mM Tris-HCl (pH 6,8)
40% (v/v) glycerol
8% (w/v) SDS
0,01% (w/v) bromphenole blue (Sigma)
5% (v/v) β -mercaptoethanol (Sigma)

SDS-PAGE

10 ml 8-15% SDS resolving gels were prepared with 2.51 ml resolving gel buffer (0.5 M Tris-HCl (Sigma) pH: 6.8, 0.4 % SDS (w/v) (Fluka)), 2-3.75 ml 40% Acrylamide (Merck), 50 μ l 10% APS (Sigma), 5 μ l TEMED (Sigma) and distilled water. 5 ml 5% stacking gel was prepared with 1.25 ml stacking gel buffer (1.5 M Tris-HCl (Sigma) pH: 8.8, 0.4 % SDS (w/v)), 0.64 ml 40% Acrylamide (Merck), 25 μ l 10% APS (Sigma), 2.5 μ l TEMED (Sigma) and distilled water. The gels were polymerized, and run at 20-30 mA for 1-2 hours.

Immunoblotting

After the gel electrophoresis, the gel was washed in transfer buffer (Table 2.8) and put together with the methanol activated PVDF membrane in between 2 Whatman papers and 2 sponges on both sides all moistened with transfer buffer. The proteins were blotted on the membrane 1-2 hours by applying 350 mA current in a wet transfer chamber (Biorad) in transfer buffer.

The membrane was blocked with 3% skim milk/PBS-0.1%Tween20 (PBS-T) for 30-60 minutes at RT and then rinsed with PBS-T. The membrane was incubated with the appropriate antibodies (for the list and conditions of the antibodies see Appendix A.2.2). The membrane was washed with PBS-T for 30-40 minutes refreshing the

buffer every 5-10 minutes and incubated with the appropriate horseradish peroxidase (HRP)-conjugated secondary antibody for 30 minutes RT in 3 % skim milk/PBS-T. The membrane was washed again for 30-40 minutes with PBS-T, and briefly dried on Whatman paper. The chemiluminescence reaction was obtained by 5 minutes incubation with ECL solution Super Signal West Pico (Thermo Scientific). The signal was detected on hypersensitive X-ray film (Thermo Scientific) after it was developed in hyper-processor (Amersham Bioscience).

Table 2.8: Transfer Buffer

0.95 M glycine
25 mM Tris base
20% (v/v) Methanol

2.2.9 Immunoprecipitation

Immunoprecipitation experiments were performed using antibodies against caspase 8 (rabbit polyclonal produced by Vandenabeele Lab) and FADD (Santa Cruz, M-19, sc-6036) with 30 minutes of antibody binding to the Protein A sepharose beads (GE Healthcare) followed by overnight incubation with protein lysates in lysis buffer. After extensive washing the beads were boiled in Laemmli buffer at 95°C for 5 minutes. The elution was subjected to immunoblot analysis.

2.2.10 Glutathionylation assay

The cells were labeled with BioGEE (Invitrogen) for one hour in DMEM at 37°C. The cells were lysed in BioGEE lysis buffer containing (50 mM tris (pH 7,5), 250 mM NaCl, 30 mM EDTA, 30 mM EGTA, 25 mM sodiumpyrophosphate, 1 % triton-X 100, 0,5 % NP40, 10 % glycerol. Biotinylated proteins were precipitated from cell lysates with streptavidin agarose beads (Thermo scientific) for 20 minutes and were eluted with BioGEE lysis buffer containing 10 mM DTT. Samples were boiled for 5 minutes at 95°C and subjected to immunoblot analysis.

2.2.11 GSH measurement

GSH measurements were done using Glutathione Assay Kit II (Calbiochem) according to the manufacturer's instructions. After preparing the cell lysates the samples were subjected to two different measurements with or without 2-vinylpyridine for the detection of GSSG and total GSH, respectively, using corresponding standards. Absorbance at 405 nm was detected and the concentrations were calculated based on the standards.

2.2.12 ELISA

Blood serum samples or cell culture supernatants stored in -20°C were used for enzyme-linked immunosorbent assay (ELISA). For the list of ELISA kits used refer to Appendix A.1. In summary, the ELISA plates coated with capture antibody were blocked for 1 hour at RT, washed extensively, incubated 2 hours with the samples and standards diluted in the dilution buffer. The plates were washed again and incubated with the detection antibody, streptavidin and substrate mix. The color reactions were detected spectrophotometrically using a plate reader at 450 nm.

Chapter 3

Results

Maintaining cellular redox balance is of vital importance for cell survival and tissue homeostasis since imbalanced production of ROS may lead to oxidative stress and cell death. Although oxidative stress has been linked to several disorders, the underlying molecular mechanisms are still not fully understood. Erythrocytes are particularly highly sensitive to ROS accumulation due to their physiological function in oxygen transport. GPx4, one of the most important ROS scavenging selenoproteins, is a unique antioxidant enzyme that can directly reduce phospholipid hydroperoxide in mammalian cells. In this study, using mice with a hematopoietic specific deletion of GPx4, it is shown that GPx4 is essential for reticulocyte maturation.

To functionally examine the role of ROS accumulation and lipid peroxidation and their effects on cellular homeostasis in the absence of GPx4 in the erythroid lineage, floxed GPx4 mice (GPx4^{fl/fl}) were crossed to Mx1-Cre transgenic mice [245] to generate Mx1-Cre/GPx4^{fl/fl} (hereafter referred to as GPx4^Δ). Deletion of GPx4 in hematopoietic cells was induced by a single intraperitoneal (i.p.) poly I:C (250μg) injection.

3.1 Anemia in the absence of GPx4

To verify the deletion of GPx4, whole protein lysates from CD71⁺/TER119⁺ bone marrow erythroblasts as well as peripheral erythrocytes were analysed by Western blot 4 weeks after the induction. Absence of GPx4 in erythroid cells is shown in Figure 3.1. The deletion is stably effective within one week after the induction.

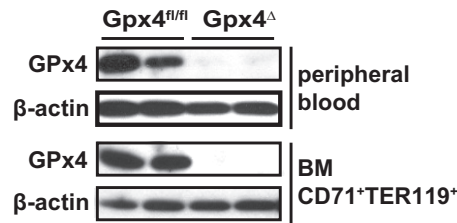


Figure 3.1: GPx4 deletion in erythroid cells. Immunoblot analysis of GPx4 in peripheral erythrocytes (TER119⁺) and bone marrow BM erythroid progenitors (CD71⁺/TER119⁺).

Within four weeks after the poly I:C administration, loss of GPx4 in hematopoietic cells lead to anemia that can be seen by the moderate yet significant decrease in red blood cell counts, hemoglobin levels and hematocrit values (Figure 3.2 A-C). In contrast, reticulocyte counts were highly increased indicating a compensatory increase of erythropoiesis (Figure 3.2 D). In parallel, serum EPO levels and the spleen weights were significantly increased (Figure 3.2 E-F). BrdU immunohistochemistry points out high proliferation rate in the spleen (Figure 3.2 G-H). Flow cytometry analysis show elevated proliferation rates of TER119⁺ erythroid cells in the spleens of GPx4^Δ mice (Figure 3.2 I). Taken together the data support the notion that anemia induced in the absence of GPx4 is largely compensated by extramedullary erythropoiesis.

3.2 ROS accumulation and lipid peroxidation in red blood cells

Since GPx4 is an antioxidant enzyme that is especially important for the reduction of lipids, lipid peroxidation and ROS accumulation were measured in GPx4^Δ erythroid cells. Figure 3.3 A shows increased levels of lipid peroxidation in unchallenged peripheral TER119⁺ erythrocytes of GPx4^Δ animals, measured by redox-sensitive dye

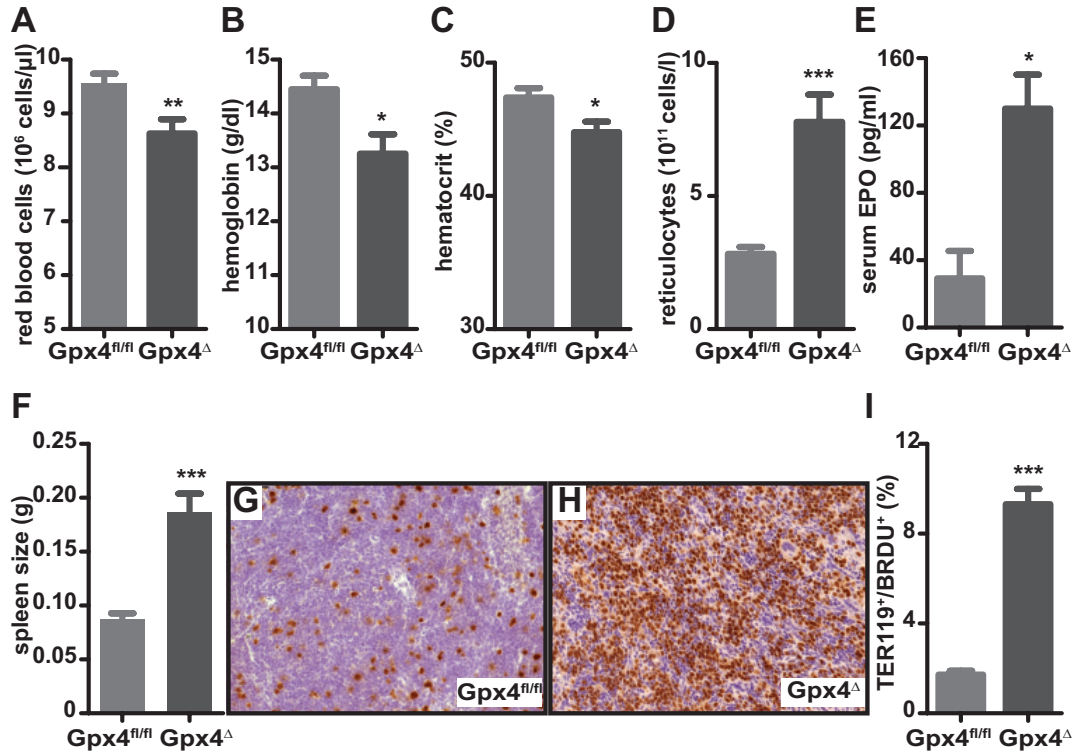


Figure 3.2: Loss of GPx4 in hematopoietic cells induces anemia that is compensated by increased erythropoiesis. Red blood cell counts (A), hemoglobin (B) and hematocrit (C) levels were decreased in GPx4 Δ mice. Number of reticulocytes was increased (D). Data are mean \pm SE; $n \geq 12$; * $p < 0.05$ ** $p < 0.01$, *** $p < 0.001$ by t-test. Elevated serum EPO levels (E) and enlarged spleens (F) in GPx4 Δ mice. Data are mean \pm SE; $n \geq 5$; * $p < 0.05$ by t-test. Immunohistochemical analysis of splenic BrdU incorporation as a marker of proliferation (G-H). Quantification of splenic BrdU⁺/TER119⁺ cells determined by flow cytometry (I). Data are mean \pm SE; $n \geq 3$; *** $p < 0.001$ by t-test. All analysis performed 4 weeks after the induction of deletion.

BODIPY 581/591, which shifts its fluorescence from red to green upon oxidation. Figure 3.3 B shows the corresponding elevated levels of ROS, measured via redox-sensitive fluorescent dye CM-H₂-DCFDA. The data indicate significant elevation of cellular ROS accumulation and lipid peroxidation in peripheral TER119⁺ erythrocytes in the absence of GPx4.

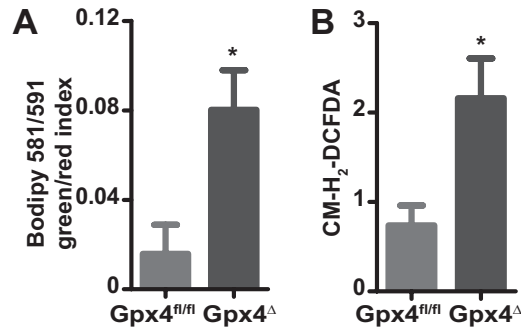


Figure 3.3: Lipid peroxidation and accumulation of ROS in red blood cells. (A) Measurement of lipid peroxidation in unchallenged peripheral TER119⁺ erythrocytes using redox-sensitive dye BODIPY 581/591. Data are mean \pm SE; $n \geq 7$; * $p < 0.05$ by t-test. (B) Measurement of ROS accumulation in unchallenged peripheral TER119⁺ erythrocytes using redox-sensitive dye CM-H₂-DCFDA. $n \geq 7$; * $p < 0.05$ by t-test.

Previous studies have shown that compromised protection from ROS in red blood cells is usually associated with shortened life span and with hemolysis [166, 167, 168, 169]. To determine whether increased lipid peroxidation and ROS formation in peripheral erythrocytes trigger their premature death, the half-life of biotin labelled peripheral CD71⁻/TER119⁺ erythrocytes and CD71⁺/TER119⁺ reticulocytes was determined using flow cytometric analysis performed weekly (Figure 3.4 A-B). The data show that the life span of GPx4^Δ cells was unaltered while the number of peripheral reticulocytes steadily increased within 4 weeks after the induction of deletion (Figure 3.4 C). The data indicate that the anemia is caused due to an interruption of erythrocyte maturation, rather than shortened life span of erythroid cells.

To exclude potential interferon-mediated effects on hematopoietic stem cells and erythroid progenitor cells [246, 247], adoptive transfer experiments using bone mar-

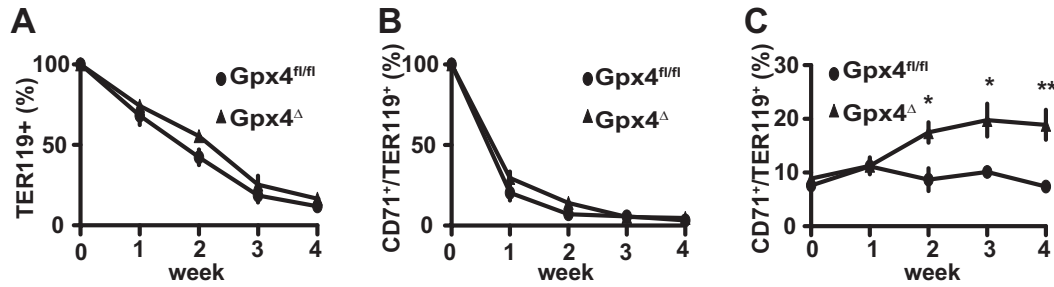


Figure 3.4: Survival of peripheral erythrocytes and reticulocytes. (A,B) Survival of biotin labelled peripheral TER119⁺ erythrocytes (A) and CD71⁺/TER119⁺ reticulocytes (B). Data are mean \pm SE; $n \geq 6$. (C) Increased number of peripheral CD71⁺/TER119⁺ reticulocytes in GPx4^Δ mice within 4 weeks after poly I:C administration. Data are mean \pm SE; $n \geq 5$; * $p < 0.05$, ** $p < 0.01$ by t-test.

row derived from tamoxifen-inducible Rosa26- CreERT2/GPx4^{fl/fl} mice were performed [239]. The defect in reticulocyte maturation was confirmed by the flow cytometric analysis of peripheral cells in GPx4^Δ BM transplanted animals. Figure 3.5 shows increased accumulation of immature reticulocytes in the periphery based on thiazol orange and mitotracker deep red staining in the CD71^{high}/TER119⁺ population in GPx4^Δ mice.

3.3 Vitamin E is essential for the increased erythropoiesis in GPx4^Δ mice

Based on the observation that the absence of GPx4 is compromising erythrocyte maturation, *in vitro* colony formation of GPx4^Δ BM cells was tested. *In vitro* erythroid colony formation in methyl cellulose semisolid media was almost completely abolished in GPx4^Δ BM indicated by o-dianisidine positive colony counts (Figure 3.6). Seiler *et al.* previously showed that in fibroblasts and neurons the cell death due to the absence of GPx4 was rescued by α -tocopherol, the most abundant form of vitamin E [103]. Figure 3.6 shows that formation of GPx4^Δ erythroid colonies was

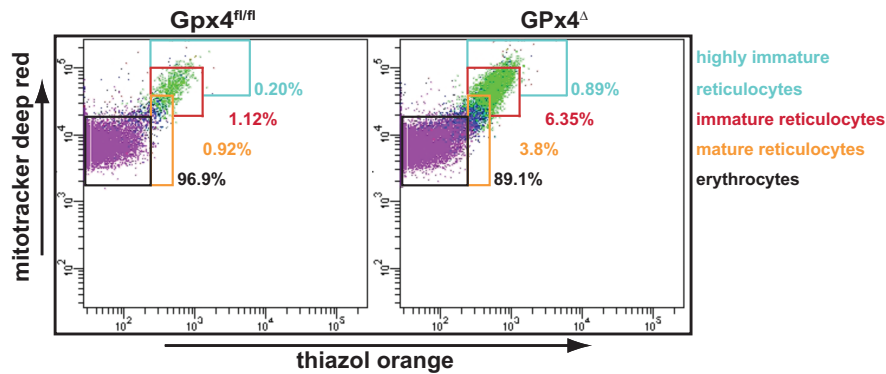


Figure 3.5: Impaired reticulocyte maturation in the absence of GPx4. Flow cytometric analysis of peripheral cells from BM transplanted animals indicating a shift to highly immature reticulocytes in $GPx4^{\Delta}$ animals. Green population represents $TER119^{+}/CD71^{high}$ cells, blue population comprises $TER119^{+}/CD71^{low}$ cells and purple population contains $TER119^{+}/CD71^{-}$ cells. Data are representative of at least three animals per group. Flow cytometry analysis performed by Helmholtz Center collaborators.

also completely restored in the presence of α -tocopherol in the medium indicating a compensatory role of vitamin E in the absence of GPx4.

Based on the *in vitro* findings of its compensatory role, the role of vitamin E is investigated *in vivo*. Regular animal chow has a high vitamin E content (55 mg/kg). In order to examine whether this accounts for the observed compensation of anemia *in vivo*, an experimental approach with a special diet lacking vitamin E was followed. Also, to exclude potential interferon-mediated effects on hematopoietic stem cells and erythroid progenitor cells [246, 247], adoptive transfer experiments using bone marrow derived from tamoxifen-inducible $Rosa26-CreERT2/GPx4^{fl/fl}$ mice were performed [239]. Eight weeks after the transplantation, mice received tamoxifen citrate (TAM) containing diet for 3 weeks to induce GPx4 deletion [248]. Afterwards, they received either a normal vitamin rich diet (ND) or a diet specifically lacking vitamin E ($vitE^{\Delta}$) for additional 3 weeks (Figure 3.7 A).

Mice kept on $vitE^{\Delta}$ diet suffer from severe anemia, indicated by dramatically low RBC counts, hemoglobin and hematocrit levels (Figure 3.7 B-D). Furthermore, the spleen size and serum EPO levels were highly increased compared to the animals fed

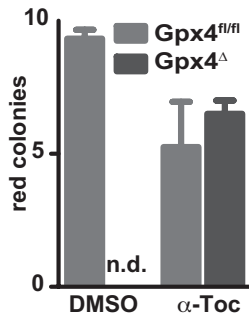


Figure 3.6: *In vitro* erythroid colony formation is abolished in GPx4^Δ BM. Formation of o-dianisidine-positive erythroid colonies from bone marrow in methyl cellulose semisolid media. Red colony formation of GPx4^Δ bone marrow cells was rescued by addition of α -tocopherol to the medium. Data are mean \pm SE; $n \geq 4$; *** $p < 0.001$ by t-test. Assay performed by Helmholtz Center collaborators.

with ND (Figure 3.7 F-G). Most importantly, dietary vitamin E-depletion caused a significant decrease in reticulocyte numbers indicating the involvement of vitamin E in the increased erythropoiesis observed in GPx4^Δ mice (Figure 3.7 E). Consequently, when mice were maintained on a vitE^Δ diet, the anemia progressed and all GPx4^Δ animals had to be sacrificed within 5 weeks following in the induction of GPx4 deletion. The data support the idea that vitamin E is essential for the compensation of anemia in the absence of GPx4. Notably, all red blood parameters were completely normal in wild type mice kept on a vitamin E-depleted diet for three months. The data indicate that vitamin E depletion further elevates anemia in GPx4^Δ mice.

3.4 Autophagic flux is inhibited in the absence of GPx4

Erythroid cells undergo enucleation and the removal of organelles during differentiation. Previous studies have shown that autophagy is required for elimination of mitochondria during erythrocyte maturation and impaired autophagy is associated with anemia development [249, 250]. Mortensen *et al.* recently showed that mice

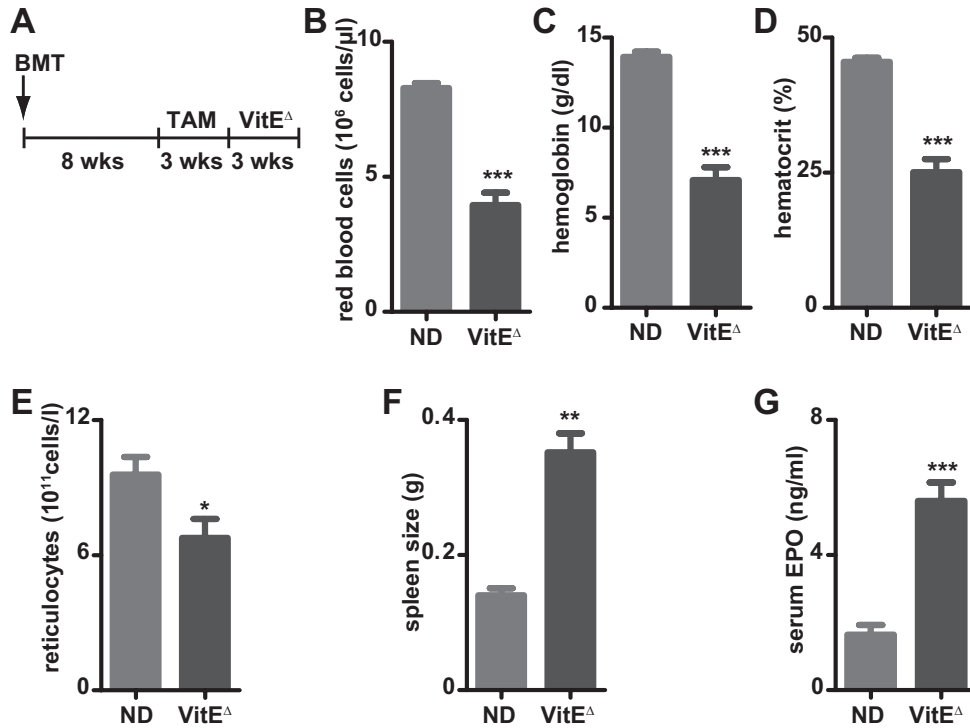


Figure 3.7: Vitamin E is essential for the increased erythropoiesis in GPx4 Δ mice (A) Schematic overview of treatment: bone marrow from Rosa26-CreERT2/GPx4 $^{fl/fl}$ mice was transplanted (BMT) into wildtype recipients and deletion was induced by tamoxifen citrate (TAM). Then mice were kept either on normal diet (ND) or vitamin E-depleted diet (vitE Δ). (B-E) Red blood cell number (B), hemoglobin (C) and hematocrit (D) levels and reticulocyte counts (E) in GPx4 Δ mice kept on vitE Δ diet compared to ND for three weeks. Data are mean \pm SE; $n \geq 10$; *** $p < 0.001$, * $p < 0.05$ by t-test. (F, G) Enlarged spleens (F) and elevated serum EPO levels (G) in transplanted mice when kept on vitE Δ diet compared to ND for three weeks. Data are mean \pm SE; $n \geq 6$; *** $p < 0.001$, ** $p < 0.001$ by t-test. *Transplantation experiments were performed by Naidu Vegi at the Helmholtz Center Munich.*

lacking the essential autophagy gene Atg7 in the hematopoietic cells develop severe anemia [249]. Therefore, whether GPx4 deletion leads to impaired autophagy in the erythroid precursor cells was tested. LC3 conversion is a commonly used marker of autophagic activation [196]. p62 is another marker that is used for the lysosomal degradation of autophagosomes and accumulation of p62 is associated with defective autophagy [251]. Quantitative PCR analysis of p62 indicated an upregulation in GPx4 Δ reticulocytes in the peripheral blood (Figure 3.8 A). Figure 3.8 B indicates activation of autophagy in CD71 $^+$ cells isolated from the blood of GPx4 Δ animals characterized by enhanced LC3-II conversion. However, higher amounts of p62 protein observed in those cells indicates impaired lysosomal degradation (Figure 3.8 B). On the other hand, p62 relative expression was significantly increased in GPx4 Δ reticulocytes (Figure 3.8 A). The elevated numbers and extended presence of autophagosomes in GPx4 Δ reticulocytes were confirmed by EM (Figure 3.8 D-G) and the number of autophagosomes per cell area was quantified in mature and immature reticulocytes (Figure 3.8 C). It is known that autophagy can be either a cytoprotective response or another mechanism of cell death when cell survival cannot be achieved [208, 252, 253]. Taken together, the data indicate that loss of GPx4 induces autophagy based on the presence of early autophagic markers, however, autophagic flux is inhibited.

3.4.1 Genetic inhibition of autophagy does not revert anemia *in vivo*

In parallel with the inhibition of autophagic degradation in the absence of GPx4, genetic inhibition of Atg7, the essential gene for autophagy, via crossing the GPx4 Δ animals with ATG7 $^{fl/fl}$ animals to obtain a double knockout, proved that inhibition of autophagy does not rescue the anemic phenotype of GPx4 Δ animals indicated by the blood parameters (Figure 3.9).

Collectively, these data suggest that GPx4 ablation triggers initiation of autophagy possibly as a counteracting mechanism against oxidative stress, however, since autophagic flux is inhibited due to loss of GPx4, autophagy is not directly

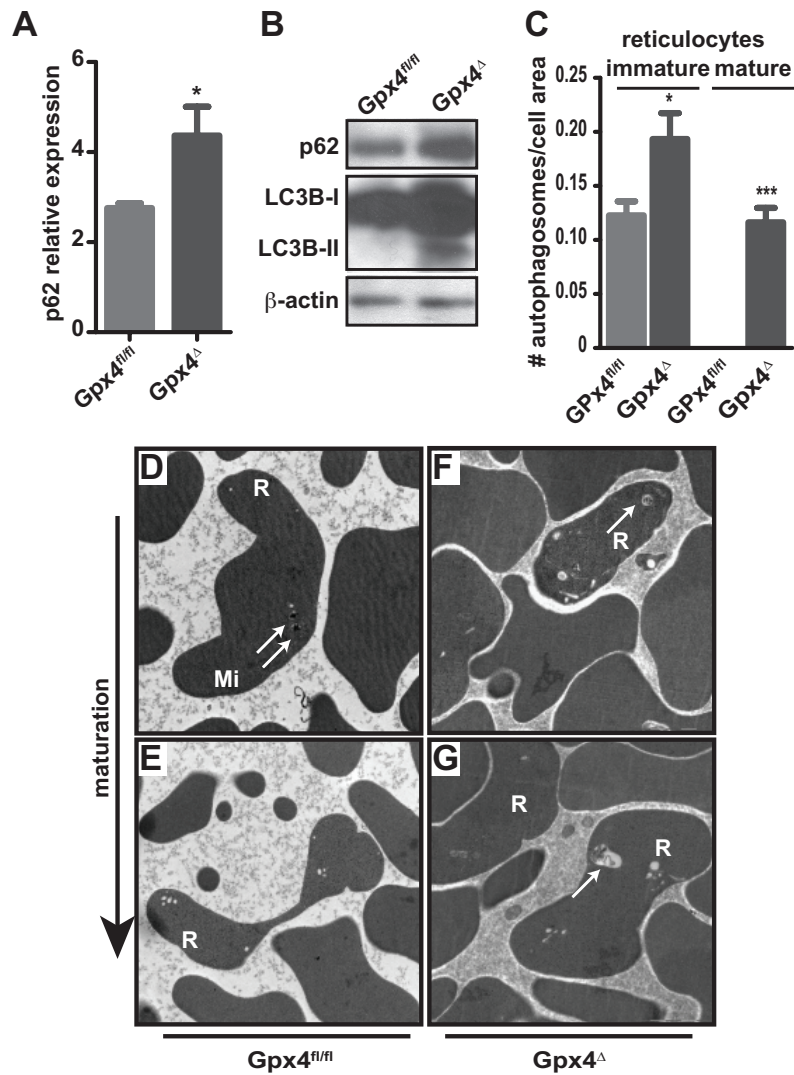


Figure 3.8: Autophagy is impaired in GPx4^Δ mice. (A) Quantitative PCR results show upregulation of p62 in GPx4^Δ peripheral CD71⁺ cells. (B) Immunoblot analysis of LC3 in blood CD71⁺ cells reveal increased conversion to LC3-II in in GPx4^Δ peripheral CD71⁺ cells. (C) Quantification of autophagosomes per cell area determined by EM (C). Data are mean ± SE; n≥4; * p < 0.05 by t-test. (D-G) Elevated numbers and persistence of autophagosomes (white arrows) determined by EM in the blood from GPx4^Δ mice (D, E) compared to control animals (F,G). R: reticulocytes; Mi: mitochondria. Data are representative of at least four animals per group. *EM analysis was performed by Dr. Michaela Aichler.*

involved in the survival of the cells, nor in cell death execution. On the other hand, malfunction of this potential countervailing mechanism might promote cell death through further elevation of ROS and reactive lipid species.

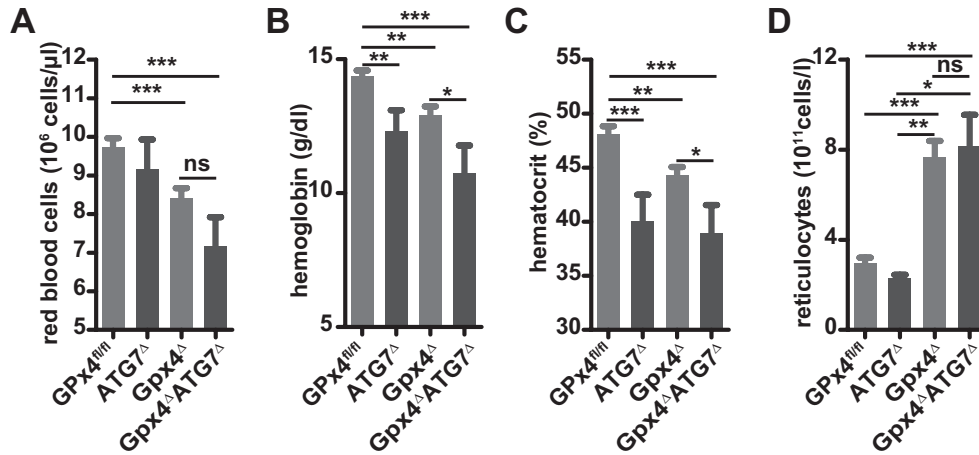


Figure 3.9: Inhibition of autophagy does not revert anemia *in vivo*. Red blood cell counts (A), hemoglobin (B) and hematocrit (C) values, reticulocyte counts (D). Data are mean \pm SE; $n \geq 5$; * $p < 0.05$ ** $p < 0.01$, *** $p < 0.001$ by t-test.

3.5 Anemia occurring in the absence of GPx4 is not dependent on 12/15-Lox

Seiler *et al.* have demonstrated that cell death due to the absence of GPx4 requires functional 12/15-Lox since specific inhibitors of 12/15-Lox efficiently protected GPx4-deficient cells from cell death. Therefore, GPx4^Δ mice were crossed with 12/15-Lox^{fl/fl} animals to obtain a double knockout in order to test whether 12/15-Lox deficiency would revert anemia. However, absence of 12/15-Lox did not affect anemia observed in GPx4^Δ mice (Figure 3.10) indicating that the impaired erythropoiesis in GPx4^Δ is not dependent on the function of 12/15-Lox.

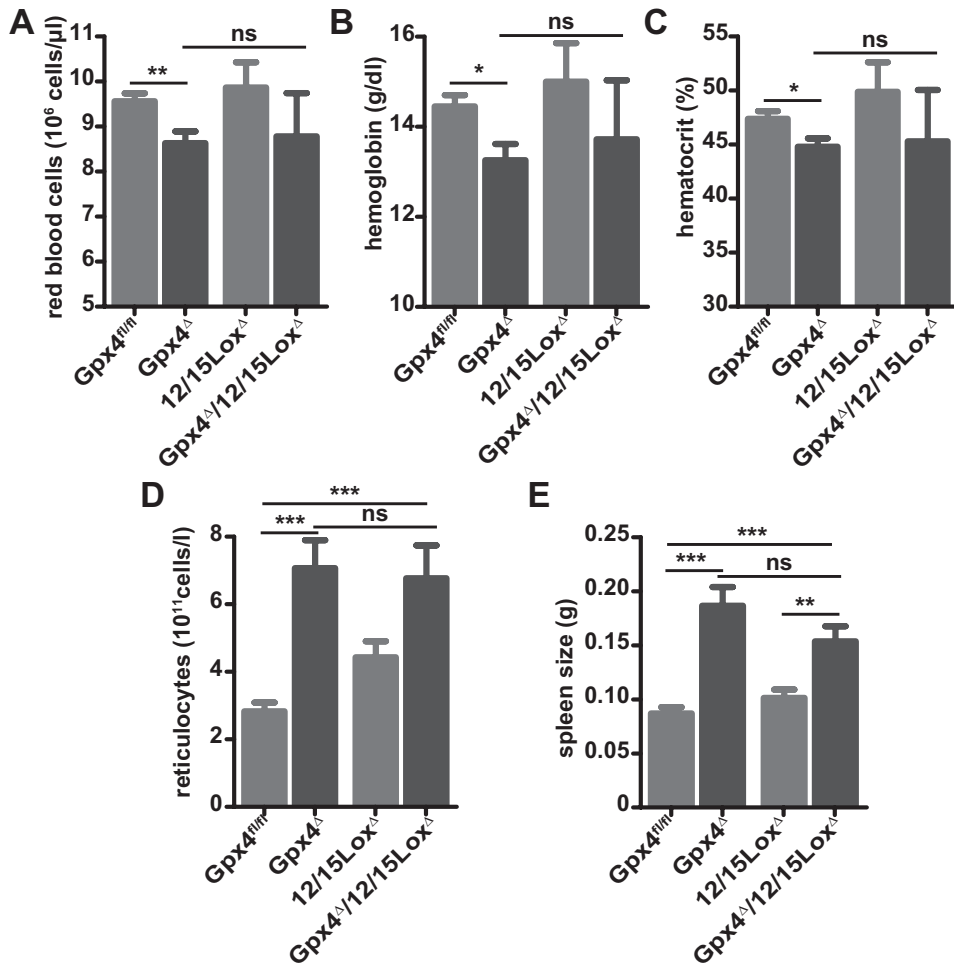


Figure 3.10: Anemia occurring in the absence of GPx4 is not dependent on 12/15-Lox. Red blood cell counts (A), hemoglobin (B) and hematocrit (C) reticulocyte counts (D). (E) Spleen size in GPx4^Δ/12/15-Lox^Δ mice. Data are mean \pm SE; $n \geq 12$; * $p < 0.05$ ** $p < 0.01$, *** $p < 0.001$ by t-test.

3.6 GPx4-deficiency does not induce apoptosis in erythroid progenitors

Seiler *et. al* previously showed that GPx4-deficient fibroblasts undergo apoptosis-independent cell death [103]. Using flow cytometric analysis of Annexin V staining on the cell surface as a marker for apoptosis, it was verified that erythroid precursor cells in GPx4 Δ mice do not activate apoptotic cell death (Figure 3.11). Similar to GPx4-deficient fibroblasts, GPx4 Δ erythroid precursors did not undergo apoptosis indicated by unaltered annexin V on the surface of bone marrow or peripheral CD71 $^+$ cells (Figure 3.11 B, C). Data indicate that the cell death in erythroid progenitors upon deletion of GPx4 is not executed via apoptosis.

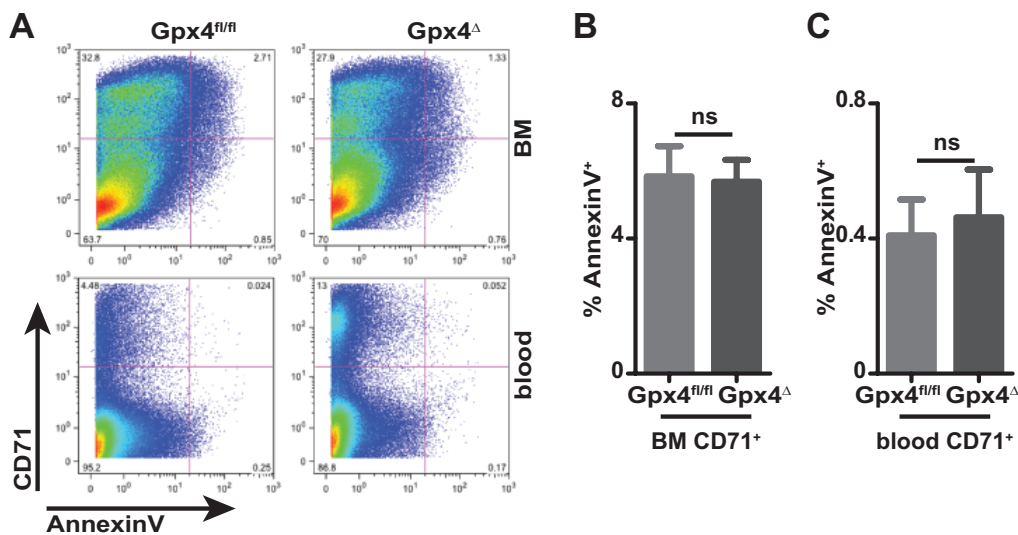


Figure 3.11: GPx4-deficiency does not induce apoptosis in erythroid progenitors. (A) Flow cytometric analysis of annexin V and CD71 in bone marrow (BM) and peripheral blood. (B, C) Quantification of annexin V $^+$ /CD71 $^+$ cells in bone marrow (B) and peripheral blood (C). Data are mean \pm SE; $n \geq 3$; ns: not significant.

3.7 Caspase 8 is functionally inhibited due to glutathionylation

Inhibition of caspases is associated with defective apoptosis resulting in activation of alternative cell death execution mechanisms [228] and caspase 8 is one of the main determinants of such alterations [254]. For detailed molecular analysis, we took advantage of murine embryonic fibroblasts harboring two loxP-flanked GPx4 alleles in addition to stably expressing 4-OHT inducible MerCreMer (Pfa1 cells), in which cell death is induced within 48 hours after 4-OHT administration [103]. Since siRNA mediated knock down of caspase 8 did not accelerate the cell death of GPx4 Δ in fibroblasts (Figure 3.12), the functionality of caspase 8 in the absence of GPx4 was tested.

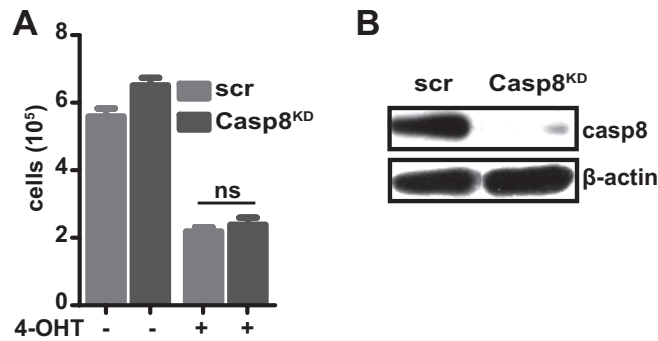


Figure 3.12: Necroptosis in the absence of GPx4 is not dependent on caspase 8. (A) Survival of 4-OHT treated Pfa1 cells was not affected by caspase 8 knockdown (casp8^{KD}). Data are mean \pm SE; $n \geq 4$. (B) Immunoblot analysis of caspase 8 in Pfa1 cells transfected with scrambled (scr) siRNA or caspase 8 siRNA pool.

Figure 3.13 A shows that whereas caspase 8 cleavage was achieved in response to TNF α treatment in the presence of TAK1 inhibitor, it was partially inhibited in GPx4 Δ cells. In a recent study with SOD1-deficient macrophages, caspase 1 was shown to be inhibited due to reversible oxidation and glutathionylation of the redox-sensitive cysteine residues and this inhibition was reversed in the presence of the reducing agent DTT [22]. Similarly, in GPx4 Δ fibroblasts, caspase 8 was shown

to be glutathionylated based on the incorporation of biotinylated glutathione ethyl ester (BioGEE), which is a cell-permanent, biotinylated glutathione analog for the detection of glutathionylation (Figure 3.13 D) consistent with the increased levels of oxidized glutathione (Figure 3.13 B-C). Presence of DTT in the culture medium did not only restore the cleavage of caspase 8 but also reversed the cell death in GPx4 Δ cells (Figure 3.13 E-F). Moreover, glutathionylation of caspase 8 due to increased oxidized glutathione was also observed for peripheral blood cells of GPx4 Δ animals (Figure 3.14). Taken together the data indicate that caspase 8 is functionally inhibited due to glutathionylation in the absence of GPx4.

3.8 RIP1/RIP3-dependent necroptosis is responsible for cell death in GPx4-deficient fibroblasts and erythroid progenitor cells

As mentioned above in Section 3.6, neither GPx4-deficient fibroblasts nor GPx4 Δ bone marrow/peripheral CD71⁺ cells undergo apoptotic cell death [103]. Inhibition of caspases results in necroptosis as the cell death execution mechanism [228] and caspase 8 is the main determinant of apoptosis-necrosis switch [254]. Functional inhibition of caspase 8 due to glutathionylation (Section 3.7) explains the inactivation of apoptosis in the loss of GPx4. Autophagy is also ruled out as the mechanism of cell death (Section 3.4). Recently, necroptosis was described as an alternative form of regulated cell death that is based on the activity of RIP1/RIP3 kinases and independent of caspase activation [219, 222, 223, 224, 225]. Therefore, it was tested whether necroptosis is the underlying mechanism of the cell death in GPx4 Δ cells. Figure 3.15 A shows that the protein levels of RIP1 and RIP3 were elevated in GPx4-deficient fibroblasts indicating that GPx4 deletion leads to the stabilization of RIP1/RIP3 complex. Moreover, addition of nec-1, specific RIP1 kinase inhibitor, to the medium reverses the elevated protein levels of the RIP1/RIP3 (Figure 3.15 A). In addition to that, immunoprecipitation for caspase 8 pulls down increased levels of RIP1 in Pfa1 cells treated with 4-OHT for 36 hours compared to untreated as well as

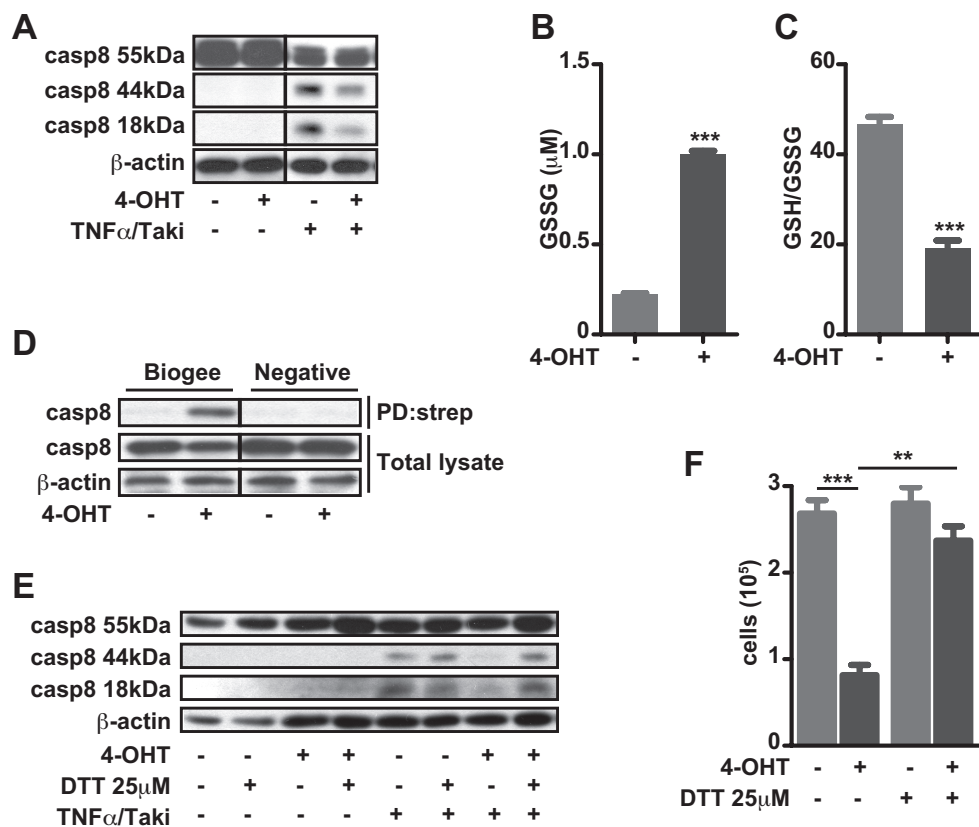


Figure 3.13: Caspase 8 is functionally inhibited due to glutathionylation *in vitro*. (A) Western blot showing reduced cleavage of caspase upon stimulation with TNF α and TAK1 inhibitor 5Z-7-Oxozeaenol in GPx4 Δ cells compared to controls. (B, C) Concentration of oxidized glutathione (GSSG) (B) and ratio of reduced to oxidized glutathione (C) in supernatants of Pfa1 cells untreated or treated with 4-OHT for 36 hours. (D) Detection of glutathionylated caspase 8 in Pfa1 cells untreated or treated with 4-OHT for 36 hours. Cells were loaded with biotinylated glutathione ethyl ester (BioGEE) and immunoblot analysis was performed after pull-down (PD) via streptavidin (strep) and with total lysate. (E, F) Addition of 25 μ M DTT reverses the inhibition of caspase 8 indicated by the western blot (E) and rescues cell death (F). Data are mean \pm SE; $n \geq 6$. ** $p < 0.01$, *** $p < 0.001$ by t-test

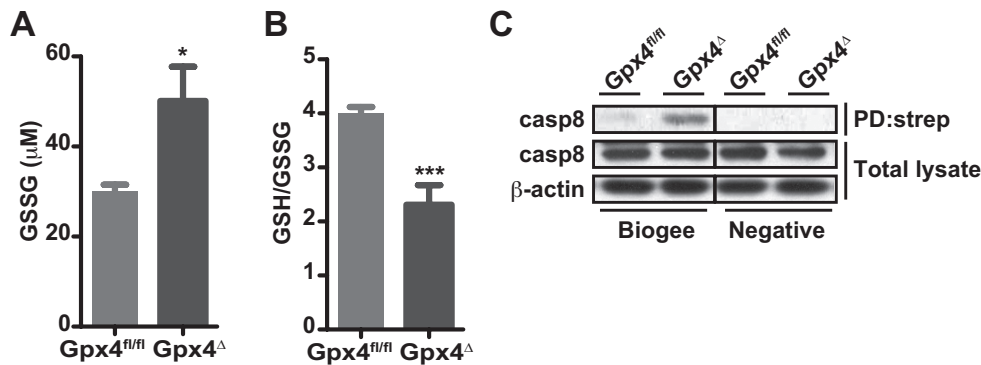


Figure 3.14: Caspase 8 is functionally inhibited due glutathionylation *in vivo*. (A, B) Concentration of oxidized glutathione (GSSG) (A) and ratio of reduced to oxidized glutathione (B) in peripheral blood of GPx4 Δ animals and controls. Data are mean \pm SE; $n \geq 6$. * $p < 0.05$, *** $p < 0.001$ by t-test. (C) Detection of glutathionylated caspase 8 in in peripheral blood of GPx4 Δ animals and controls. Cells were loaded with biotinylated glutathione ethyl ester (BioGEE) and immunoblot analysis was performed after pull-down (PD) via streptavidin (strep) and with total lysate.

in TNF α treated cells compared to TAK1 inhibitor and zVAD (Figure 3.15 B) More importantly, nec-1 but not its inactive derivative nec-1i, completely rescued the cell death in GPx4-deficient fibroblasts starting from the concentration of 10 μ M in a dose dependent manner (Figure 3.15 C). Furthermore, siRNA mediated knock down of RIP1 or RIP3 increases the survival of GPx4-deficient fibroblasts (Figure 3.15 D, E).

It was tested whether inhibition of necroptosis would also have an affect on almost completely abolished *in vitro* erythroid colony formation of GPx4 Δ BM cells. Similar to the fibroblasts, addition of nec-1 into the culture medium increases the colony formation of GPx4 Δ cells to a significant extent (Figure 3.15 F). The data provide evidence that GPx4 deficiency induces necroptosis in fibroblasts and necroptosis is the underlying mechanism of cell death based on the observations that both chemical and biological inhibition of the pathway significantly increase cell survival.

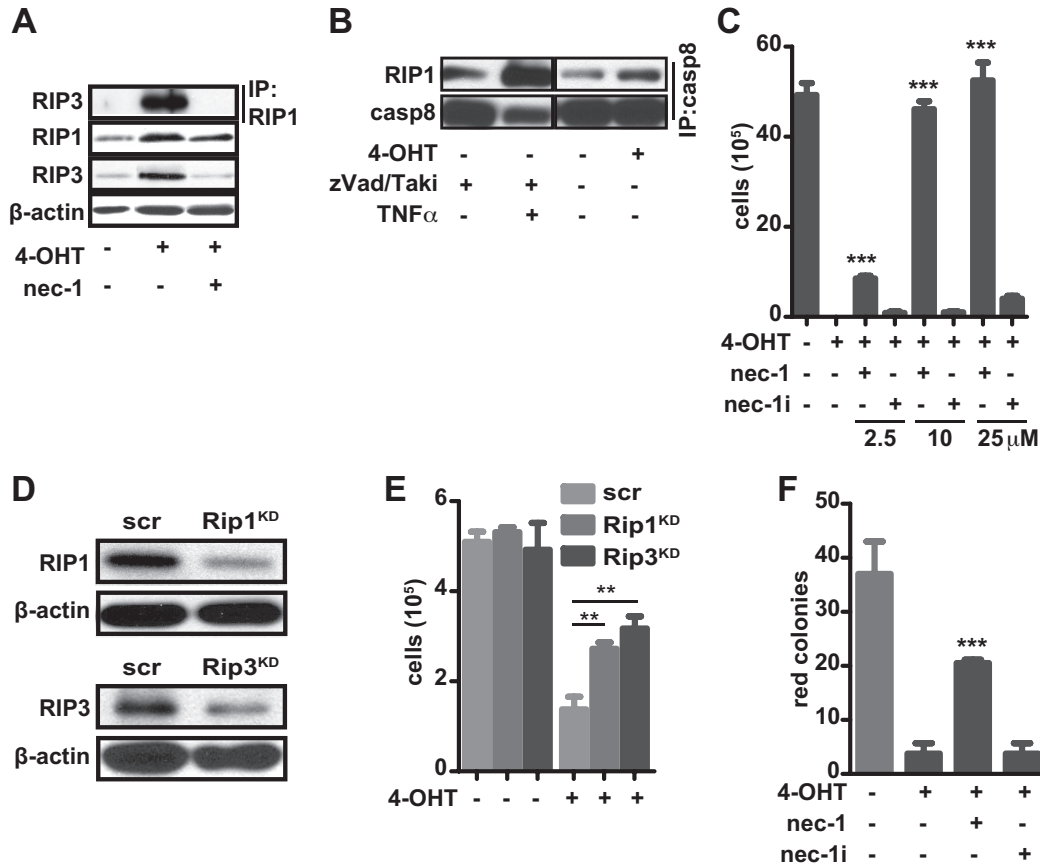


Figure 3.15: RIP1/RIP3-dependent necroptosis is responsible for cell death in GPx4-deficient fibroblasts and erythroid progenitor cells. (A) Immunoprecipitation (IP) and immunoblot analysis of RIP1 and RIP3 in Pfa1 cells untreated or treated with 4-OHT for 48 hours with or without nec-1 (10 μ M). (B) Immunoprecipitation for caspase 8 showing increased levels of RIP1 in Pfa1 cells treated with 4-OHT for 18 hours and 36 hours compared to untreated as well as in TNF α treated cells compared to TAK1 inhibitor and zVAD. (C) nec-1 in the culture medium increases the survival of Pfa1 cells 48 hours after 4-OHT administration. (D) Immunoblot analysis of RIP1 and RIP3 in Pfa1 cells transfected with scrambled (scr) siRNA, RIP1 or RIP3 siRNA pools. (E) RIP1 or RIP3 knock down increases survival of Pfa1 cells 48 hours after 4-OHT administration. Data are mean \pm SE; $n \geq 6$; ** $p < 0.01$ by t-test. (F) Formation of erythroid o-dianisidine-positive GPx4 Δ colonies was significantly improved in the presence of nec-1 (10 μ M). Data are mean \pm SE; $n \geq 3$; *** $p < 0.001$ by t-test.

3.8.1 Inhibition of necroptosis rescues anemia

The data from the *in vitro* experiments suggested necroptosis as the underlying mechanism of cell death observed in the absence of GPx4. Therefore, whether inhibition of necroptosis would reverse anemia observed in GPx4 Δ mice was tested by nec-1 treatment *in vivo*. For the experiments, the animals have been treated 3 times a week with either nec-1 (2 mg/kg) or nec-1i (1.89 mg/kg) two weeks after the induction of GPx4 knockout. Within 2 weeks of treatment, all red blood cell parameters were normalized for the GPx4 Δ mice treated with nec-1 but not for the animals treated with the inactive compound (Figure 3.16).

More importantly, genetic inhibition of necroptosis using RIP3 deficient mice [242] rescues anemia in GPx4 Δ animals confirming the data obtained with the nec-1 treatment. Figure 3.17 shows that the blood count values were normalized in RIP3 Δ mice 4 weeks after the induction of GPx4 deletion. Collectively, the data support the notion that necroptosis is responsible for the cell death observed in GPx4 Δ erythroid progenitor cells that is leading to an interruption of erythrocyte maturation, and subsequently to anemia.

3.8.2 ROS levels and lipid peroxidation are not affected by nec-1

Since nec-1 administration showed profound effects on the phenotype observed in the absence of GPx4, it was tested whether it acts as an antioxidant and reverse the observed ROS accumulation and lipid peroxidation. Flow cytometric analysis reveal that nec-1 does not affect accumulation of lipid peroxides or ROS in GPx4 Δ fibroblasts (Figure 3.18). Data indicate that nec-1 inhibits the cell death triggered in the absence of GPx4 without reducing the elevated lipid peroxidation and ROS levels, suggesting lipid peroxidation and ROS per se are not sufficient to induce cell death but rather act as upstream signaling activators of RIP1/RIP3 induced necroptosis.

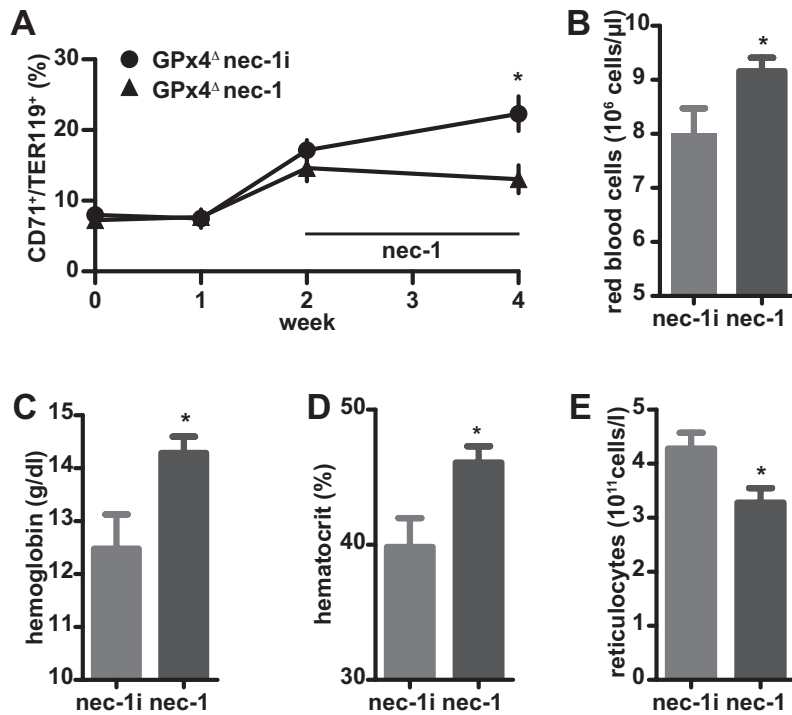


Figure 3.16: Nec-1 treatment reverts anemia in GPx4^Δ mice. GPx4^Δ mice have been treated with nec-1 (2 mg/kg) or nec-1i (1.89 mg/kg) for two weeks starting from two weeks after the induction of GPx4 deletion. (A) Weekly flow cytometric analysis of peripheral CD71⁺/TER119⁺ showing normalization in nec-1 treated animals. Data are mean \pm SE; $n \geq 5$; * $p < 0.05$ by t-test. (B-E) Normalization of red blood cell number (B), hemoglobin level (C), hematocrit values (D) and number of reticulocytes (E) in nec-1 treated animals after 2 weeks of treatment. Data are mean \pm SE; $n \geq 5$; * $p < 0.05$ by t-test.

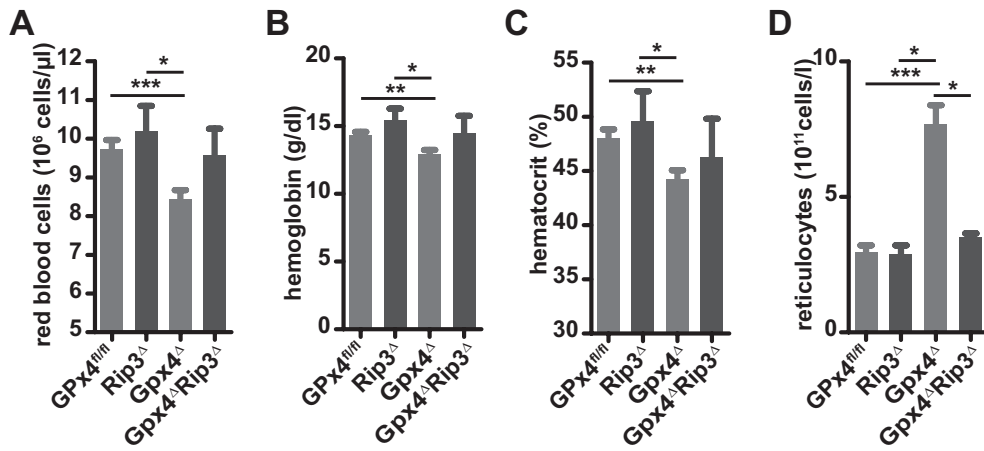


Figure 3.17: Necroptosis is responsible for the anemia in GPx4^Δ mice. Deletion of RIP3 normalizes red blood cell parameters. (A-D) Normalization of red blood cell number (A), hemoglobin level (B), hematocrit values (C) and number of reticulocytes (D) Data are mean ± SE; n≥4; * p < 0.05, ** p<0.01, *** p<0.001 by t-test.

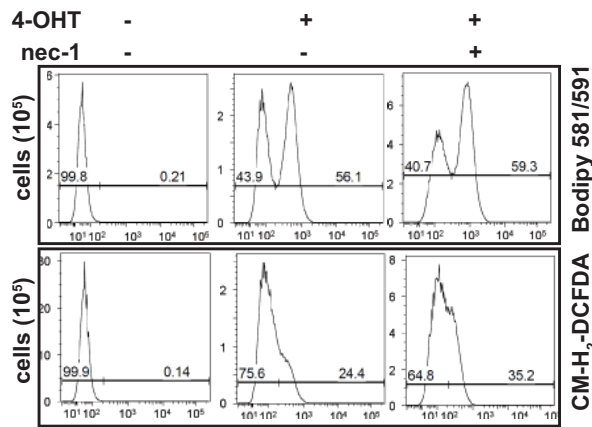


Figure 3.18: Nec-1 does not reverse ROS levels or lipid peroxidation. Unaltered lipid peroxidation or ROS accumulation in Pfa1 cells untreated or treated with 4-OHT for 48 hours in the presence of nec-1 (10 μM) as assessed by flow cytometric analysis of BODIPY 581/591 and CM-H₂-DCFDA staining. *This experiment has been performed by Marcus Conrad and Josef Mysliwicz at the Helmholtz Center Munich.*

3.8.3 Necrosome formed in the absence of GPx4 is independent of FADD recruitment

The best described necrosome complex involves FADD in addition to RIP1, RIP3 and caspase 8. However, immunoprecipitation using anti-FADD antibody indicated that FADD is not recruited to RIP1/Casp8 complex in Pfa1 cells (Figure 3.19). Data suggest that the necrosome formed in the absence of GPx4 differs from the conventional necrosome complex.

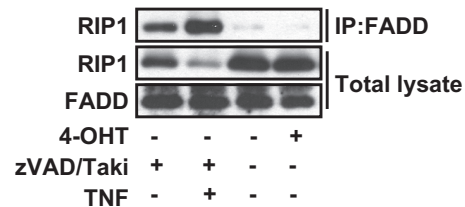


Figure 3.19: Necrosome formed in the absence of GPx4 is independent of FADD recruitment. Immunoprecipitation analysis indicating that there is no recruitment of FADD to RIP1 in Pfa1 cells untreated or treated with 4-OHT for 48 hours. Positive control confirms enhanced recruitment in Pfa1 cells upon TNF α stimulation in the presence of zVAD and TAK inhibitor 5Z-7-Oxozeaenol (Taki) which potently induces TNF α -dependent necroptosis.

3.8.4 Necroptosis in the absence of GPx4 is not dependent on TNF α or CD95L

To date, the best characterized pathways for the activation of necroptosis involve Fas and TNF signaling upstream of RIP1/RIP3 kinases [221, 219]. Evidence is provided that loss of GPx4 leads to RIP1/RIP3 dependent necroptosis through lipid peroxidation and ROS accumulation. Whether TNF α is involved in the cell death triggered by GPx4 loss was tested by inhibition of TNF signaling.

To functionally examine the role of TNF signaling, GPx4 Δ fibroblasts were cul-

tured in the presence of a specific TNF antagonist (enbrel, etanercept). As shown in Figure 3.20 A, inhibition of TNF signaling did not have any affect on cell death.

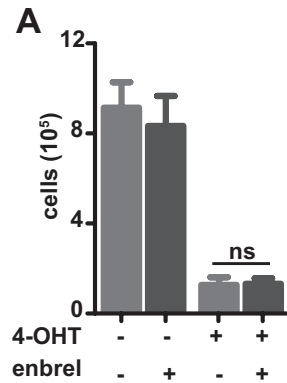


Figure 3.20: Necroptosis in the absence of GPx4 is not dependent on TNF α . Survival of 4-OHT treated Pfa1 cells cannot be rescued in the presence of TNF antagonist (enbrel, etanercept). Data are mean \pm SE; $n \geq 4$.

Involvement of TNF α and CD95L was also checked *in vivo*. GPx4 Δ mice were treated either with enbrel or a neutralizing antibody against CD95L for 2 weeks starting from 2 weeks after the induction of deletion. However, as shown in Figure 3.21 the anemia and the compensatory reticulocytosis observed in those animals remain unaffected.

Both *in vitro* and *in vivo* experiments rule out the possible involvement of the TNF α and CD95L in necroptosis triggered by GPx4 loss. These observations provide basis for a novel pathway for the induction of necroptosis triggered directly by ROS and lipid peroxidation independent of so far described upstream regulators.

3.9 Despite the DNA damage, inhibition of PARP does not rescue cell death of GPx4-deficient fibroblasts and the anemia in GPx4 Δ mice

Finally, whether activation of PARP plays a role in the cell death induced upon loss of GPx4 was tested. PARP is a nuclear enzyme activated in response to DNA damage and may lead to PARP-mediated cell death that is known to be caspase-independent

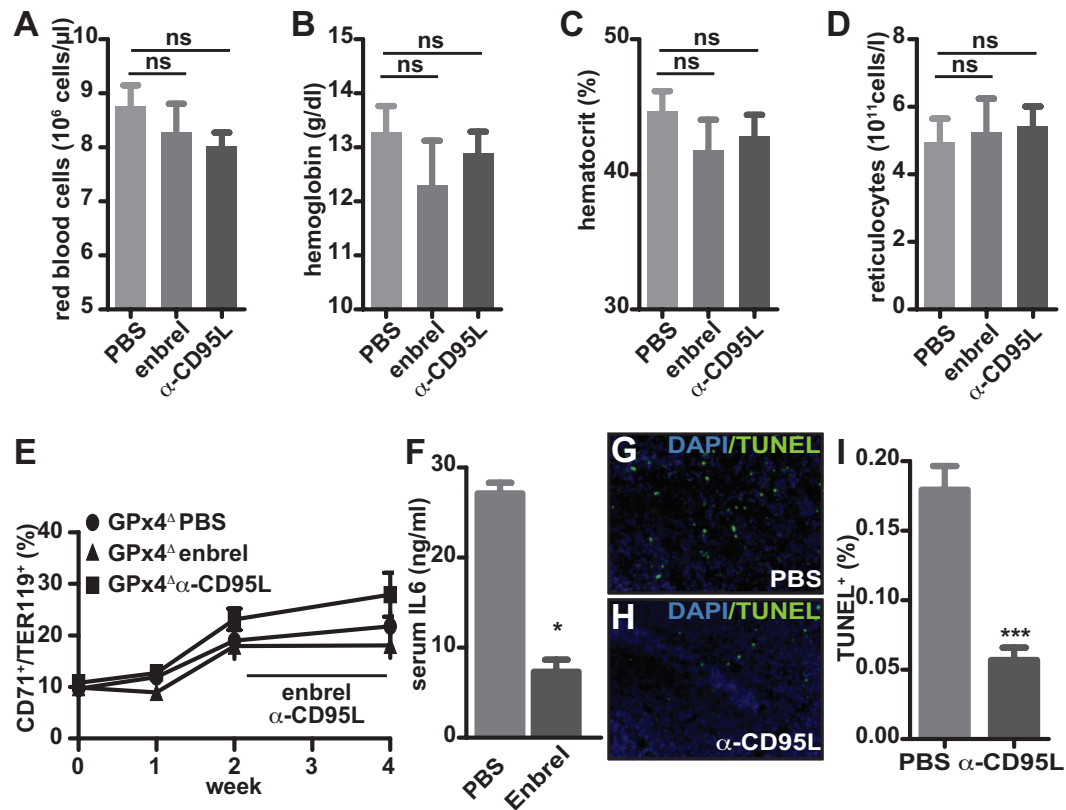


Figure 3.21: TNF α or CD95 neutralization do not rescue anemia *in vivo*. GPx4 Δ mice were treated for 2 weeks with enbrel (5 mg/kg) or α -CD95L neutralizing antibody (50 μ g) starting 2 weeks after the induction of deletion. (A-D) Red blood cells parameters; red blood cells (A), hemoglobin (B), hematocrit (C) and reticulocytes (D) were not affected. Data are mean \pm SE; $n \geq 5$. (E) The number of peripheral CD71⁺/TER119⁺ cells remains unaffected. Data are mean \pm SE; $n \geq 5$. (F) Control experiments for the efficiency of enbrel treatment. Serum IL6 level was detected by ELISA 4 hours after LPS (5 μ g/kg) treatment applied 4 hours after a single enbrel injection. Data are mean \pm SE; $n \geq 2$; * $p < 0.05$ by t-test. (G-I) Control experiments for the efficiency of α -CD95L neutralizing antibody. (G-H) TUNEL assay in the spleens of the mice treated with α -CD95L neutralizing antibody (H) or PBS (G) upon treatment with soluble CD95L (1 μ g/kg). (I) Quantification of TUNEL positive cells. Data are mean \pm SE; $n \geq 2$; *** $p < 0.001$ by t-test.

and considered as a type of necrotic cell death [255, 256]. To investigate the role of PARP in the absence of GPx4, specific inhibitor of PARP, Olaparib, was used on fibroblasts. Despite elevated DNA damage in GPx4^Δ cells (Figure 3.22 A-E) indicated by increased levels of phospho-H2A.X (pH2A.X), inhibition of PARP did not rescue the cell death (Figure 3.22 F). Xu *et al.* demonstrated that PARP mediated cell death requires tumor necrosis factor receptor-associated factor 2 (TRAF2) [257], therefore, it was checked whether siRNA mediated knockdown of TRAF2 would have any effect on cell survival. Consistent with the inhibition of PARP, successful knockdown of TRAF2 also did not affect the survival of GPx4-deficient fibroblasts (Figure 3.22 G,H).

In addition to the *in vitro* data, inhibition of PARP *in vivo* and its effects on erythropoiesis in GPx4^Δ mice were tested since there was significantly more phospho-H2A.X positive cells in the spleens of knockout animals (Figure 3.23 A-C). In consistency with the fibroblasts, inhibition of PARP also did not reverse the observed anemia and increased reticulocytosis in GPx4^Δ mice (Figure 3.23 A-C).

Taken altogether, despite a remarkable phospho-H2A.X in the absence of GPx4, observed cell death and anemia are not dependent on PARP activation.

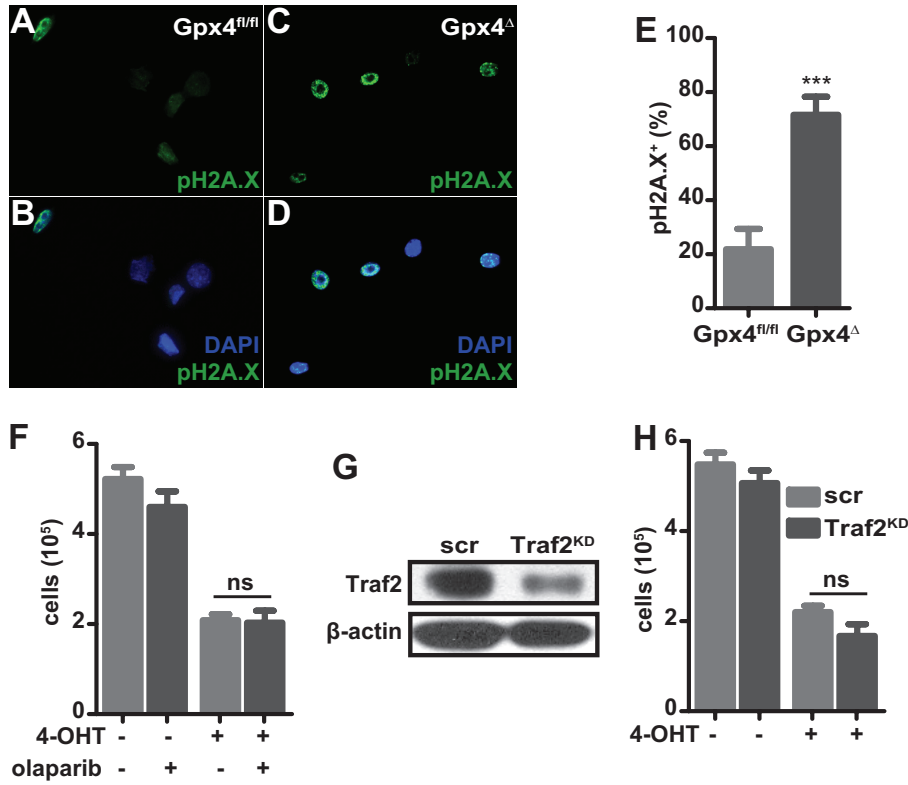


Figure 3.22: Inhibition of PARP does not rescue cell death of GPx4^Δ fibroblasts despite presence of marked DNA damage. (A-E) Immunofluorescent staining demonstrates significant increase in phospho-H2A.X positive nuclei in GPx4-deficient fibroblasts (C, D) compared to controls (A, B). (E) Quantification of phospho-H2A.X (pH2A.X) positive cells. Data are mean \pm SE; $n \geq 50$; *** $p < 0.001$ by t-test. (F) Survival of 4-OHT treated Pfa1 cells was not affected by the PARP inhibitor Olaparib (50 nM). Data are mean \pm SE; $n \geq 6$; ns: not significant. (G) Immunoblot analysis of TRAF2 in Pfa1 cells transfected with scrambled (scr) siRNA or TRAF2 siRNA pool. (H) Consistent with the PARP inhibition TRAF2 knockdown did not affect the survival of GPx4-deficient fibroblasts. Data are mean \pm SE; $n \geq 6$; ns: not significant.

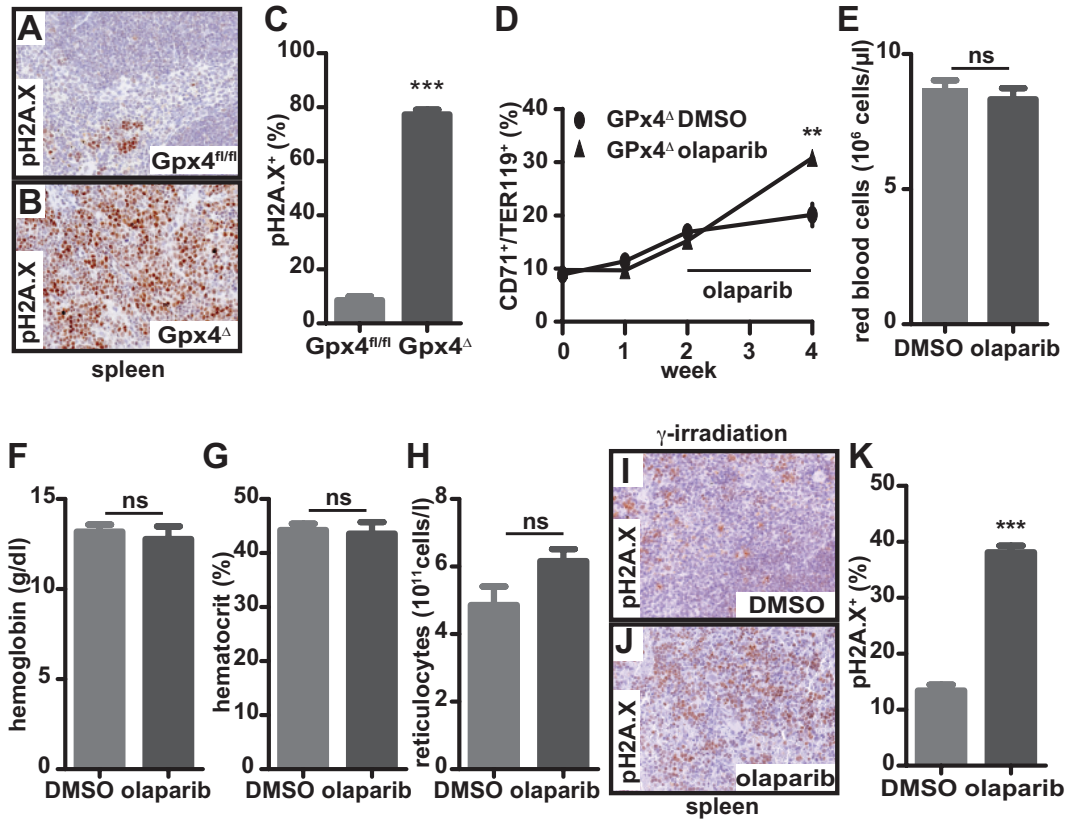


Figure 3.23: Inhibition of PARP does not rescue the anemia in *GPx4^Δ* mice despite the presence of marked DNA damage in the spleen. (A-C) Immunohistochemical analysis of phospho-H2A.X in spleen demonstrating significant DNA damage in *GPx4^Δ* mice (B) compared to controls (A). (C) Quantification of phospho-H2A.X positive cells. Data are mean \pm SE; $n \geq 5$; *** $p < 0.001$ by t-test. (D-H) *GPx4^Δ* mice were treated for 2 weeks with olaparib (5 mg/kg) or DMSO 2 weeks after the induction of deletion. (D) The number of peripheral CD71⁺/TER119⁺ cells was not decreased upon olaparib treatment. Data are mean \pm SE; $n \geq 5$ ** $p < 0.01$ by t-test. (E-H) Red blood cell parameters; red blood cells (E), hemoglobin (F), hematocrit (G) and reticulocytes (H) were not affected. Data are mean \pm SE; $n \geq 5$; ns: not significant. (I-K) Proof of olaparib efficiency in vivo. (I-J) Immunohistochemical analysis of phospho-H2A.X in spleen of the animals treated with a single dose of (J) olaparib or DMSO (I) upon 6 Gy γ -irradiation 4 hours after the treatment. The animals were sacrificed 4 hours after the irradiation. (H) Quantification of the phospho-H2A.X staining. Data are mean \pm SE; $n \geq 2$; *** $p < 0.001$ by t-test.

Chapter 4

Discussion

GPx4, with its unique characteristics and high hierarchy within mammalian seleno-proteins, is a major antioxidant, implicated in the regulation of several cellular processes including cell survival and cell death [94, 100, 101, 103, 104, 95]. The fact that its deletion is lethal during embryogenesis [95, 96] emphasizes the functional significance of GPx4 among all redox regulation enzymes. Even though the importance of GPx4 was underlined in many clinical concepts, its detailed mode of action is not clearly defined. Therefore, the study presented here provides valuable information, proposing a detailed model for the action of GPx4 in cellular homeostasis, which is supported by both *in vivo* and *in vitro* models. Based on the anemia observed in its absence, GPx4 is proved to be especially important for RBCs.

4.1 GPx4 deletion impairs cellular redox balance leading to accumulation of ROS and lipid peroxidation

The study confirms the expected elevation of ROS accumulation and lipid peroxidation in the absence of GPx4, one of the most important antioxidant enzymes, in RBCs as well as in murine embryonic fibroblasts. Due to their high reactivity, ROS cause damage to most biomolecules and are therefore potentially toxic, mutagenic or carcinogenic. Since an imbalanced cellular redox state can alter cellular homeostasis, not surprisingly, several cellular mechanisms are affected in the absence of GPx4.

Based on the results of *in vivo* and *in vitro* experiments, the data strongly suggest

that GPx4, via suppressing ROS accumulation and lipid peroxidation, maintains cellular homeostasis and protects cells from cell death.

4.1.1 Oxidative stress in RBCs causes anemia

Given the particular importance of ROS in RBCs, the role of GPx4, a unique antioxidant enzyme, has been investigated in this study using mouse models with GPx4 deletion in the hematopoietic system. The data enlighten crucial roles of GPx4 in the homeostasis of red blood cell lineage based on the anemia observed in GPx4 Δ mice. It has been shown in several studies that compromised protection from ROS results in diseases of red blood cells, often in anemia [166, 167, 168, 169]. Most of these studies suggested associations between accumulation of ROS and reduced survival of RBCs. The data obtained from the GPx4 deficient mice indicated that the ROS accumulation and lipid peroxidation lead to impaired maturation of reticulocytes, however, do not directly affect the life span of circulating erythrocytes (Figure 3.4) supporting previously known significance of GPx4 in differentiation and development [95, 96].

4.1.2 Vitamin E acts as a ROS scavenger in the absence of GPx4

The study pointed out the crucial role of vitamin E as a ROS scavenger in the absence of GPx4. Vitamin E supplementation reverts *in vitro* erythroid colony formation, which is completely abolished in GPx4 Δ BM (Figure 3.6). Furthermore, the cell death in fibroblasts under GPx4 depletion was rescued by vitamin E [103]. Most strikingly, anemia observed in GPx4 Δ mice is highly pronounced under vitamin E deficiency indicating that absence of vitamin E further elevates impaired maturation of reticulocytes and hinders the compensatory increase of erythropoiesis in GPx4 Δ mice (Figure 3.7). Given the role of vitamin E as a ROS scavenger, the data propose that the ROS accumulation under GPx4 depletion is partially suppressed in the presence of vitamin E. Therefore, it is not surprising that the downstream events, such as, cell death and impaired reticulocyte maturation are partially or completely

reversed by vitamin E by the maintenance of the cellular redox balance. Significantly less pronounced effects of vitamin E depletion on the red cell parameters in the presence of GPx4 prove that GPx4 and vitamin E are both important regulators of ROS accumulation and lipid peroxidation and compensate one another to a certain extent. The model proposed here clearly emphasize the clinical significance of dietary vitamin E.

4.2 Impaired autophagy in the absence of GPx4

It is shown that in the absence of GPx4, the resulting ROS and lipid peroxidation, interfering with the cellular redox regulation and homoeostasis, are triggering the activation of autophagy. Enhanced autophagy initiation in GPx4 deficient cells, is implied to be a survival mechanism activated to eliminate damaged cellular components. In the absence of GPx4, autophagy is shown to be initiated based on the early markers such as conversion of LC3, however, the process seems to be impaired and not finalized, based on p62 accumulation (Figure 3.8). Since, ROS is known to cause damage to all kinds of macromolecules in the cells and consequently causing alterations and defects in cellular mechanisms, it is not surprising to observe that among other pathways, autophagic machinery is affected by the cellular redox imbalance. LC3 conversion, which is used as a marker for autophagic vesicle formation, is established successfully, suggesting that the alterations are in the later stages of the process. The data suggest a possible defect in autophagy during fusion, vesicle elongation or degradation steps in GPx4 deficient systems based on the fact that the autophagy is progressed until the fusion of the autophagosomes with the lysosomes. Anemia associated with the impaired autophagy in the absence of GPx4 supports the findings in the study by Mortensen *et al.* supporting the essential role of autophagy during erythropoiesis using a mouse model lacking the essential autophagy gene Atg7 [249].

It has been suggested by Scherz-Shouval *et al.* that ROS is essential for the oxidative regulation of autophagy via inactivation of Atg4 at the site of autophagosome

formation that is promoting autophagy [212]. The presence of ROS can be beneficial for the cells in the initiation of autophagy at low doses and could support cell survival with the successive elimination of damaged cellular compartments. On the other hand, a defect in the process can give rise to higher doses of cellular ROS since autophagic degradation cannot be achieved. ROS accumulation provokes further damage and finally triggers cell death.

Remarkably, autophagy provides capacity for cell regeneration and restoration of proliferation and this recovery process is strongly impaired by defects in autophagy [258, 259]. Thus autophagy deficient cells are not only unable to tolerate metabolic stress but are also defective in the recovery process leading to elevation of stress, and to accumulation of damaged molecules and organelles.

Combined impairment of autophagy and apoptosis promotes necrotic cell death as shown previously in studies with apoptosis deficient tumor cells [258]. Therefore, impaired autophagy, observed in GPx4 deficient cells, might be a possible trigger for the activation of alternative cell death mechanisms. It is hypothesized that impaired autophagy is another way to account for the marked RIP1/RIP3 dependent necroptosis.

Whether the successful implementation of autophagy in GPx4 deficient cells would have achieved cell survival via elimination of damaged material or would have led to autophagic cell death is currently unknown and should be further investigated by means of description of the affected crucial elements of the pathway.

4.3 Loss of GPx4 leads to necroptosis

4.3.1 Inhibition of caspase dependent cell death in GPx4 deficient cells

In the GPx4 deficient models used in this study, the observed cell death is shown to be caspase independent as was previously suggested by Seiler *et al.* [103]. Not surprisingly, caspase 8, one of the main regulators of the cell fate, is found to be functionally inactivated in GPx4 deficient cells due to glutathionylation of the en-

zyme (Section 3.7). The functional inactivation of caspase 8 explains the activation of necroptosis as an alternative cell death mechanism in the absence of GPx4. A similar phenomenon was observed for caspase-1 inactivation in a study with SOD1-deficient macrophages [22].

Whereas reversible glutathionylation is an important regulatory mechanism for protection of proteins against oxidative stress, guiding correct protein folding, regulating protein activity, and modulating proteins based on redox signalling under normal conditions, irreversible glutathionylation might alter pathways, which regulate cell survival. Previous studies demonstrated that glutathione depletion or indirect depletion of glutathione as a consequence of a decrease in GSH/GSSH ratio plays a role in the regulation of cell death, including TNFR regulated mechanisms [260, 261, 22]. In the absence of GPx4, caspase 8 dependent apoptotic pathways are inhibited possibly due to imbalanced GSH/GSSH ratio (Section 3.7). It is highly possible that other apoptosis regulators are also affected by irreversible glutathionylation, yet, inhibition of caspase 8 has particular importance due to its key regulatory role for the decision of apoptotic or necroptotic cell death execution.

In light of the finding that treatment with DTT, a reducing agent targeting S-glutathionylation, reversed the observed cell death in fibroblasts (Figure 3.13), it is highly reasonable to assume that in addition to caspase 8, other molecules, especially the regulators of cell survival can be suffering from uncontrolled glutathionylation. One possible pathway affected is the $\text{NF}\kappa\text{B}$ pathway, a very important signalling pathway involved in the cellular responses to a wide variety of factors including oxidative stress. Previous studies reported that glutathionylation and deglutathionylation have been suggested to play important roles in the regulation of $\text{NF}\kappa\text{B}$ signalling [262, 263]. In addition to $\text{NF}\kappa\text{B}$ and caspase-1, other elements with particular importance on the cell survival, have been previously reported to be regulated by glutathionylation such as; caspase-3 [23], p53 [264], MEKK1 [265] and many others (reviewed in [15]). Whether the glutathionylation occurring in the absence of GPx4 also has impact on one or more of these elements is subject for further investigation. Possible effects of GPx4 deletion on the glutathionylation of those candidate path-

ways might provide information for defining the mechanistic role of GPx4 in other diseases such as neurodegenerative diseases or cancer.

4.3.2 Necroptosis as a cell death mechanism in the absence of GPx4

It is an important point for the proposed model in this study that ROS and lipid hydroperoxides act as upstream regulators of necroptosis independent of TNF α and FasL. Even though ROS have been implicated in previous studies as a mediator of TNF α induced necrosis in L929 cells [231, 266, 233], it was considered as downstream effector of necroptosis. Alternatively, emerging ROS and lipid peroxidation in GPx4 deficient cells constitute the upstream signaling of RIP1/RIP3 dependent necroptosis. This hypothesis is strongly supported based on several facts. The cell death observed in GPx4 deficient cells is not dependent on any of the known upstream activators of necroptosis such as TNFR or Fas (Section 3.8.4). Despite the presence of marked DNA damage, inhibition of PARP does not rescue cell death, ruling out PARP as an activator. The death complex harboring RIP1 and RIP3 formed in the absence of GPx4 does not involve the recruitment of FADD, which is described as a member of the conventional necrosome (Section 3.8.3). Although, nec-1 successfully inhibits the cell death, lipid peroxidation and ROS accumulation is not inhibited in GPx4 Δ cells, positioning ROS and lipid peroxidation upstream of RIP1/RIP3 dependent cell death.

Primary mechanisms of cell death involve apoptosis, autophagy and necrosis. Given the previous discussions about the inactivation of caspase 8 and impaired autophagy in GPx4 Δ cells, necrotic cell death was the presumable execution mechanism for the elimination of cells suffering from high doses of ROS accumulation and this is strongly supported by genetic and pharmacological evidence provided in the study (Section 3.8).

Taken together the results postulate a novel receptor-independent pathway for the intracellular initiation of necroptosis through the enhanced accumulation of ROS formation and lipid peroxides as upstream signaling components leading to activation of

RIP1/RIP3. Protein modification is induced either directly by ROS or indirectly by reaction with secondary products of oxidative stress. Whether there are particularly important lipid metabolites or ROS regulated elements, acting as secondary messenger molecules in the absence of GPx4, remains for further investigation. Reactive lipid derivatives have been implicated in apoptosis initiation governed by mitochondria with their high reactivity with nucleophiles such as the amino acids cysteine, lysine and histidine [267]. Several reactive lipid species have been implicated in pathological conditions involving cell death [268] therefore, identification of possible specific lipid derivatives arising in the absence of GPx4 might provide valuable information for understanding mechanistic events underlying indicated diseases.

It is known that oxidative stress causes an increase in redox active iron. Iron ions have been shown to exert a strong influence on the toxicity of reactive oxygen species [231]. Recently, ferroptosis is described as a unique iron-dependent form of nonapoptotic cell death, triggered by the lethal oncogenic Ras-selective small molecule erastin in cancer cells in an iron-dependent fashion [178]. The authors describe that ferroptosis is dependent on intracellular iron, but not other metals, and is morphologically, biochemically, and genetically distinct from apoptosis, necrosis, and autophagy and clearly, cannot be inhibited by nec-1 but with a potent inhibitor of ferroptosis ferrostatin-1. Despite its differences, ferroptosis might share common mechanisms with the cell death observed under GPx4 deficiency based on the common phenotype with glutamate induced cell death of neuronal cells [236].

Chapter 5

Conclusion

ROS are formed as normal by-products of aerobic metabolism. When kept under control they take part in the regulation of cellular pathways, however, elevated rates may lead to pathophysiological conditions. Hence, maintaining cellular redox balance is of vital importance for cell survival and tissue homeostasis since imbalanced production of ROS may lead to oxidative stress and cell death. In particular, erythrocytes are highly sensitive to ROS accumulation due to their physiological function in oxygen transport and several antioxidant mechanisms take part in the regulation of ROS in this lineage. GPx4, one of the most important ROS scavenging selenoproteins, is a unique antioxidant enzyme that can directly reduce phospholipid hydroperoxide in mammalian cells, yet, its specific function in RBCs has not been investigated to date.

Taking advantage of mice with hematopoietic specific deletion of GPx4, GPx4 is shown to be essential for reticulocyte maturation. Loss of GPx4 in erythroid cells results in ROS accumulation and lipid peroxidation leading to impaired reticulocyte maturation and subsequently to anemia. Anemia is compensated to a certain extent, as indicated by the high reticulocyte counts and serum EPO levels. Additional depletion of vitamin E strongly elevates the anemia and attenuates compensatory erythropoiesis indicating the crucial role of vitamin E as a ROS scavenger in the absence of GPx4.

Moreover, the data provide evidence that the autophagic flux is impaired in the absence of GPx4. Imbalanced ROS accumulation triggers initiation of autophagy,

which acts as a reliable detoxification mechanism. Absence of GPx4, however, inhibits autophagic flux and therefore excludes autophagy as a counteracting mechanism.

The use of an *in vitro* model of murine embryonic fibroblasts provided insights for the mechanism of cell death in GPx4^Δ cells. The scheme depicted in Figure 5.1 illustrates the cellular homeostasis controlled by GPx4 and vitamin E and the cell death mechanism activated in their absence, supported by both *in vitro* and *in vivo* findings. The model suggests that GPx4 and vitamin E act as ROS scavengers to control the cellular redox state and they can compensate each other to a certain extent. Accumulation of ROS and lipid peroxidation in the absence of GPx4 and vitamin E inhibit autophagic flux, which is a potential counteracting mechanism for elimination of oxidized cellular material. Additionally, caspase 8, one of the main regulatory elements of cell death execution, is inhibited due to glutathionylation. Therefore, inhibition of both autophagy and caspase dependent cell death mechanisms constitute the basis for the induction of the alternative cell death mechanism, namely RIP1/RIP3 dependent necroptosis. The cell death observed in the absence of GPx4, shares common features with the recently described necroptosis and can also be inhibited with the specific necroptosis inhibitor nec-1, however, its activation is independent of the previously described upstream TNFR signaling. The model proposes a novel receptor-independent pathway for the initiation of necroptosis that is initiated intracellularly through enhanced accumulation of ROS and formation of lipid peroxides as upstream signaling components leading to activation of RIP1/RIP3 (Figure 5.1 B, C).

This study provides findings of clinical importance that will contribute to deciphering the underlying mechanisms of diseases and pathological conditions associated with GPx4 as well as other antioxidant enzymes.

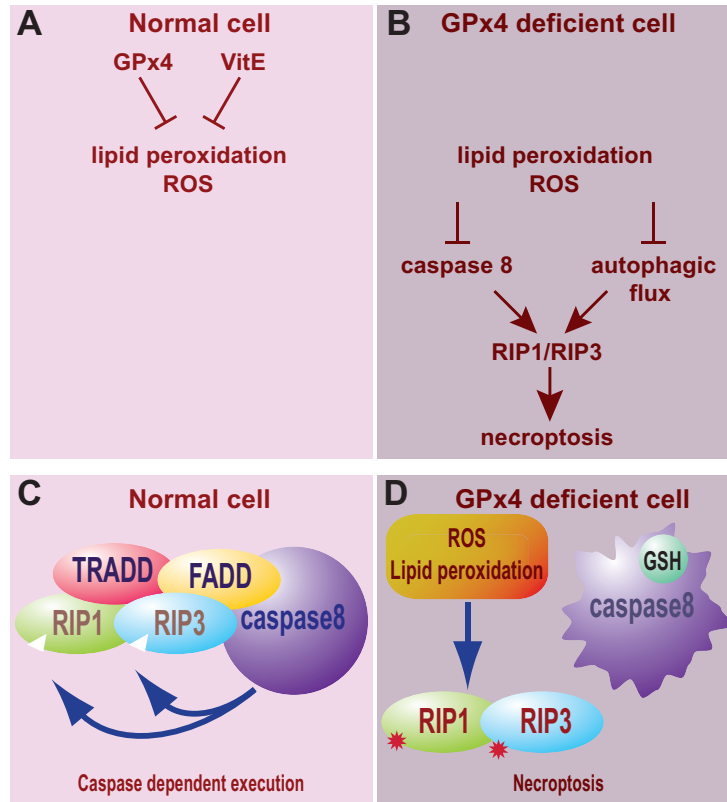


Figure 5.1: Summary of the proposed model explaining the cellular role of GPx4. (A-B) The model presented here suggest that GPx4 and vitamin E act as ROS scavengers and control the cellular redox state. In the absence of GPx4, autophagic flux, which would have been a counteracting mechanism for elimination of oxidized cellular material is inhibited. Also, caspase 8, one of the main regulatory elements of cell death execution, is inhibited due to glutathionylation. Inhibition of both caspase dependent cell death mechanisms and autophagy constitutes the basis for the execution of the alternative cell death mechanism, namely RIP1/RIP3 dependent necroptosis. Although the cell death observed in the absence of GPx4, shares common features with the recently described necroptosis, the pathway, which is activated, differs in the regulatory phase. (C-D) The model proposes a novel receptor-independent pathway for the initiation of necroptosis that is regulated intracellularly trough the enhanced accumulation of ROS and formation of lipid peroxides as upstream signaling components leading to activation of RIP1/RIP3.

Bibliography

- [1] E. L. Thomas, R. I. Lehrer, and R. F. Rest. Human neutrophil antimicrobial activity. *Rev Infect Dis*, 10 Suppl 2:S450–S456, Jan 1988.
- [2] F. Rossi, P. Bellavite, G. Berton, M. Grzeskowiak, and E. Papini. Mechanism of production of toxic oxygen radicals by granulocytes and macrophages and their function in the inflammatory process. *Pathol Res Pract*, 180:136–142, Aug 1985.
- [3] H. Rosen, J. Orman, R. M. Rakita, B. R. Michel, and D. R. VanDevanter. Loss of dna-membrane interactions and cessation of dna synthesis in myeloperoxidase-treated escherichia coli. *Proc Natl Acad Sci U S A*, 87:10048–10052, Dec 1990.
- [4] M. Valko, D. Leibfritz, J. Moncol, M. T. D. Cronin, M. Mazur, and J. Telser. Free radicals and antioxidants in normal physiological functions and human disease. *Int J Biochem Cell Biol*, 39:44–84, Jan 2007.
- [5] L. J. Marnett. Oxyradicals and dna damage. *Carcinogenesis*, 21:361–370, Mar 2000.
- [6] H. Kasai and S. Nishimura. Hydroxylation of deoxyguanosine at the c-8 position by ascorbic acid and other reducing agents. *Nucleic Acids Res*, 12:2137–2145, Feb 1984.
- [7] B. Halliwell. The role of oxygen radicals in human disease, with particular reference to the vascular system. *Haemostasis*, 23 Suppl 1:118–126, Mar 1993.
- [8] B. Frei. On the role of vitamin c and other antioxidants in atherogenesis and vascular dysfunction. *Proc Soc Exp Biol Med*, 222:196–204, Dec 1999.
- [9] N. A. Porter. Mechanisms for the autoxidation of polyunsaturated lipids. 19:262–268, Jan 1986.
- [10] D. Steinberg. Low density lipoprotein oxidation and its pathobiological significance. *J Biol Chem*, 272:20963–20966, Aug 1997.
- [11] A. Higdon, A. R. Diers, J. Y. Oh, A. Landar, and V. M. Darley-Usmar. Cell signalling by reactive lipid species: new concepts and molecular mechanisms. *Biochem J*, 442:453–464, Mar 2012.
- [12] E. R. Stadtman and B. S. Berlett. Reactive oxygen-mediated protein oxidation in aging and disease. *Drug Metab Rev*, 30:225–243, May 1998.
- [13] E. R. Stadtman and R. L. Levine. Free radical-mediated oxidation of free amino acids and amino acid residues in proteins. *Amino Acids*, 25:207–218, Dec 2003.
- [14] W. T. Lowther, N. Brot, H. Weissbach, J. F. Honek, and B. W. Matthews. Thiol-disulfide exchange is involved in the catalytic mechanism of peptide methionine sulfoxide reductase. *Proc Natl Acad Sci U S A*, 97:6463–6468, Jun 2000.
- [15] A. J. Cooper, J. T. Pinto, and P. S. Callery. Reversible and irreversible protein glutathionylation: biological and clinical aspects. *Expert Opin Drug Metab Toxicol*, 7:891–910, Jul 2011.
- [16] R. J. Mallis, M. J. Hamann, W. Zhao, T. Zhang, S. Hendrich, and J. A. Thomas. Irreversible thiol oxidation in carbonic anhydrase iii: protection by s-glutathiolation and detection in aging rats. *Biol Chem*, 383:649–662, Jan 2002.
- [17] B. S. Berlett and E. R. Stadtman. Protein oxidation in aging, disease, and oxidative stress. *J Biol Chem*, 272:20313–20316, Aug 1997.
- [18] E. R. Stadtman. Protein oxidation and aging. *Science*, 257:1220–1224, Aug 1992.
- [19] R. L. Levine. Carbonyl modified proteins in cellular regulation, aging, and disease. *Free Radic Biol Med*, 32:790–796, May 2002.

- [20] I. Dalle-Donne, R. Rossi, D. Giustarini, R. Colombo, and A. Milzani. S-glutathionylation in protein redox regulation. *Free Radic Biol Med*, 43:883–898, Sep 2007.
- [21] A. Delaunay, A. D. Isnard, and M. B. Toledano. H₂O₂ sensing through oxidation of the yap1 transcription factor. *EMBO J*, 19:5157–5166, Oct 2000.
- [22] F. Meissner, K. Molawi, and A. Zychlinsky. Superoxide dismutase 1 regulates caspase-1 and endotoxic shock. *Nat Immunol*, 9:866–872, Aug 2008.
- [23] Z. Huang, J. T. Pinto, H. Deng, and J. P. Richie. Inhibition of caspase-3 activity and activation by protein glutathionylation. *Biochem Pharmacol*, 75:2234–2244, Jun 2008.
- [24] D. Trachootham, W. Lu, M. A. Ogasawara, R. D. Nilsa, and P. Huang. Redox regulation of cell survival. *Antioxid Redox Signal*, 10:1343–1374, Aug 2008.
- [25] R. Brigelius-Flohé and M. G. Traber. Vitamin e: function and metabolism. *FASEB J*, 13:1145–1155, Jul 1999.
- [26] M. G. Traber and J. Atkinson. Vitamin e, antioxidant and nothing more. *Free Radic Biol Med*, 43:4, Jul 2007.
- [27] J. Neuzil, P. K. Witting, and R. Stocker. Alpha-tocopheryl hydroquinone is an efficient multifunctional inhibitor of radical-initiated oxidation of low density lipoprotein lipids. *Proc Natl Acad Sci U S A*, 94:7885–7890, Jul 1997.
- [28] S. J. Padayatty, A. Katz, Y. Wang, P. Eck, O. Kwon, J. H. Lee, S. Chen, C. Corpe, A. Dutta, S. K. Dutta, and M. Levine. Vitamin c as an antioxidant: evaluation of its role in disease prevention. *J Am Coll Nutr*, 22:18–35, Feb 2003.
- [29] S. Englund and S. Seifter. The biochemical functions of ascorbic acid. *Annu Rev Nutr*, 6:365–406, Jan 1986.
- [30] B. H. Bielski, H. W. Richter, and P. C. Chan. Some properties of the ascorbate free radical. *Ann N Y Acad Sci*, 258:231–237, Sep 1975.
- [31] B. Halliwell. Vitamin c: antioxidant or pro-oxidant in vivo? *Free Radic Res*, 25:439–454, Nov 1996.
- [32] I. D. Podmore, H. R. Griffiths, K. E. Herbert, N. Mistry, P. Mistry, and J. Lunec. Vitamin c exhibits pro-oxidant properties. *Nature*, 392:559, Apr 1998.
- [33] A. Meister and M. E. Anderson. Glutathione. *Annu Rev Biochem*, 52:711–760, Jan 1983.
- [34] O. Carmel-Harel and G. Storz. Roles of the glutathione- and thioredoxin-dependent reduction systems in the escherichia coli and saccharomyces cerevisiae responses to oxidative stress. *Annu Rev Microbiol*, 54:439–461, Jan 2000.
- [35] P. M. Kidd. Glutathione: systemic protectant against oxidative and free radical damage. *Altern Med Rev*, 1:155–176, 1997.
- [36] I. A. Cotgreave and R. G. Gerdes. Recent trends in glutathione biochemistry—glutathione-protein interactions: a molecular link between oxidative stress and cell proliferation? *Biochem Biophys Res Commun*, 242:1–9, Jan 1998.
- [37] D. J. van den Dobbela, C. S. Nobel, J. Schlegel, I. A. Cotgreave, S. Orrenius, and A. F. Slater. Rapid and specific efflux of reduced glutathione during apoptosis induced by anti-fas/apo-1 antibody. *J Biol Chem*, 271:15420–15427, Jun 1996.
- [38] D. W. Voehringer. Bcl-2 and glutathione: alterations in cellular redox state that regulate apoptosis sensitivity. *Free Radic Biol Med*, 27:945–950, Nov 1999.
- [39] R. Franco and J. A. Cidlowski. Apoptosis and glutathione: beyond an antioxidant. *Cell Death Differ*, 16:1303–1314, Oct 2009.
- [40] J. M. McCord and I. Fridovich. Superoxide dismutase. an enzymic function for erythrocyte hemocuprein. *J Biol Chem*, 244:6049–6055, Nov 1969.
- [41] A. F. Miller. Superoxide dismutases: ancient enzymes and new insights. *FEBS Lett*, 586:585–595, Mar 2012.
- [42] R. E. Blankenship. Early evolution of photosynthesis. *Plant Physiol*, 154:434–438, Oct 2010.
- [43] T. Fukui and M. Ushio-Fukai. Superoxide dismutases: role in redox signaling, vascular function, and diseases. *Antioxid Redox Signal*, 15:1583–1606, Sep 2011.
- [44] D. R. Rosen, T. Siddique, D. Patterson, D. A. Figlewicz, P. Sapp, A. Hentati, D. Donaldson, J. Goto, J. P. O’Regan, and H. X. Deng. Mutations in cu/zn superoxide dismutase gene are associated with familial amyotrophic lateral sclerosis. *Nature*, 362:59–62, Mar 1993.

- [45] R. W. Orrell. Amyotrophic lateral sclerosis: copper/zinc superoxide dismutase (sod1) gene mutations. *Neuromuscul Disord*, 10:63–68, Jan 2000.
- [46] J. S. Friedman, M. F. Lopez, M. D. Fleming, A. Rivera, F. M. Martin, M. L. Welsh, A. Boyd, S. R. Doctrow, and S. J. Burakoff. Sod2-deficiency anemia: protein oxidation and altered protein expression reveal targets of damage, stress response, and antioxidant responsiveness. *Blood*, 104:2565–2573, Oct 2004.
- [47] F. M. Martin, X. Xu, Löhneysen K. von, T. J. Gilmartin, and J. S. Friedman. Sod2 deficient erythroid cells up-regulate transferrin receptor and down-regulate mitochondrial biogenesis and metabolism. *PLoS One*, 6:e16894, Jan 2011.
- [48] H. N. Kirkman and G. F. Gaetani. Catalase: a tetrameric enzyme with four tightly bound molecules of nadph. *Proc Natl Acad Sci U S A*, 81:4343–4347, Jul 1984.
- [49] J. Nordberg and E. S. Arnér. Reactive oxygen species, antioxidants, and the mammalian thioredoxin system. *Free Radic Biol Med*, 31:1287–1312, Dec 2001.
- [50] M. M. Goyal and A. Basak. Human catalase: looking for complete identity. *Protein Cell*, 1:888–897, Oct 2010.
- [51] G. F. Gaetani, S. Galiano, L. Canepa, A. M. Ferraris, and H. N. Kirkman. Catalase and glutathione peroxidase are equally active in detoxification of hydrogen peroxide in human erythrocytes. *Blood*, 73:334–339, Jan 1989.
- [52] B. Halliwell and J. M. Gutteridge. Oxygen toxicity, oxygen radicals, transition metals and disease. *Biochem J*, 219:1, Apr 1984.
- [53] M. Vuillaume. Reduced oxygen species, mutation, induction and cancer initiation. *Mutat Res*, 186:43–72, Jul 1987.
- [54] T. Miyamoto, M. Hayashi, A. Takeuchi, T. Okamoto, S. Kawashima, T. Takii, H. Hayashi, and K. Onozaki. Identification of a novel growth-promoting factor with a wide target cell spectrum from various tumor cells as catalase. *J Biochem*, 120:725–730, Oct 1996.
- [55] K. N. Islam, Y. Kayanoki, H. Kaneto, K. Suzuki, M. Asahi, J. Fujii, and N. Taniguchi. Tgf-beta1 triggers oxidative modifications and enhances apoptosis in hit cells through accumulation of reactive oxygen species by suppression of catalase and glutathione peroxidase. *Free Radic Biol Med*, 22:1007–1017, Jan 1997.
- [56] A. Holmgren. Thioredoxin. *Annu Rev Biochem*, 54:237–271, Jan 1985.
- [57] A. Rubartelli, N. Bonifaci, and R. Sitia. High rates of thioredoxin secretion correlate with growth arrest in hepatoma cells. *Cancer Res*, 55:675–680, Feb 1995.
- [58] M. Aota, K. Matsuda, N. Isowa, H. Wada, J. Yodoi, and T. Ban. Protection against reperfusion-induced arrhythmias by human thioredoxin. *J Cardiovasc Pharmacol*, 27:727–732, May 1996.
- [59] E. S. Arnér and A. Holmgren. Physiological functions of thioredoxin and thioredoxin reductase. *Eur J Biochem*, 267:6102–6109, Oct 2000.
- [60] K. Becker, S. Gromer, R. H. Schirmer, and S. Müller. Thioredoxin reductase as a pathophysiological factor and drug target. *Eur J Biochem*, 267:6118–6125, Oct 2000.
- [61] H. Z. Chae, H. J. Kim, S. W. Kang, and S. G. Rhee. Characterization of three isoforms of mammalian peroxiredoxin that reduce peroxides in the presence of thioredoxin. *Diabetes Res Clin Pract*, 45:101–112, Sep 1999.
- [62] R. Bryk, P. Griffin, and C. Nathan. Peroxynitrite reductase activity of bacterial peroxiredoxins. *Nature*, 407:211–215, Sep 2000.
- [63] Z. A. Wood, L. B. Poole, and P. A. Karplus. Peroxiredoxin evolution and the regulation of hydrogen peroxide signaling. *Science*, 300:650–653, Apr 2003.
- [64] J. Fujii and Y. Ikeda. Advances in our understanding of peroxiredoxin, a multifunctional, mammalian redox protein. *Redox Rep*, 7:123–130, Jan 2002.
- [65] L. H. Butterfield, A. Merino, S. H. Golub, and H. Shau. From cytoprotection to tumor suppression: the multifactorial role of peroxiredoxins. *Antioxid Redox Signal*, 1:385–402, Jan 1999.
- [66] S. G. Rhee, H. A. Woo, I. S. Kil, and S. H. Bae. Peroxiredoxin functions as a peroxidase and a regulator and sensor of local peroxides. *J Biol Chem*, 287:4403–4410, Feb 2012.
- [67] Y. Zhou, K. H. Kok, A. C. Chun, C. M. Wong, H. W. Wu, M. C. Lin, P. C. Fung, H. Kung, and D. Y. Jin. Mouse peroxiredoxin v is a thioredoxin peroxidase that inhibits p53-induced apoptosis. *Biochem Biophys Res Commun*, 268:921–927, Feb 2000.

- [68] P. Zhang, B. Liu, S. W. Kang, M. S. Seo, S. G. Rhee, and L. M. Obeid. Thioredoxin peroxidase is a novel inhibitor of apoptosis with a mechanism distinct from that of bcl-2. *J Biol Chem*, 272:30615–30618, Dec 1997.
- [69] G. C. Mills. Hemoglobin catabolism. i. glutathione peroxidase, an erythrocyte enzyme which protects hemoglobin from oxidative breakdown. *J Biol Chem*, 229:189–197, Nov 1957.
- [70] L. Flohe, W. A. Günzler, and H. H. Schock. Glutathione peroxidase: A selenoenzyme. 32:132–134, Jan 1973.
- [71] K. Wingler and R. Brigelius-Flohé. Gastrointestinal glutathione peroxidase. *Biofactors*, 10:245–249, Jan 1999.
- [72] F. F. Chu, J. H. Doroshov, and R. S. Esworthy. Expression, characterization, and tissue distribution of a new cellular selenium-dependent glutathione peroxidase, gshpx-gi. *J Biol Chem*, 268:2571–2576, Feb 1993.
- [73] K. Takahashi, M. Akasaka, Y. Yamamoto, C. Kobayashi, J. Mizoguchi, and J. Koyama. Primary structure of human plasma glutathione peroxidase deduced from cdna sequences. *J Biochem*, 108:145–148, Aug 1990.
- [74] E. A. Knopp, T. L. Arndt, K. L. Eng, M. Caldwell, R. C. LeBoeuf, S. S. Deeb, and K. D. O'Brien. Murine phospholipid hydroperoxide glutathione peroxidase: cdna sequence, tissue expression, and mapping. *Mamm Genome*, 10:601–605, Jun 1999.
- [75] R. S. Esworthy, K. Doan, J. H. Doroshov, and F. F. Chu. Cloning and sequencing of the cdna encoding a human testis phospholipid hydroperoxide glutathione peroxidase. *Gene*, 144:317–318, Jul 1994.
- [76] A. Borchert, N. E. Savaskan, and H. Kuhn. Regulation of expression of the phospholipid hydroperoxide/sperm nucleus glutathione peroxidase gene. tissue-specific expression pattern and identification of functional cis- and trans-regulatory elements. *J Biol Chem*, 278:2571–2580, Jan 2003.
- [77] P. Vernet, N. Rigaudière, N. Ghyselinck, J. P. Dufaure, and J. R. Drevet. In vitro expression of a mouse tissue specific glutathione-peroxidase-like protein lacking the selenocysteine can protect stably transfected mammalian cells against oxidative damage. *Biochem Cell Biol*, 74:125–131, Jan 1996.
- [78] A. Utomo, X. Jiang, S. Furuta, J. Yun, D. S. Levin, Y. J. Wang, K. V. Desai, J. E. Green, P. L. Chen, and W. H. Lee. Identification of a novel putative non-selenocysteine containing phospholipid hydroperoxide glutathione peroxidase (npgpx) essential for alleviating oxidative stress generated from polyunsaturated fatty acids in breast cancer cells. *J Biol Chem*, 279:43522–43529, Oct 2004.
- [79] J. R. Arthur. The glutathione peroxidases. *Cell Mol Life Sci*, 57:1825–1835, Dec 2000.
- [80] A. Grossmann and A. Wendel. Non-reactivity of the selenoenzyme glutathione peroxidase with enzymatically hydroperoxidized phospholipids. *Eur J Biochem*, 135:549–552, Oct 1983.
- [81] X. G. Lei and W. H. Cheng. New roles for an old selenoenzyme: evidence from glutathione peroxidase-1 null and overexpressing mice. *J Nutr*, 135:2295–2298, Oct 2005.
- [82] U. Schweizer and L. Schomburg. New insights into the physiological actions of selenoproteins from genetically modified mice. *IUBMB Life*, 57:737–744, Nov 2005.
- [83] Y. S. Ho, J. L. Magnenat, R. T. Bronson, J. Cao, M. Gargano, M. Sugawara, and C. D. Funk. Mice deficient in cellular glutathione peroxidase develop normally and show no increased sensitivity to hyperoxia. *J Biol Chem*, 272:16644–16651, Jun 1997.
- [84] J. B. de Haan, C. Bladier, P. Griffiths, M. Kelner, R. D. O'Shea, N. S. Cheung, R. T. Bronson, M. J. Silvestro, S. Wild, S. S. Zheng, P. M. Beart, P. J. Hertzog, and I. Kola. Mice with a homozygous null mutation for the most abundant glutathione peroxidase, gpx1, show increased susceptibility to the oxidative stress-inducing agents paraquat and hydrogen peroxide. *J Biol Chem*, 273:22528–22536, Aug 1998.
- [85] W. H. Cheng, Y. S. Ho, B. A. Valentine, D. A. Ross, G. F. Combs, and X. G. Lei. Cellular glutathione peroxidase is the mediator of body selenium to protect against paraquat lethality in transgenic mice. *J Nutr*, 128:1070–1076, Jul 1998.
- [86] R. S. Esworthy, R. Aranda, M. G. Martín, J. H. Doroshov, S. W. Binder, and F. F. Chu. Mice with combined disruption of gpx1 and gpx2 genes have colitis. *Am J Physiol Gastrointest Liver Physiol*, 281:G848–G855, Sep 2001.
- [87] R. Brigelius-Flohé. Tissue-specific functions of individual glutathione peroxidases. *Free Radic Biol Med*, 27:951–965, Nov 1999.
- [88] D. Behne and A. Kyriakopoulos. Mammalian selenium-containing proteins. *Annu Rev Nutr*, 21:453–473, Jan 2001.
- [89] F. Ursini, M. Maiorino, M. Valente, L. Ferri, and C. Gregolin. Purification from pig liver of a protein which protects liposomes and biomembranes from peroxidative degradation and exhibits glutathione peroxidase activity on phosphatidylcholine hydroperoxides. *Biochim Biophys Acta*, 710:197–211, Feb 1982.

- [90] F. Ursini, M. Maiorino, and C. Gregolin. The selenoenzyme phospholipid hydroperoxide glutathione peroxidase. *Biochim Biophys Acta*, 839:62–70, Mar 1985.
- [91] M. Maiorino, F. F. Chu, F. Ursini, K. J. Davies, J. H. Doroshov, and R. S. Esworthy. Phospholipid hydroperoxide glutathione peroxidase is the 18-kda selenoprotein expressed in human tumor cell lines. *J Biol Chem*, 266:7728–7732, Apr 1991.
- [92] R. Schuckelt, R. Brigelius-Flohé, M. Maiorino, A. Roveri, J. Reumkens, W. Strassburger, F. Ursini, B. Wolf, and L. Flohé. Phospholipid hydroperoxide glutathione peroxidase is a selenoenzyme distinct from the classical glutathione peroxidase as evident from cdna and amino acid sequencing. *Free Radic Res Commun*, 14:343–361, Jan 1991.
- [93] F. Ursini, S. Heim, M. Kiess, M. Maiorino, A. Roveri, J. Wissing, and L. Flohé. Dual function of the selenoprotein phgpx during sperm maturation. *Science*, 285:1393–1396, Aug 1999.
- [94] R. Brigelius-Flohé. Glutathione peroxidases and redox-regulated transcription factors. *Biol Chem*, 387:1329–1335, Jan 2006.
- [95] H. Imai and Y. Nakagawa. Biological significance of phospholipid hydroperoxide glutathione peroxidase (phgpx, gpx4) in mammalian cells. *Free Radic Biol Med*, 34:145–169, Jan 2003.
- [96] L. J. Yant, Q. Ran, L. Rao, R. H. Van, T. Shibata, J. G. Belter, L. Motta, A. Richardson, and T. A. Prolla. The selenoprotein gpx4 is essential for mouse development and protects from radiation and oxidative damage insults. 34:496–502, Jan 2003.
- [97] F. Weitzel and A. Wendel. Selenoenzymes regulate the activity of leukocyte 5-lipoxygenase via the peroxide tone. *J Biol Chem*, 268:6288–6292, Mar 1993.
- [98] M. Conrad, S. G. Moreno, F. Sinowatz, F. Ursini, S. Kölle, A. Roveri, M. Brielmeier, W. Wurst, M. Maiorino, and G. W. Bornkamm. The nuclear form of phospholipid hydroperoxide glutathione peroxidase is a protein thiol peroxidase contributing to sperm chromatin stability. *Mol Cell Biol*, 25:7637–7644, Sep 2005.
- [99] Y. Bao, P. Jemth, B. Mannervik, and G. Williamson. Reduction of thymine hydroperoxide by phospholipid hydroperoxide glutathione peroxidase and glutathione transferases. *FEBS Lett*, 410:210–212, Jun 1997.
- [100] M. Arai, H. Imai, T. Koumura, M. Yoshida, K. Emoto, M. Umeda, N. Chiba, and Y. Nakagawa. Mitochondrial phospholipid hydroperoxide glutathione peroxidase plays a major role in preventing oxidative injury to cells. *J Biol Chem*, 274:4924–4933, Feb 1999.
- [101] K. Nomura, H. Imai, T. Koumura, M. Arai, and Y. Nakagawa. Mitochondrial phospholipid hydroperoxide glutathione peroxidase suppresses apoptosis mediated by a mitochondrial death pathway. *J Biol Chem*, 274:29294–29302, Oct 1999.
- [102] K. Yagi, S. Komura, H. Kojima, Q. Sun, N. Nagata, N. Ohishi, and M. Nishikimi. Expression of human phospholipid hydroperoxide glutathione peroxidase gene for protection of host cells from lipid hydroperoxide-mediated injury. *Biochem Biophys Res Commun*, 219:486–491, Feb 1996.
- [103] A. Seiler, M. Schneider, H. Förster, S. Roth, E. K. Wirth, C. Culmsee, N. Plesnila, E. Kremmer, O. Radmark, W. Wurst, G. W. Bornkamm, U. Schweizer, and M. Conrad. Glutathione peroxidase 4 senses and translates oxidative stress into 12/15-lipoxygenase dependent- and aif-mediated cell death. *Cell Metab*, 8:237–248, Sep 2008.
- [104] A. Borchert, C. C. Wang, C. Ufer, H. Schiebel, N. E. Savaskan, and H. Kuhn. The role of phospholipid hydroperoxide glutathione peroxidase isoforms in murine embryogenesis. *J Biol Chem*, 281:19655–19664, Jul 2006.
- [105] C. Ufer and C. C. Wang. The roles of glutathione peroxidases during embryo development. *Front Mol Neurosci*, 4:12, Jan 2011.
- [106] J. P. Thomas, P. G. Geiger, M. Maiorino, F. Ursini, and A. W. Girotti. Enzymatic reduction of phospholipid and cholesterol hydroperoxides in artificial bilayers and lipoproteins. *Biochim Biophys Acta*, 1045:252–260, Aug 1990.
- [107] W. Sattler, M. Maiorino, and R. Stocker. Reduction of hdl- and ldl-associated cholesterylester and phospholipid hydroperoxides by phospholipid hydroperoxide glutathione peroxidase and ebselen (pz 51). *Arch Biochem Biophys*, 309:214–221, Mar 1994.
- [108] C. Godeas, F. Tramer, F. Micali, M. Soranzo, G. Sandri, and E. Panfilì. Distribution and possible novel role of phospholipid hydroperoxide glutathione peroxidase in rat epididymal spermatozoa. *Biol Reprod*, 57:1502–1508, Dec 1997.
- [109] P. Scheerer, A. Borchert, N. Krauss, H. Wessner, C. Gerth, W. Höhne, and H. Kuhn. Structural basis for catalytic activity and enzyme polymerization of phospholipid hydroperoxide glutathione peroxidase-4 (gpx4). *Biochemistry*, 46:9041–9049, Aug 2007.

- [110] A. M. Mannes, A. Seiler, V. Bosello, M. Maiorino, and M. Conrad. Cysteine mutant of mammalian gpx4 rescues cell death induced by disruption of the wild-type selenoenzyme. *FASEB J*, 25:2135–2144, Jul 2011.
- [111] H. Imai, K. Suzuki, K. Ishizaka, S. Ichinose, H. Oshima, I. Okayasu, K. Emoto, M. Umeda, and Y. Nakagawa. Failure of the expression of phospholipid hydroperoxide glutathione peroxidase in the spermatozoa of human infertile males. *Biol Reprod*, 64:674–683, Feb 2001.
- [112] M. Diaconu, Y. Tangat, D. Böhm, H. Kühn, H. W. Michelmann, G. Schreiber, G. Haidl, H. J. Glander, W. Engel, and K. Nayernia. Failure of phospholipid hydroperoxide glutathione peroxidase expression in oligoasthenozoospermia and mutations in the phgpx gene. *Andrologia*, 38:152–157, Aug 2006.
- [113] M. J. Kelner and M. A. Montoya. Structural organization of the human selenium-dependent phospholipid hydroperoxide glutathione peroxidase gene (gpx4): chromosomal localization to 19p13.3. *Biochem Biophys Res Commun*, 249:53–55, Aug 1998.
- [114] A. Borchert, K. Schnurr, B. J. Thiele, and H. Kühn. Cloning of the mouse phospholipid hydroperoxide glutathione peroxidase gene. *FEBS Lett*, 446:223–227, Mar 1999.
- [115] H. Pfeifer, M. Conrad, D. Roethlein, A. Kyriakopoulos, M. Brielmeier, G. W. Bornkamm, and D. Behne. Identification of a specific sperm nuclei selenoenzyme necessary for protamine thiol cross-linking during sperm maturation. *FASEB J*, 15:1236–1238, May 2001.
- [116] M. Maiorino, K. D. Aumann, R. Brigelius-Flohé, D. Doria, J. van den Heuvel, J. McCarthy, A. Roveri, F. Ursini, and L. Flohé. Probing the presumed catalytic triad of selenium-containing peroxidases by mutational analysis of phospholipid hydroperoxide glutathione peroxidase (phgpx). *Biol Chem Hoppe Seyler*, 376:651–660, Nov 1995.
- [117] Y. Shidoji, K. Okamoto, Y. Muto, S. Komura, N. Ohishi, and K. Yagi. Prevention of geranylgeranoic acid-induced apoptosis by phospholipid hydroperoxide glutathione peroxidase gene. *J Cell Biochem*, 97:178–187, Jan 2006.
- [118] M. Brielmeier, J. M. Béchet, S. Suppmann, M. Conrad, G. Laux, and G. W. Bornkamm. Cloning of phospholipid hydroperoxide glutathione peroxidase (phgpx) as an anti-apoptotic and growth promoting gene of burkitt lymphoma cells. *Biofactors*, 14:179–190, Jan 2001.
- [119] K. Nomura, H. Imai, T. Koumura, T. Kobayashi, and Y. Nakagawa. Mitochondrial phospholipid hydroperoxide glutathione peroxidase inhibits the release of cytochrome c from mitochondria by suppressing the peroxidation of cardiolipin in hypoglycaemia-induced apoptosis. *Biochem J*, 351:183–193, Oct 2000.
- [120] M. Schneider, H. Förster, A. Boersma, A. Seiler, H. Wehnes, F. Sinowatz, C. Neumüller, M. J. Deutsch, A. Walch, M. Hrabé de Angelis, W. Wurst, F. Ursini, A. Roveri, M. Maleszewski, M. Maiorino, and M. Conrad. Mitochondrial glutathione peroxidase 4 disruption causes male infertility. *FASEB J*, 23:3233–3242, Sep 2009.
- [121] H. Liang, S. E. Yoo, R. Na, C. A. Walter, A. Richardson, and Q. Ran. Short form glutathione peroxidase 4 is the essential isoform required for survival and somatic mitochondrial functions. *J Biol Chem*, 284:30836–30844, Nov 2009.
- [122] R. Brigelius-Flohé, S. Maurer, K. Lötzer, G. Böl, H. Kallionpää, P. Lehtolainen, H. Viita, and S. Ylä-Herttuala. Overexpression of phgpx inhibits hydroperoxide-induced oxidation, nf-kappab activation and apoptosis and affects oxldl-mediated proliferation of rabbit aortic smooth muscle cells. *Atherosclerosis*, 152:307–316, Oct 2000.
- [123] H. P. Wang, S. Y. Qian, F. Q. Schafer, F. E. Domann, L. W. Oberley, and G. R. Buettner. Phospholipid hydroperoxide glutathione peroxidase protects against singlet oxygen-induced cell damage of photodynamic therapy. *Free Radic Biol Med*, 30:825–835, Apr 2001.
- [124] R. Hurst, W. Korytowski, T. Kriska, R. S. Esworthy, F. F. Chu, and A. W. Girotti. Hyperresistance to cholesterol hydroperoxide-induced peroxidative injury and apoptotic death in a tumor cell line that overexpresses glutathione peroxidase isotype-4. *Free Radic Biol Med*, 31:1051–1065, Nov 2001.
- [125] H. Liang, Q. Ran, Y. C. Jang, D. Holstein, J. Lechleiter, T. McDonald-Marsh, A. Musatov, W. Song, Remmen H. Van, and A. Richardson. Glutathione peroxidase 4 differentially regulates the release of apoptogenic proteins from mitochondria. *Free Radic Biol Med*, 47:312–320, Aug 2009.
- [126] C. Ufer, C. C. Wang, M. Föhling, H. Schiebel, B. J. Thiele, E. E. Billett, H. Kuhn, and A. Borchert. Translational regulation of glutathione peroxidase 4 expression through guanine-rich sequence-binding factor 1 is essential for embryonic brain development. *Genes Dev*, 22:1838–1850, Jul 2008.
- [127] U. Schweizer, A. U. Bräuer, J. Köhrle, R. Nitsch, and N. E. Savaskan. Selenium and brain function: a poorly recognized liaison. *Brain Res Brain Res Rev*, 45:164–178, Jul 2004.
- [128] H. Imai, D. Sumi, H. Sakamoto, A. Hanamoto, M. Arai, N. Chiba, and Y. Nakagawa. Overexpression of phospholipid hydroperoxide glutathione peroxidase suppressed cell death due to oxidative damage in rat basophilic leukemia cells (rbl-2h3). *Biochem Biophys Res Commun*, 222:432–438, May 1996.

- [129] H. Kühn and A. Borchert. Regulation of enzymatic lipid peroxidation: the interplay of peroxidizing and peroxide reducing enzymes. *Free Radic Biol Med*, 33:154–172, Jul 2002.
- [130] M. J. Schilstra, G. A. Veldink, J. Verhagen, and J. F. Vliegthart. Effect of lipid hydroperoxide on lipoxygenase kinetics. *Biochemistry*, 31:7692–7699, Aug 1992.
- [131] H. Imai, K. Narashima, M. Arai, H. Sakamoto, N. Chiba, and Y. Nakagawa. Suppression of leukotriene formation in rbl-2h3 cells that overexpressed phospholipid hydroperoxide glutathione peroxidase. *J Biol Chem*, 273:1990–1997, Jan 1998.
- [132] C. J. Chen, H. S. Huang, and W. C. Chang. Depletion of phospholipid hydroperoxide glutathione peroxidase up-regulates arachidonate metabolism by 12s-lipoxygenase and cyclooxygenase 1 in human epidermoid carcinoma a431 cells. *FASEB J*, 17:1694–1696, Sep 2003.
- [133] I. Heirman, D. Ginneberge, R. Brigelius-Flohé, N. Hendrickx, P. Agostinis, P. Brouckaert, P. Rottiers, and J. Grooten. Blocking tumor cell eicosanoid synthesis by gpx4 impedes tumor growth and malignancy. *Free Radic Biol Med*, 40:285–294, Jan 2006.
- [134] M. Conrad, A. Sandin, H. Förster, A. Seiler, J. Frijhoff, M. Dagnell, G. W. Bornkamm, O. Radmark, H. R. Hoof, P. Aspenström, F. Böhmer, and A. Ostman. 12/15-lipoxygenase-derived lipid peroxides control receptor tyrosine kinase signaling through oxidation of protein tyrosine phosphatases. *Proc Natl Acad Sci U S A*, 107:15774–15779, Sep 2010.
- [135] M. Schneider, M. Wortmann, P. K. Mandal, W. Arpornchayanon, K. Jannasch, F. Alves, S. Strieth, M. Conrad, and H. Beck. Absence of glutathione peroxidase 4 affects tumor angiogenesis through increased 12/15-lipoxygenase activity. *Neoplasia*, 12:254–263, Mar 2010.
- [136] R. Brigelius-Flohé, B. Friedrichs, S. Maurer, M. Schultz, and R. Streicher. Interleukin-1-induced nuclear factor kappa b activation is inhibited by overexpression of phospholipid hydroperoxide glutathione peroxidase in a human endothelial cell line. *Biochem J*, 328 (Pt 1):199–203, Nov 1997.
- [137] A. Banning and R. Brigelius-Flohé. Nf-kappab, nrf2, and ho-1 interplay in redox-regulated vcam-1 expression. *Antioxid Redox Signal*, 7:889–899, Jan 2005.
- [138] A. Banning, S. Deubel, D. Kluth, Z. Zhou, and R. Brigelius-Flohé. The gi-gpx gene is a target for nrf2. *Mol Cell Biol*, 25:4914–4923, Jun 2005.
- [139] J. Wenk, J. Schüller, C. Hinrichs, T. Syrovets, N. Azoitei, M. Podda, M. Wlaschek, P. Brenneisen, L. A. Schneider, A. Sabiwalsky, T. Peters, S. Sulyok, J. Dissemond, M. Schauen, T. Krieg, T. Wirth, T. Simmet, and K. Scharfetter-Kochanek. Overexpression of phospholipid-hydroperoxide glutathione peroxidase in human dermal fibroblasts abrogates uva irradiation-induced expression of interstitial collagenase/matrix metalloproteinase-1 by suppression of phosphatidylcholine hydroperoxide-mediated nfkappab activation and interleukin-6 release. *J Biol Chem*, 279:45634–45642, Oct 2004.
- [140] A. A. Beg, W. C. Sha, R. T. Bronson, S. Ghosh, and D. Baltimore. Embryonic lethality and liver degeneration in mice lacking the rela component of nf-kappa b. *Nature*, 376:167–170, Jul 1995.
- [141] T. R. Pushpa-Rekha, A. L. Burdsall, L. M. Oleksa, G. M. Chisolm, and D. M. Driscoll. Rat phospholipid-hydroperoxide glutathione peroxidase. cDNA cloning and identification of multiple transcription and translation start sites. *J Biol Chem*, 270:26993–26999, Nov 1995.
- [142] S. G. Moreno, G. Laux, M. Brielmeier, G. W. Bornkamm, and M. Conrad. Testis-specific expression of the nuclear form of phospholipid hydroperoxide glutathione peroxidase (phgpx). *Biol Chem*, 384:635–643, Apr 2003.
- [143] R. Brigelius-Flohé, K. D. Aumann, H. Blöcker, G. Gross, M. Kiess, K. D. Klöppel, M. Maiorino, A. Roveri, R. Schuckelt, and F. Usani. Phospholipid-hydroperoxide glutathione peroxidase. genomic dna, cDNA, and deduced amino acid sequence. *J Biol Chem*, 269:7342–7348, Mar 1994.
- [144] C. Ufer, A. Borchert, and H. Kuhn. Functional characterization of cis- and trans-regulatory elements involved in expression of phospholipid hydroperoxide glutathione peroxidase. *Nucleic Acids Res*, 31:4293–4303, Aug 2003.
- [145] M. Schneider, Weisenhorn DM Vogt, A. Seiler, G. W. Bornkamm, M. Brielmeier, and M. Conrad. Embryonic expression profile of phospholipid hydroperoxide glutathione peroxidase. *Gene Expr Patterns*, 6:489–494, Jun 2006.
- [146] D. Schnabel, E. Salas-Vidal, V. Narváez, Mdel R. Sánchez-Carbente, D. Hernández-García, R. Cuervo, and L. Covarrubias. Expression and regulation of antioxidant enzymes in the developing limb support a function of ros in interdigital cell death. *Dev Biol*, 291:291–299, Mar 2006.
- [147] H. Imai, M. Saito, N. Kirai, J. Hasegawa, K. Konishi, H. Hattori, M. Nishimura, S. Naito, and Y. Nakagawa. Identification of the positive regulatory and distinct core regions of promoters, and transcriptional regulation in three types of mouse phospholipid hydroperoxide glutathione peroxidase. *J Biochem*, 140:573–590, Oct 2006.

- [148] M. Maiorino, M. Scapin, F. Ursini, M. Biasolo, V. Bosello, and L. Flohé. Distinct promoters determine alternative transcription of gpx-4 into phospholipid-hydroperoxide glutathione peroxidase variants. *J Biol Chem*, 278:34286–34290, Sep 2003.
- [149] F. Tramer, F. Micali, G. Sandri, A. Bertoni, A. Lenzi, L. Gandini, and E. Panfili. Enzymatic and immunohistochemical evaluation of phospholipid hydroperoxide glutathione peroxidase (phgpx) in testes and epididymal spermatozoa of rats of different ages. *Int J Androl*, 25:72–83, Apr 2002.
- [150] R. Puglisi, F. Tramer, E. Panfili, F. Micali, G. Sandri, and C. Boitani. Differential splicing of the phospholipid hydroperoxide glutathione peroxidase gene in diploid and haploid male germ cells in the rat. *Biol Reprod*, 68:405–411, Feb 2003.
- [151] A. A. Sneddon, H. C. Wu, A. Farquharson, I. Grant, J. R. Arthur, D. Rotondo, S. N. Choe, and K. W. J. Wahle. Regulation of selenoprotein gpx4 expression and activity in human endothelial cells by fatty acids, cytokines and antioxidants. *Atherosclerosis*, 171:57–65, Nov 2003.
- [152] G. Daniels. A century of human blood groups. *Wien Klin Wochenschr*, 113:781–786, Oct 2001.
- [153] L. M. van Putten. The life span of red cells in the rat and the mouse as determined by labeling with dfp32 in vivo. *Blood*, 13:789–794, Aug 1958.
- [154] H. Zhu, T. Jackson, and H. F. Bunn. Detecting and responding to hypoxia. *Nephrol Dial Transplant*, 17 Suppl 1:3–7, Jan 2002.
- [155] T. D. Richmond, M. Chohan, and D. L. Barber. Turning cells red: signal transduction mediated by erythropoietin. *Trends Cell Biol*, 15:146–155, Mar 2005.
- [156] G. L. Semenza. Hif-1: mediator of physiological and pathophysiological responses to hypoxia. *J Appl Physiol*, 88:1474–1480, Apr 2000.
- [157] P. J. Ratcliffe, J. F. O'Rourke, P. H. Maxwell, and C. W. Pugh. Oxygen sensing, hypoxia-inducible factor-1 and the regulation of mammalian gene expression. *J Exp Biol*, 201:1153–1162, Apr 1998.
- [158] H. F. Bunn and R. O. Poyton. Oxygen sensing and molecular adaptation to hypoxia. *Physiol Rev*, 76:839–885, Jul 1996.
- [159] M. Socolovsky. Molecular insights into stress erythropoiesis. *Curr Opin Hematol*, 14:215–224, May 2007.
- [160] H. Ludwig and K. Strasser. Symptomatology of anemia. *Semin Oncol*, 28:7, Apr 2001.
- [161] R. Njalsson. Glutathione synthetase deficiency. *Cell Mol Life Sci*, 62:1938–1945, Sep 2005.
- [162] S. C. Grubb, T. P. Maddatu, C. J. Bult, and M. A. Bogue. Mouse phenome database. *Nucleic Acids Res*, 37:D720–D730, Jan 2009.
- [163] S. Ghaffari. Oxidative stress in the regulation of normal and neoplastic hematopoiesis. *Antioxid Redox Signal*, 10:1923–1940, Nov 2008.
- [164] C. C. Winterbourn. Oxidative reactions of hemoglobin. *Methods Enzymol*, 186:265–272, Jan 1990.
- [165] J. F. Turrens. Mitochondrial formation of reactive oxygen species. *J Physiol*, 552:335–344, Oct 2003.
- [166] J. S. Friedman, V. I. Rebel, R. Derby, K. Bell, T. T. Huang, F. A. Kuypers, C. J. Epstein, and S. J. Burakoff. Absence of mitochondrial superoxide dismutase results in a murine hemolytic anemia responsive to therapy with a catalytic antioxidant. *J Exp Med*, 193:925–934, Apr 2001.
- [167] R. P. Hebbel. The sickle erythrocyte in double jeopardy: autoxidation and iron decompartmentalization. *Semin Hematol*, 27:51–69, Jan 1990.
- [168] Y. Kong, S. Zhou, A. J. Kihm, A. M. Katein, X. Yu, D. A. Gell, J. P. Mackay, K. Adachi, L. Foster-Brown, C. S. Loudon, A. J. Gow, and M. J. Weiss. Loss of alpha-hemoglobin-stabilizing protein impairs erythropoiesis and exacerbates beta-thalassemia. *J Clin Invest*, 114:1457–1466, Nov 2004.
- [169] J. M. Lee, K. Chan, Y. W. Kan, and J. A. Johnson. Targeted disruption of nrf2 causes regenerative immune-mediated hemolytic anemia. *Proc Natl Acad Sci U S A*, 101:9751–9756, Jun 2004.
- [170] R. M. Johnson, G. Goyette, Y. Ravindranath, and Y. S. Ho. Hemoglobin autoxidation and regulation of endogenous h2o2 levels in erythrocytes. *Free Radic Biol Med*, 39:1407–1417, Dec 2005.
- [171] J. Y. Chan, M. Kwong, M. Lo, R. Emerson, and F. A. Kuypers. Reduced oxidative-stress response in red blood cells from p45nfe2-deficient mice. *Blood*, 97:2151–2158, Apr 2001.

- [172] J. Y. Chan, M. Kwong, R. Lu, J. Chang, B. Wang, T. S. Yen, and Y. W. Kan. Targeted disruption of the ubiquitous cnc-bzip transcription factor, nr1, results in anemia and embryonic lethality in mice. *EMBO J*, 17:1779–1787, Mar 1998.
- [173] M. Kwong. The cnc basic leucine zipper factor, nr1, is essential for cell survival in response to oxidative stress-inducing agents. role for nr1 in gamma -gcsf and gss expression in mouse fibroblasts. 274:37491–37498, Jan 1999.
- [174] T. H. Lee, S. U. Kim, S. L. Yu, S. H. Kim, D. S. Park, H. B. Moon, S. H. Dho, K. S. Kwon, H. J. Kwon, Y. H. Han, S. Jeong, S. W. Kang, H. S. Shin, K. K. Lee, S. G. Rhee, and D. Y. Yu. Peroxiredoxin ii is essential for sustaining life span of erythrocytes in mice. *Blood*, 101:5033–5038, Jun 2003.
- [175] J. S. Friedman, M. F. Lopez, M. D. Fleming, A. Rivera, F. M. Martin, M. L. Welsh, A. Boyd, S. R. Doctrow, and S. J. Burakoff. Sod2-deficiency anemia: protein oxidation and altered protein expression reveal targets of damage, stress response, and antioxidant responsiveness. *Blood*, 104:2565–2573, Oct 2004.
- [176] G. Kroemer, L. Galluzzi, P. Vandenabeele, J. Abrams, E. S. Alnemri, E. H. Baehrecke, M. V. Blagosklonny, W. S. El-Deiry, P. Golstein, D. R. Green, M. Hengartner, R. A. Knight, S. Kumar, S. A. Lipton, W. Malorni, G. Nuñez, M. E. Peter, J. Tschopp, J. Yuan, M. Piacentini, B. Zhivotovsky, and G. Melino. Classification of cell death: recommendations of the nomenclature committee on cell death 2009. *Cell Death Differ*, 16:3, Jan 2009.
- [177] Y. Wang, V. L. Dawson, and T. M. Dawson. Poly(adp-ribose) signals to mitochondrial aif: a key event in parthanatos. *Exp Neurol*, 218:193–202, Aug 2009.
- [178] S. J. Dixon, K. M. Lemberg, M. R. Lamprecht, R. Skouta, E. M. Zaitsev, C. E. Gleason, D. N. Patel, A. J. Bauer, A. M. Cantley, W. S. Yang, B. Morrison, and B. R. Stockwell. Ferroptosis: an iron-dependent form of nonapoptotic cell death. *Cell*, 149:1060–1072, May 2012.
- [179] J. F. Kerr, A. H. Wyllie, and A. R. Currie. Apoptosis: a basic biological phenomenon with wide-ranging implications in tissue kinetics. *Br J Cancer*, 26:239–257, Aug 1972.
- [180] R. S. Hotchkiss, A. Strasser, J. E. McDunn, and P. E. Swanson. Cell death. *N Engl J Med*, 361:1570–1583, Oct 2009.
- [181] L. A. Tartaglia, T. M. Ayres, G. H. Wong, and D. V. Goeddel. A novel domain within the 55 kd tnf receptor signals cell death. *Cell*, 74:845–853, Sep 1993.
- [182] C. Scaffidi, S. Fulda, A. Srinivasan, C. Friesen, F. Li, K. J. Tomaselli, K. M. Debatin, P. H. Krammer, and M. E. Peter. Two cd95 (apo-1/fas) signaling pathways. *EMBO J*, 17:1675–1687, Mar 1998.
- [183] H. Hsu, J. Xiong, and D. V. Goeddel. The tnf receptor 1-associated protein tradd signals cell death and nf-kappa b activation. *Cell*, 81:495–504, May 1995.
- [184] A. Strasser. The role of bh3-only proteins in the immune system. *Nat Rev Immunol*, 5:189–200, Mar 2005.
- [185] J. C. Goldstein, C. Muñoz-Pinedo, J. E. Ricci, S. R. Adams, A. Kelekar, M. Schuler, R. Y. Tsien, and D. R. Green. Cytochrome c is released in a single step during apoptosis. *Cell Death Differ*, 12:453–462, May 2005.
- [186] N. N. Danial and S. J. Korsmeyer. Cell death: critical control points. *Cell*, 116:205–219, Jan 2004.
- [187] P. Li, D. Nijhawan, I. Budihardjo, S. M. Srinivasula, M. Ahmad, E. S. Alnemri, and X. Wang. Cytochrome c and datp-dependent formation of apaf-1/caspase-9 complex initiates an apoptotic protease cascade. *Cell*, 91:479–489, Nov 1997.
- [188] J. E. Chipuk and D. R. Green. Do inducers of apoptosis trigger caspase-independent cell death? *Nat Rev Mol Cell Biol*, 6:268–275, Mar 2005.
- [189] D. R. Green. Apoptotic pathways: ten minutes to dead. *Cell*, 121:671–674, Jun 2005.
- [190] N. Mizushima, B. Levine, A. M. Cuervo, and D. J. Klionsky. Autophagy fights disease through cellular self-digestion. *Nature*, 451:1069–1075, Feb 2008.
- [191] C. Gordy and Y. W. He. The crosstalk between autophagy and apoptosis: where does this lead? *Protein Cell*, 3:17–27, Jan 2012.
- [192] C. deDuve. The lysosome. *Sci Am*, 208:64–72, May 1963.
- [193] C. deDuve and R. Wattiaux. Functions of lysosomes. *Annu Rev Physiol*, 28:435–492, Jan 1966.
- [194] C. deDuve. Lysosomes revisited. *Eur J Biochem*, 137:391–397, Dec 1983.

- [195] J. Lee, S. Giordano, and J. Zhang. Autophagy, mitochondria and oxidative stress: cross-talk and redox signalling. *Biochem J*, 441:523–540, Jan 2012.
- [196] C. He and D. J. Klionsky. Regulation mechanisms and signaling pathways of autophagy. *Annu Rev Genet*, 43:67–93, Jan 2009.
- [197] Y. Chen and D. J. Klionsky. The regulation of autophagy - unanswered questions. *J Cell Sci*, 124:161–170, Jan 2011.
- [198] G. E. Mortimore, N. J. Hutson, and C. A. Surmacz. Quantitative correlation between proteolysis and macro- and microautophagy in mouse hepatocytes during starvation and refeeding. *Proc Natl Acad Sci U S A*, 80:2179–2183, Apr 1983.
- [199] D. Mijaljica, M. Prescott, and R. J. Devenish. Microautophagy in mammalian cells: revisiting a 40-year-old conundrum. *Autophagy*, 7:673–682, Jul 2011.
- [200] R. Sahu, S. Kaushik, C. C. Clement, E. S. Cannizzo, B. Scharf, A. Follenzi, I. Potolicchio, E. Nieves, A. M. Cuervo, and L. Santambrogio. Microautophagy of cytosolic proteins by late endosomes. *Dev Cell*, 20:131–139, Jan 2011.
- [201] E. Bejarano and A. M. Cuervo. Chaperone-mediated autophagy. *Proc Am Thorac Soc*, 7:29–39, Feb 2010.
- [202] H. L. Chiang, S. R. Terlecky, C. P. Plant, and J. F. Dice. A role for a 70-kilodalton heat shock protein in lysosomal degradation of intracellular proteins. *Science*, 246:382–385, Oct 1989.
- [203] Y. Kabeya, N. Mizushima, T. Ueno, A. Yamamoto, T. Kirisako, T. Noda, E. Kominami, Y. Ohsumi, and T. Yoshimori. Lc3, a mammalian homologue of yeast apg8p, is localized in autophagosome membranes after processing. *EMBO J*, 19:5720–5728, Nov 2000.
- [204] I. Tanida, T. Ueno, and E. Kominami. Lc3 conjugation system in mammalian autophagy. *Int J Biochem Cell Biol*, 36:2503–2518, Dec 2004.
- [205] R. I. Morimoto and A. M. Cuervo. Protein homeostasis and aging: taking care of proteins from the cradle to the grave. *J Gerontol A Biol Sci Med Sci*, 64:167–170, Feb 2009.
- [206] F. Cecconi and B. Levine. The role of autophagy in mammalian development: cell makeover rather than cell death. *Dev Cell*, 15:344–357, Sep 2008.
- [207] G. Kroemer and B. Levine. Autophagic cell death: the story of a misnomer. *Nat Rev Mol Cell Biol*, 9:1004–1010, Dec 2008.
- [208] H. M. Shen and P. Codogno. Autophagic cell death: Loch ness monster or endangered species? *Autophagy*, 7:457–465, May 2011.
- [209] R. Scherz-Shouval and Z. Elazar. Regulation of autophagy by ros: physiology and pathology. *Trends Biochem Sci*, 36:30–38, Jan 2011.
- [210] J. Huang, G. Y. Lam, and J. H. Brumell. Autophagy signaling through reactive oxygen species. *Antioxid Redox Signal*, 14:2215–2231, Jun 2011.
- [211] Y. Chen, M. B. Azad, and S. B. Gibson. Superoxide is the major reactive oxygen species regulating autophagy. *Cell Death Differ*, 16:1040–1052, Jul 2009.
- [212] R. Scherz-Shouval, E. Shvets, E. Fass, H. Shorer, L. Gil, and Z. Elazar. Reactive oxygen species are essential for autophagy and specifically regulate the activity of atg4. *EMBO J*, 26:1749–1760, Apr 2007.
- [213] R. A. Gottlieb and R. S. Carreira. Autophagy in health and disease. 5. mitophagy as a way of life. *Am J Physiol Cell Physiol*, 299:C203–C210, Aug 2010.
- [214] R. Kiffin, C. Christian, E. Knecht, and A. M. Cuervo. Activation of chaperone-mediated autophagy during oxidative stress. *Mol Biol Cell*, 15:4829–4840, Nov 2004.
- [215] M. Pan, V. Maitin, S. Parathath, U. Andreo, S. X. Lin, C. St Germain, Z. Yao, F. R. Maxfield, K. J. Williams, and E. A. Fisher. Presecretory oxidation, aggregation, and autophagic destruction of apoprotein-b: a pathway for late-stage quality control. *Proc Natl Acad Sci U S A*, 105:5862–5867, Apr 2008.
- [216] Y. Xiong, A. L. Contento, P. Q. Nguyen, and D. C. Bassham. Degradation of oxidized proteins by autophagy during oxidative stress in arabidopsis. *Plant Physiol*, 143:291–299, Jan 2007.
- [217] D. E. Christofferson and J. Yuan. Necroptosis as an alternative form of programmed cell death. *Curr Opin Cell Biol*, 22:263–268, Apr 2010.

- [218] A. Degterev and J. Yuan. Expansion and evolution of cell death programmes. *Nat Rev Mol Cell Biol*, 9:378–390, May 2008.
- [219] P. Vandenabeele, L. Galluzzi, Berghe T. Vanden, and G. Kroemer. Molecular mechanisms of necroptosis: an ordered cellular explosion. *Nat Rev Mol Cell Biol*, 11:700–714, Oct 2010.
- [220] D. Vercammen, P. Vandenabeele, R. Beyaert, W. Declercq, and W. Fiers. Tumour necrosis factor-induced necrosis versus anti-fas-induced apoptosis in 1929 cells. *Cytokine*, 9:801–808, Nov 1997.
- [221] J. Han, C. Q. Zhong, and D. W. Zhang. Programmed necrosis: backup to and competitor with apoptosis in the immune system. *Nat Immunol*, 12:1143–1149, Dec 2011.
- [222] A. Degterev, Z. Huang, M. Boyce, Y. Li, P. Jagtap, N. Mizushima, G. D. Cuny, T. J. Mitchison, M. A. Moskowitz, and J. Yuan. Chemical inhibitor of nonapoptotic cell death with therapeutic potential for ischemic brain injury. *Nat Chem Biol*, 1:112–119, Jul 2005.
- [223] L. Wang, F. Du, and X. Wang. Tnf-alpha induces two distinct caspase-8 activation pathways. *Cell*, 133:693–703, May 2008.
- [224] S. He, L. Wang, L. Miao, T. Wang, F. Du, L. Zhao, and X. Wang. Receptor interacting protein kinase-3 determines cellular necrotic response to tnf-alpha. *Cell*, 137:1100–1111, Jun 2009.
- [225] Y. S. Cho, S. Challa, D. Moquin, R. Genga, T. D. Ray, M. Guildford, and F. K. Chan. Phosphorylation-driven assembly of the rip1-rip3 complex regulates programmed necrosis and virus-induced inflammation. *Cell*, 137:1112–1123, Jun 2009.
- [226] D. W. Zhang, J. Shao, J. Lin, N. Zhang, B. J. Lu, S. C. Lin, M. Q. Dong, and J. Han. Rip3, an energy metabolism regulator that switches tnf-induced cell death from apoptosis to necrosis. *Science*, 325:332–336, Jul 2009.
- [227] O. Micheau and J. Tschopp. Induction of tnf receptor i-mediated apoptosis via two sequential signaling complexes. *Cell*, 114:181–190, Jul 2003.
- [228] D. Vercammen, R. Beyaert, G. Denecker, V. Goossens, G. Van Loo, W. Declercq, J. Grooten, W. Fiers, and P. Vandenabeele. Inhibition of caspases increases the sensitivity of 1929 cells to necrosis mediated by tumor necrosis factor. *J Exp Med*, 187:1477–1485, May 1998.
- [229] W. X. Zong, D. Ditsworth, D. E. Bauer, Z. Q. Wang, and C. B. Thompson. Alkylating dna damage stimulates a regulated form of necrotic cell death. *Genes Dev*, 18:1272–1282, Jun 2004.
- [230] H. Boujrad, O. Gubkina, N. Robert, S. Krantic, and S. A. Susin. Aif-mediated programmed necrosis: a highly regulated way to die. *Cell Cycle*, 6:2612–2619, Nov 2007.
- [231] K. Schulze-Osthoff, A. C. Bakker, B. Vanhaesebroeck, R. Beyaert, W. A. Jacob, and W. Fiers. Cytotoxic activity of tumor necrosis factor is mediated by early damage of mitochondrial functions. evidence for the involvement of mitochondrial radical generation. *J Biol Chem*, 267:5317–5323, Mar 1992.
- [232] V. Goossens, G. Stangé, K. Moens, D. Pipeleers, and J. Grooten. Regulation of tumor necrosis factor-induced, mitochondria- and reactive oxygen species-dependent cell death by the electron flux through the electron transport chain complex i. *Antioxid Redox Signal*, 1:285–295, Jan 1999.
- [233] Y. S. Kim, M. J. Morgan, S. Choksi, and Z. G. Liu. Tnf-induced activation of the nox1 nadph oxidase and its role in the induction of necrotic cell death. *Mol Cell*, 26:675–687, Jun 2007.
- [234] J. Hitomi, D. E. Christofferson, A. Ng, J. Yao, A. Degterev, R. J. Xavier, and J. Yuan. Identification of a molecular signaling network that regulates a cellular necrotic cell death pathway. *Cell*, 135:1311–1323, Dec 2008.
- [235] A. Degterev, J. Hitomi, M. Gernscheid, I. L. Ch'en, O. Korkina, X. Teng, D. Abbott, G. D. Cuny, C. Yuan, G. Wagner, S. M. Hedrick, S. A. Gerber, A. Lugovskoy, and J. Yuan. Identification of rip1 kinase as a specific cellular target of necrostatins. *Nat Chem Biol*, 4:313–321, May 2008.
- [236] X. Xu, C. C. Chua, J. Kong, R. M. Kostrzewa, U. Kumaraguru, R. C. Hamdy, and B. H. Chua. Necrostatin-1 protects against glutamate-induced glutathione depletion and caspase-independent cell death in ht-22 cells. *J Neurochem*, 103:2004–2014, Dec 2007.
- [237] C. Xie, N. Zhang, H. Zhou, J. Li, Q. Li, T. Zarubin, S. C. Lin, and J. Han. Distinct roles of basal steady-state and induced h-ferritin in tumor necrosis factor-induced death in 1929 cells. *Mol Cell Biol*, 25:6673–6681, Aug 2005.
- [238] R. Kühn, F. Schwenk, M. Aguet, and K. Rajewsky. Inducible gene targeting in mice. *Science*, 269:1427–1429, Sep 1995.

- [239] D. Hameyer, A. Loonstra, L. Eshkind, S. Schmitt, C. Antunes, A. Groen, E. Bindels, J. Jonkers, P. Krimpenfort, R. Meuwissen, L. Rijswijk, A. Bex, A. Berns, and E. Bockamp. Toxicity of ligand-dependent cre recombinases and generation of a conditional cre deleter mouse allowing mosaic recombination in peripheral tissues. *Physiol Genomics*, 31:32–41, Sep 2007.
- [240] D. Sun and C. D. Funk. Disruption of 12/15-lipoxygenase expression in peritoneal macrophages. enhanced utilization of the 5-lipoxygenase pathway and diminished oxidation of low density lipoprotein. *J Biol Chem*, 271:24055–24062, Sep 1996.
- [241] M. Komatsu, S. Waguri, T. Ueno, J. Iwata, S. Murata, I. Tanida, J. Ezaki, N. Mizushima, Y. Ohsumi, Y. Uchiyama, E. Kominami, K. Tanaka, and T. Chiba. Impairment of starvation-induced and constitutive autophagy in atg7-deficient mice. *J Cell Biol*, 169:425–434, May 2005.
- [242] K. Newton, X. Sun, and V. M. Dixit. Kinase rip3 is dispensable for normal nf- κ b signaling by the b-cell and t-cell receptors, tumor necrosis factor receptor 1, and toll-like receptors 2 and 4. *J Biol Chem*, 279:1464–1469, Jan 2004.
- [243] G. Hoffmann-Fezer, J. Mysliwicz, W. Mörtlbauer, H. J. Zeitler, E. Eberle, U. Hönle, and S. Thierfelder. Biotin labeling as an alternative nonradioactive approach to determination of red cell survival. *Ann Hematol*, 67:81–87, Aug 1993.
- [244] C. Verrou, Y. Zhang, C. Zürn, W. W. Schamel, and M. Reth. Comparison of the tamoxifen regulated chimeric cre recombinases mercrer and cremer. *Biol Chem*, 380:1435–1438, Dec 1999.
- [245] F. Schwenk, U. Baron, and K. Rajewsky. A cre-transgenic mouse strain for the ubiquitous deletion of loxp-flanked gene segments including deletion in germ cells. *Nucleic Acids Res*, 23:5080–5081, Dec 1995.
- [246] H. E. Broxmeyer, L. Lu, E. Platzer, C. Feit, L. Juliano, and B. Y. Rubin. Comparative analysis of the influences of human gamma, alpha and beta interferons on human multipotential (cfu-gemm), erythroid (bfu-e) and granulocyte-macrophage (cfu-gm) progenitor cells. *J Immunol*, 131:1300–1305, Sep 1983.
- [247] M. A. G. Essers, S. Offner, W. E. Blanco-Bose, Z. Waibler, U. Kalinke, M. A. Duchosal, and A. Trumpp. Ifn α activates dormant haematopoietic stem cells in vivo. *Nature*, 458:904–908, Apr 2009.
- [248] C. Kiermayer, M. Conrad, M. Schneider, J. Schmidt, and M. Brielmeier. Optimization of spatiotemporal gene inactivation in mouse heart by oral application of tamoxifen citrate. *Genesis*, 45:11–16, Jan 2007.
- [249] M. Mortensen, D. J. P. Ferguson, M. Edelmann, B. Kessler, K. J. Morten, M. Komatsu, and A. K. Simon. Loss of autophagy in erythroid cells leads to defective removal of mitochondria and severe anemia in vivo. *Proc Natl Acad Sci U S A*, 107:832–837, Jan 2010.
- [250] H. Sandoval, P. Thiagarajan, S. K. Dasgupta, A. Schumacher, J. T. Prchal, M. Chen, and J. Wang. Essential role for nix in autophagic maturation of erythroid cells. *Nature*, 454:232–235, Jul 2008.
- [251] M. Komatsu, S. Waguri, M. Koike, Y. S. Sou, T. Ueno, T. Hara, N. Mizushima, J. I. Iwata, J. Ezaki, S. Murata, J. Hamazaki, Y. Nishito, S. I. Iemura, T. Natsume, T. Yanagawa, J. Uwayama, E. Warabi, H. Yoshida, T. Ishii, A. Kobayashi, M. Yamamoto, Z. Yue, Y. Uchiyama, E. Kominami, and K. Tanaka. Homeostatic levels of p62 control cytoplasmic inclusion body formation in autophagy-deficient mice. *Cell*, 131:1149–1163, Dec 2007.
- [252] H. M. Shen and P. Codogno. Autophagy is a survival force via suppression of necrotic cell death. *Exp Cell Res*, 318:1304–1308, Jul 2012.
- [253] Y. Jin, A. Tanaka, A. M. K. Choi, and S. W. Ryter. Autophagic proteins: New facets of the oxygen paradox. *Autophagy*, 8, Mar 2012.
- [254] W. Fiers, R. Beyaert, E. Boone, S. Cornelis, W. Declercq, E. Decoster, G. Denecker, B. Depuydt, D. De Valck, G. De Wilde, V. Goossens, J. Grooten, G. Haegeman, K. Heyninck, L. Penning, S. Plaisance, K. Vancompernelle, W. Van Criekeinghe, P. Vandenabeele, W. Vanden Berghe, M. Van de Craen, V. Vandevoorde, and D. Vercammen. Tnf-induced intracellular signaling leading to gene induction or to cytotoxicity by necrosis or by apoptosis. *J Inflamm*, 47:67–75, Jan 1995.
- [255] D. D’Amours, S. Desnoyers, I. D’Silva, and G. G. Poirier. Poly(adp-ribosyl)ation reactions in the regulation of nuclear functions. *Biochem J*, 342 (Pt 2):249–268, Sep 1999.
- [256] H. C. Ha and S. H. Snyder. Poly(adp-ribose) polymerase is a mediator of necrotic cell death by atp depletion. *Proc Natl Acad Sci U S A*, 96:13978–13982, Nov 1999.
- [257] Y. Xu, S. Huang, Z. G. Liu, and J. Han. Poly(adp-ribose) polymerase-1 signaling to mitochondria in necrotic cell death requires rip1/traf2-mediated jnk1 activation. *J Biol Chem*, 281:8788–8795, Mar 2006.
- [258] K. Degenhardt, R. Mathew, B. Beaudoin, K. Bray, D. Anderson, G. Chen, C. Mukherjee, Y. Shi, C. Gélinas, Y. Fan, D. A. Nelson, S. Jin, and E. White. Autophagy promotes tumor cell survival and restricts necrosis, inflammation, and tumorigenesis. *Cancer Cell*, 10:51–64, Jul 2006.

- [259] J. J. Lum, D. E. Bauer, M. Kong, M. H. Harris, C. Li, T. Lindsten, and C. B. Thompson. Growth factor regulation of autophagy and cell survival in the absence of apoptosis. *Cell*, 120:237–248, Jan 2005.
- [260] D. M. Sullivan, N. B. Wehr, M. M. Fergusson, R. L. Levine, and T. Finkel. Identification of oxidant-sensitive proteins: Tnf-alpha induces protein glutathiolation. *Biochemistry*, 39:11121–11128, Sep 2000.
- [261] G. Filomeni, K. Aquilano, P. Civitareale, G. Rotilio, and M. R. Ciriolo. Activation of c-jun-n-terminal kinase is required for apoptosis triggered by glutathione disulfide in neuroblastoma cells. *Free Radic Biol Med*, 39:345–354, Aug 2005.
- [262] N. L. Reynaert, A. van der Vliet, A. S. Guala, T. McGovern, M. Hristova, C. Pantano, N. H. Heintz, J. Heim, Y. S. Ho, D. E. Matthews, Emiel F. M. Wouters, and Yvonne M. W. Janssen-Heininger. Dynamic redox control of nf-kappab through glutaredoxin-regulated s-glutathionylation of inhibitory kappab kinase beta. *Proc Natl Acad Sci U S A*, 103:13086–13091, Aug 2006.
- [263] S. Qanungo, D. W. Starke, H. V. Pai, J. J. Mieyal, and A. L. Nieminen. Glutathione supplementation potentiates hypoxic apoptosis by s-glutathionylation of p65-nfkappab. *J Biol Chem*, 282:18427–18436, Jun 2007.
- [264] C. S. Velu, S. K. Niture, C. E. Doneanu, N. Pattabiraman, and K. S. Srivenugopal. Human p53 is inhibited by glutathionylation of cysteines present in the proximal dna-binding domain during oxidative stress. *Biochemistry*, 46:7765–7780, Jul 2007.
- [265] J. V. Cross and D. J. Templeton. Oxidative stress inhibits mekk1 by site-specific glutathionylation in the atp-binding domain. *Biochem J*, 381:675–683, Aug 2004.
- [266] H. Kamata, S. Honda, S. Maeda, L. Chang, H. Hirata, and M. Karin. Reactive oxygen species promote tnfalpa-induced death and sustained jnk activation by inhibiting map kinase phosphatases. *Cell*, 120:649–661, Mar 2005.
- [267] A. R. Diers, A. N. Higdon, K. C. Ricart, M. S. Johnson, A. Agarwal, B. Kalyanaraman, A. Landar, and V. M. Darley-Usmar. Mitochondrial targeting of the electrophilic lipid 15-deoxy-delta12,14-prostaglandin j2 increases apoptotic efficacy via redox cell signalling mechanisms. *Biochem J*, 426:31–41, Feb 2010.
- [268] A. Negre-Salvayre, N. Auge, V. Ayala, H. Basaga, J. Boada, R. Brenke, S. Chapple, G. Cohen, J. Feher, T. Grune, G. Lengyel, G. E. Mann, R. Pamplona, G. Poli, M. Portero-Otin, Y. Riahi, R. Salvayre, S. Sasson, J. Serrano, O. Shammi, W. Siems, R. C. M. Siow, I. Wiswedel, K. Zarkovic, and N. Zarkovic. Pathological aspects of lipid peroxidation. *Free Radic Res*, 44:1125–1171, Oct 2010.

Appendix A

Appendix

A.1 Chemicals, Reagents and Kits

Chemical	Company	Catalog No.
5Z-7-Oxozeaenol	Sigma	O9890
Annexin V	BD Pharmingen	550464
anti-CD178	BD Pharmingen	555291
Antigen Unmasking Solution	Vector Lab	H-3300
Anti-FITC MicroBeads	Miltenyi	130-048-701
Anti-PE MicroBeads	Miltenyi	130-048-801
APO Alert (Tunel)	Clontech	630107
Avidin/Biotin Blocking Kit	Vector Lab	SP-2001
Bodipy C11	Invitrogen, USA	D3861
BrdU detection kit	eBioscience	17-5071-41
Caspase inhibitor 1 (zVAD)	Calbiochem	627610
CM-H2DCFDA	Invitrogen, USA	C6827
Ciprobay 500mg	Bayer	
DAPI	Invitrogen	P36931
DTT	Sigma	43815
dNTP Mix	Invitrogen	18427-088
Fas (Soluble) Recombinant	BD Pharmingen	554336
Mitotracker Deep Red	Invitrogen	M22426
Mouse EPO Elisa Kit	R&D Systems	DY959
Mouse IL-6 Elisa Kit	R&D Systems	DY406
Olaparib (AZD2281)	Selleckchem	S1060
Oligo (dT) Primer	Invitrogen	AM5730G
poly I:C	Sigma	P1530
QIAshredder Kit	Qiagen	79656
Recombinant Human TNF α	R&D Systems	210-TA-001MG/CF
RNaseOUT	Invitrogen	10777-019
RNeasy Mini Kit	Qiagen	74104
Streptovivin/Biotin Blocking Kit	Vector Lab	SP-2001
SuperScriptII Reverse Transcriptase	Invitrogen	18064-014
SuperSignal West Femto Substrate	Thermo Scientific	34095
SuperSignal West Pico Substrate	Thermo Scientific	34080
SYBR Green Master (Rox)	Roche	79656
Thiazol orange	Biomol	ABD-17518
VectaMount Mounting Medium	Vector Lab	H-5000

A.2 Antibodies

A.2.1 Flow cytometry antibodies

Target	Company	Catalog Number	Conditions
CD16/CD32	BD Pharmingen	553142	1:100
CD3	BD Pharmingen	555274	1:200
CD71	BD Pharmingen	553266	1:200
TER119	BD Pharmingen	561071	1:100

A.2.2 Western blot antibodies

Target	Company	Catalog Number	Conditions
β -actin	Sigma	A4700	1:2000 3% Skim milk 4°C ON
caspase 8	Abnova	MAB3429	1:1000 4% Skim milk 4°C ON
GPx4	raised against PQVIEKDLPCYL	[103]	3% BSA 4°C ON
LC3B	Cell Signaling	2775	1:1000 3% BSA 4°C ON
p62	Progen	GP62-C	1:1000 3% Skim milk 4°C ON
RIP1	BD Pharmingen	610459	1:1000 4% Skim milk 4°C ON
RIP3	Abcam	AB62344	1:1000 4% Skim milk 4°C ON
TRAF2	Cell Signaling	4724	1:1000 4% Skim milk 4°C ON

A.2.3 Antibodies used for histology

Target	Company	Catalog Number	Conditions
BRDU	AbDSerotec	MCA2060	1:400 3% BSA 4°C ON
Phospho-Histone H2A.X	Cell Signaling	2577	1:200 3% BSA 4°C ON

A.3 siRNA

Target	Company	Catalog Number
caspase 8	Thermo Scientific	L-043044-00
RIP1	Thermo Scientific	L-040150-00
RIP3	Thermo Scientific	D-049919-04
TRAF2	Thermo Scientific	L-042814-01

A.4 Genotyping

Table A.6: 12/15-Lox Genotyping PCR

Primers (5'-3')	Temperature(°C)	Time(second)	Cycle
CTGAATGAACTGCAGGACGA	94	30	35
CGTGGTTGAAGACTCTCAAGG	73	60	
CGAAATCGCTGGTCTACAGG	72	60	

Table A.7: ATG7 Genotyping PCR

Primers (5'-3')	Temperature(°C)	Time(second)	Cycle
TGGCTGCTACTTCTGCAATGATGT	94	30	35
CAGGACAGAGACCATCAGCTCCAC	62	60	
TTGCCAACATCCCTGGATAC	72	60	
TGGCACCCACTGACCAATAG			

Table A.8: Cre Genotyping PCR

Primers (5'-3')	Temperature(°C)	Time(second)	Cycle
ACCTGAAGATGTTTCGCGATTATCT	94	30	35
ACCGTCAGTACGTGAGATATCTT	58	30	
	72	30	

Table A.9: GPx4 Genotyping PCR

Primers (5'-3')	Temperature°C	Time	Cycle
ACTCCCCGTGGAAGCTGTGAGCTTTGTGC	94	30	40
GGATCTAAGGATCACAGAGCTGAGGCTGC	68	30	
	72	90	

Table A.10: RIP3 Genotyping PCR

Primers (5'-3')	Temperature(°C)	Time(second)	Cycle
CGCTTTAGAAGCCTTCAGGTTGAC	94	30	30
GCCTGCCCAATCAGCAACTC	60	30	
CCAAGAGGCCACTTGTGTAGCG	72	60	